ANALYSIS OF WHIPLASH DURING REAR CRASH AND DEVELOPMENT OF AN ANTI-WHIPLASH SEAT MECHANISM

A THESIS SUBMITTED TO
THE GRADUATE SCHOOL OF NATURAL AND APPLIED SCIENCES
OF
MIDDLE EAST TECHNICAL UNIVERSITY

BY

MUSTAFA ÖZDEMİR

IN PARTIAL FULFILLMENT OF THE REQUIREMENTS FOR
THE DEGREE OF DOCTOR OF PHILOSOPHY

IN

MECHANICAL ENGINEERING

JUNE 2013

Approval of the thesis:

ANALYSIS OF WHIPLASH DURING REAR CRASH AND DEVELOPMENT OF AN ANTI-WHIPLASH SEAT MECHANISM

submitted by **MUSTAFA ÖZDEMİR** in partial fulfillment of the requirements for the degree of **Doctor of Philosophy in Mechanical Engineering Department, Middle East Technical University** by,

Prof. Dr. Canan Özgen _____
Dean, Graduate School of **Natural and Applied Sciences**

Prof. Dr. Süha Oral _____
Head of Department, **Mechanical Engineering**

Prof. Dr. Sıtkı Kemal İder _____
Supervisor, **Mechanical Engineering Dept., METU**

Prof. Dr. Mustafa İlhan Gökler _____
Co-Supervisor, **Mechanical Engineering Dept., METU**

Examining Committee Members:

Prof. Dr. Reşit Soylu _____
Mechanical Engineering Dept., METU

Prof. Dr. Sıtkı Kemal İder _____
Mechanical Engineering Dept., METU

Prof. Dr. Raif Tuna Balkan _____
Mechanical Engineering Dept., METU

Prof. Dr. Mehmet Utku _____
Civil Engineering Dept., METU

Prof. Dr. Müfit Gülgeç _____
Mechatronics Engineering Dept., Çankaya University

Date: 04.06.2013

I hereby declare that all information in this document has been obtained and presented in accordance with academic rules and ethical conduct. I also declare that, as required by these rules and conduct, I have fully cited and referenced all material and results that are not original to this work.

Name, Last name : Mustafa Özdemir

Signature :

ABSTRACT

ANALYSIS OF WHIPLASH DURING REAR CRASH AND DEVELOPMENT OF AN ANTI-WHIPLASH SEAT MECHANISM

Özdemir, Mustafa
Ph.D., Department of Mechanical Engineering
Supervisor: Prof. Dr. Sıtkı Kemal İder
Co-Supervisor: Prof. Dr. Mustafa İlhan Gökler

June 2013, 167 pages

Whiplash injury is one of the most important types of injuries when its resulting long-term pain is considered. This neck injury is frequently seen in the motor vehicle collisions, especially in the low-speed rear collisions. In this thesis, it is aimed to analyze the whiplash syndrome in low-speed rear-end impacts and develop an anti-whiplash seat mechanism that reduces the risk of occurrence of whiplash injuries. Firstly, using the commercially available finite element model of the BioRID II dummy, backset reducing and slidable seat design concepts have been analyzed. Based on the strategy of moving the head restraint forward during a rear crash in order to reduce the backset, two novel seat mechanisms have been developed. One of these is an anti-whiplash system having a lock unit, and the other is a quick forward anti-whiplash seat mechanism. Three identical prototype seats have been produced for the quick forward anti-whiplash mechanism and tested by sled tests that have been performed at the Vehicle Safety Unit of the METU-BILTIR Center according to the Euro NCAP whiplash testing procedure using BioRID II dummy. For comparative purposes, three identical standard seats that do not have any anti-whiplash action, and three identical anti-whiplash seats with a different headrest moving mechanism have been also tested using the same procedure. The test results have been assessed according to the Euro NCAP and RCAR-IIWPG rating systems, and the seat with the developed quick forward anti-whiplash mechanism has been shown to be effective for reducing the risk of whiplash injury.

Keywords: Whiplash Injury, Anti-whiplash System, Vehicle Safety, Euro NCAP, RCAR-IIWPG

ÖZ

ARKADAN ÇARPMALARDA WHIPLASH ANALİZİ VE BİR ANTI-WHIPLASH KOLTUK MEKANİZMASININ GELİŞTİRİLMESİ

Özdemir, Mustafa
Doktora, Makina Mühendisliği Bölümü
Tez Yöneticisi: Prof. Dr. Sıtkı Kemal İder
Ortak Tez Yöneticisi: Prof. Dr. Mustafa İlhan Gökler

Haziran 2013, 167 sayfa

Whiplash incinmesi neden olduğu uzun süreli ağrı göz önüne alındığında en önemli incinmeler türlerinden biridir. Bu boyun incinmesi motorlu araç çarpışmalarında, özellikle de düşük hızlarda gerçekleşen arkadan çarpmalarda, sıklıkla görülmektedir. Bu tezde düşük hızlı arkadan çarpmalarda görülen whiplash sendromunun analiz edilmesi ve whiplash incinmelerinin ortaya çıkma riskini azaltacak bir anti-whiplash koltuk mekanizmasının geliştirilmesi amaçlanmıştır. İlk olarak, BioRID II çarpışma mankeninin ticari olarak satılan sonlu elemanlar modeli kullanılarak backset azaltan ve kayabilir koltuk tasarım konseptleri analiz edilmiştir. Backseti azaltmak için kaza sırasında koltuk başlığının öne doğru hareket ettirilmesi stratejisine dayalı olarak iki özgün koltuk mekanizması geliştirilmiştir. Bunlardan biri kilit ünitesine sahip bir ani-whiplash sistemi, diğeri ise hızlı dönüş anti-whiplash koltuk mekanizmasıdır. Hızlı dönüş anti-whiplash mekanizması için üç özdeş prototip koltuk üretilmiş ve ODTÜ-BİLTİR Merkezi Taşıt Güvenliği Biriminde BioRID II mankeni kullanılarak Euro NCAP test protokolüne göre gerçekleştirilen kızak testleri ile test edilmiştir. Kıyaslama amacıyla herhangi bir anti-whiplash özelliğine sahip olmayan üç özdeş standart koltuk ve farklı bir koltuk başlığı hareket ettirme mekanizmasına sahip üç özdeş koltuk da aynı prosedür kullanılarak test edilmiştir. Test sonuçları Euro NCAP ve RCAR-IIWPG değerlendirme sistemlerine göre değerlendirilmiş ve geliştirilen hızlı dönüş anti-whiplash mekanizmasının whiplash incinme riskini azaltmada etkili olduğu gösterilmiştir.

Anahtar Kelimeler: Whiplash Yaralanması, Anti-whiplash Sistemi, Taşıt Güvenliği Euro NCAP, RCAR-IIWPG

To My Family

ACKNOWLEDGEMENTS

The author wishes to express his deepest gratitude to his supervisor Prof. Dr. Sıtkı Kemal İder and co-supervisor Prof. Dr. Mustafa İlhan Gökler for their guidance, advice, criticism, encouragements, and insight throughout the research.

This thesis work is supported by TOFAŞ, which is gratefully acknowledged. The author would also like to thank to Hüseyin Dicle, Evren Anık, Murat Sefa İnce, and İpek Beyhan working in the Seat Design Management of TOFAŞ R&D Directorate.

The author is grateful to his family for their endless love and support throughout his life.

The author is supported by the Scientific and Technological Research Council of Turkey (TÜBİTAK) National Scholarship Program for Ph.D. Students.

Last but not least, thanks to the METU-BILTIR Center for the facilities provided.

TABLE OF CONTENTS

ABSTRACT v
ÖZ vi
ACKNOWLEDGEMENTS viii
TABLE OF CONTENTS ix
LIST OF TABLES xii
LIST OF FIGURES xiv
LIST OF SYMBOLS AND ABBREVIATIONS xix
CHAPTERS
1. INTRODUCTION 1
1.1 Motivation 1
1.2 Occupant Motion during a Rear Crash and the Injury Mechanism 2
1.3 Influence of Different Factors Regarding Vehicle Seat Design on Whiplash Injury Risk 3
1.4 Objective and Scope of the Thesis 5
2. CLASSIFICATION OF ANTI-WHIPLASH SYSTEMS: A PATENT SURVEY 7
2.1 Systems where the Head Restraint is Moved Forward by an Electrical Control System 7
2.2 Systems where the Head Restraint is Moved Forward by a Mechanical Trigger Mechanism 11
2.3 Systems where the Backrest Moves 15
2.4 Systems where the Entire Seat Moves 19
2.5 Special-Shaped Backrest and Head Restraint Designs Made of Special Materials 23
2.6 Air-Bagged Head Restraints 27
2.7 Other Headrest Forms 31
2.8 Helmet and Collar Designs 35
3. WHIPLASH SIMULATION WITH SIMPLIFIED VEHICLE SEAT MODEL . 39
3.1 Finite Element Model Development 39
3.2 Selection and Validation of the Seat Model Parameters 43
4. EVALUATION OF ALTERNATIVE FUNCTIONAL DESIGNS 51
4.1 Alternative Functional Designs 51
4.2 Effect of Backset Distance on Whiplash Syndrome 52
4.3 Parametric Analysis of an Anti-whiplash Seat Suspension 54
4.4 Selection of the System 60

5. TWO NOVEL ANTI-WHIPLASH VEHICLE SEAT MECHANISMS BASED ON REDUCING BACKSET 61
5.1 An Anti-whiplash Vehicle Seat Mechanism Having a Lock 61
5.2 An Anti-whiplash Vehicle Seat with a Quick Forward Anti-whiplash Mechanism 80
5.3 Kinematic Synthesis and Analysis of the Quick Forward Anti-whiplash Seat Mechanism 86
5.4 Assessment of the Quick Forward Anti-whiplash Seat Mechanism 88
6. SLED TESTS OF THE SEAT WITH THE PROPOSED QUICK FORWARD ANTI-WHIPLASH SEAT MECHANISM 91
6.1 Sled Test System 92
6.2 Basic Steps in Euro NCAP Whiplash Assessment Tests 93
6.3 Test Sample Preparation 94
6.3.1 Seat Mounting and Adjustment 95
6.3.2 Seat Belt Anchorage Arrangement 96
6.3.3 HPM and HRMD Measurements 97
6.4 Generation of the Target Sled Pulses 104
6.5 Dummy Positioning, Adjustments, Measurements and Performing of the Sled Test 106
7. WHIPLASH ASSESSMENT SYSTEMS 117
7.1 Euro NCAP Assessment 117
7.1.1 Static Assessment 117
7.1.2 Dynamic Assessment 118
7.1.3 Dynamic Assessment Criteria 119
7.1.3.1 T-HRC 119
7.1.3.2 T1 119
7.1.3.3 NIC 121
7.1.3.4 F_x and F_z 121
7.1.3.5 N_{km} 121
7.1.3.6 $V_{rebound}$ 124
7.1.4 Modifiers 124
7.1.4.1 Seatback Deflection 124
7.1.5 Overall Scoring 125
7.2 RCAR-IIWPG Assessment 126
8. EURO NCAP AND RCAR-IIWPG EVALUATION RESULTS OF THE TESTED SEATS 133
8.1 Euro NCAP Assessment Results 133
8.2 RCAR-IIWPG Assessment Results 142
9. CONCLUSIONS 147
9.1 General Conclusions 147
9.2 Recommendations for Future Works 151

REFERENCES 153
CURRICULUM VITAE..... 165

LIST OF TABLES

TABLES

Table 1 The foam material parameters (Tabiei, et al., 2007) 41
Table 2 Simulations performed 52
Table 3 Simulation results 53
Table 4 The effect of *k* and *c* on the NIC_{max} (F_b=320 N, *b*=59 mm) 58
Table 5 The performances of slidable seats that have different *k* and *c* values, but same *d* value (F_b=309 N, *b*=59 mm) 60
Table 6 Target and tolerance values of the BioRID installation parameters (Euro NCAP whiplash testing protocol, 2011) 104
Table 7 The numbering system used for the tested seats 108
Table 8 Dummy transducer channels used (Euro NCAP whiplash testing protocol, 2011) 108
Table 9 Sled pulse specifications 110
Table 10 Geometry assessment parameters and their lower and higher performance limits (Euro NCAP whiplash assessment protocol, 2011) 118
Table 11 Higher and lower performance and capping limits for each dynamic assessment criteria (Euro NCAP whiplash assessment protocol, 2011) 120
Table 12 CFC filter classes used for the dummy transducer channels during the calculation of the injury criteria (Euro NCAP whiplash testing protocol, 2011) 120
Table 13 Critical intercept values for calculation of N_{km} (Euro NCAP whiplash testing protocol, 2011) 122
Table 14 Raw scoring (Euro NCAP whiplash assessment protocol, 2011) 126
Table 15 RCAR-IIWPG dynamic rating scale (RCAR-IIWPG dynamic evaluation protocol, 2008) 129
Table 16 RCAR-IIWPG overall rating scale (RCAR-IIWPG dynamic evaluation protocol, 2008) 130
Table 17 CFC filter classes used for the RCAR-IIWPG dynamic rating (RCAR-IIWPG dynamic evaluation protocol, 2008) 131
Table 18 HRMD backset and height measurements summary for the head restraint geometry assessment of seat type #1 134
Table 19 HRMD backset and height measurements summary for the head restraint geometry assessment of seat type #2 134
Table 20 HRMD backset and height measurements summary for the head restraint geometry assessment of seat type #3 135
Table 21 Head restraint geometry assessment scores of each seat type 135

Table 22 HRMD backset and height measurements summary for the worst case assessment of seat type #1 136
Table 23 HRMD backset and height measurements summary for the worst case assessment of seat type #2 136
Table 24 HRMD backset and height measurements summary for the worst case assessment of seat type #3 137
Table 25 Worst case assessment scores of each seat type 137
Table 26 Dynamic test results of seat type #1 138
Table 27 Dynamic test results of seat type #2 139
Table 28 Dynamic test results of seat type #3 140
Table 29 Overall Euro NCAP rating of each tested seat type..... 141
Table 30 BioRID backset distances recorded prior to each test 141
Table 31 Seatback deflections in each test 142
Table 32 Head restraint static rating of each seat type 144
Table 33 Neck force classification of each seat type..... 144
Table 34 Dynamic rating of each seat type..... 145
Table 35 Overall RCAR-IIWPG rating of each seat type..... 145

LIST OF FIGURES

FIGURES

Figure 1 Hyperextension of the cervical spine (Svensson, et al., 2000) 3
Figure 2 Backset and height (Chapline, et al., 2000) 4
Figure 3 GB Patent No. 2301906 and US Patent Nos. 6088640, 2006186713, and 2008042477 8
Figure 4 US Patent Nos. 6017086, and 6149232 9
Figure 5 US Patent No. 2002195846 9
Figure 6 US Patent No. 2005280304 10
Figure 7 WO Patent No. 0050258 11
Figure 8 GB Patent No. 2395114 12
Figure 9 GB Patent No. 2403137 13
Figure 10 EP Patent No. 1842717 14
Figure 11 US Patent No. 2008129092 14
Figure 12 US Patent No. 2004061362 15
Figure 13 GB Patent No. 2311212 16
Figure 14 An alternative embodiment in GB Patent No. 2311212 16
Figure 15 The force limiter of the design of GB Patent No. 2311212 17
Figure 16 EP Patent No. 1084901 18
Figure 17 US Patent No. 6179379 18
Figure 18 An alternative embodiment in US Patent No. 6179379 19
Figure 19 EP Patent No. 1551664 and US Patent No. 2005253408 20
Figure 20 The seat apparatus devised in EP Patent No. 1551664 and US Patent No. 2005253408 20
Figure 21 The invention in GB Patent No. 2354936 in an initial position 21
Figure 22 The catch mechanism used in GB Patent No. 2354936 21
Figure 23 The invention in GB Patent No. 2354936 after a crash 22
Figure 24 GB Patent No. 2359482 22
Figure 25 US Patent Nos. 6435591 and 2001011830 23
Figure 26 WO Patent No. 9204847 and US Patent Nos. 5181763, and 5290091 24
Figure 27 US Patent No. 5580124 25
Figure 28 WO Patent No. 9743142 25
Figure 29 WO Patent No. 0156830 26
Figure 30 WO Patent No. 9511818 26
Figure 31 US Patent No. 2003001413 27
Figure 32 US Patent No. 2002014760 28
Figure 33 US Patent No. 2004075252 29

Figure 34 US Patent No. 2008073886 29
Figure 35 US Patent No. 2007158933 30
Figure 36 US Patent No. 5833312 30
Figure 37 US Patent No. 2004070239 31
Figure 38 CA Patent No. 1273375 32
Figure 39 US Patent Nos. 2002056980 and 2002180197 32
Figure 40 US Patent No. 3643972 33
Figure 41 US Patent No. 3151911 34
Figure 42 US Patent No. 3222084 34
Figure 43 US Patent No. 2007241594 35
Figure 44 GB Patent No. 1348239 36
Figure 45 GB Patent No. 2296855 37
Figure 46 WO Patent No. 9818356 37
Figure 47 US Patent No. 2007209667 38
Figure 48 Chalmers seat (Deter, et al., 2007) 40
Figure 49 The simplified standard seat model 40
Figure 50 The nominal stress strain plot of the foam (Tabiei, et al., 2007) 42
Figure 51 The pivot point of the seatback (Stahlschmidt, et al., 2006a) 42
Figure 52 Low, medium and high severity Euro NCAP sled pulses (Van Ratingen, et al., 2009) 44
Figure 53 Head x-acceleration [g] vs. time [ms] (Stahlschmitd, et al., 2006b) 45
Figure 54 T1 x-acceleration [g] vs. time [ms] (Stahlschmitd, et al., 2006b) 45
Figure 55 NIC vs. time calculated with the results given by Stahlschmitd, et al., (2006b) 46
Figure 56 The test set-up of Yuen, et al. (2004) 47
Figure 57 The sled pulse used by Yuen, et al. (2004) to simulate a rear crash where whiplash may occur 47
Figure 58 The NIC curve obtained by Yuen, et al. (2004) 48
Figure 59 Head x-acceleration vs. time result obtained with the developed model when the same acceleration pulse with that of Stahlschmitd, et al., (2006b) is used 48
Figure 60 T1 x-acceleration vs. time result obtained with the developed model when the same acceleration pulse with that of Stahlschmitd, et al., (2006b) is used 49
Figure 61 NIC vs. time result obtained with the developed model when the same acceleration pulse with that of Stahlschmitd, et al., (2006b) is used 49
Figure 62 NIC vs. time result obtained with the developed model when the same acceleration pulse with that of Yuen, et al. (2004) is used 50
Figure 63 A sketch of the slidable vehicle seat and the horizontal anti-whiplash seat suspension arrangement (a) during normal driving and (b) during crash. .. 56

Figure 64 A general view of the finite element model of the conceptual slidable vehicle seat and the BioRID II dummy 57
Figure 65 A view showing the details of the suspension arrangement used in the finite element model 57
Figure 66 NIC_{max} vs. the seat's maximum sliding distance, d (F_b=320 N, b=59 mm) . 59
Figure 67 Front perspective view of the vehicle seat mechanism 66
Figure 68 Rear perspective view of the vehicle seat mechanism 67
Figure 69 Perspective view of the lower assembly 68
Figure 70 Right side view of the lower assembly before accident 69
Figure 71 Right side view of the lower assembly after accident 70
Figure 72 Perspective view of the upper assembly 71
Figure 73 Right side view of the upper assembly before accident (A) and after accident (B) 72
Figure 74 Detailed front view of the trigger lock 73
Figure 75 View of the trigger lock holding the upper assembly in its nominal position under normal driving conditions 73
Figure 76 View of the trigger lock at the moment when it is released by the Bowden cable after the lower assembly moves backwards 74
Figure 77 View of the trigger lock after the released upper assembly is rotated forward by the headrest springs 74
Figure 78 Detailed front view of the alternative secondary lock 77
Figure 79 Front perspective view of the alternative secondary lock 77
Figure 80 View of the alternative secondary lock at its nominal configuration under normal driving conditions 78
Figure 81 View of the alternative secondary lock at the moment when the trigger lock is released by the Bowden cable after the lower assembly rotates backwards 78
Figure 82 View of the alternative secondary lock after the released upper assembly is rotated forward by the headrest springs 79
Figure 83 View wherein the alternative secondary lock locks the upper assembly at its frontmost position brought by the headrest springs 79
Figure 84 A quick return mechanisms 81
Figure 85 Perspective view of a vehicle seat with a quick forward mechanism 83
Figure 86 Detailed perspective view of the lower assembly 84
Figure 87 Detailed perspective view of the upper assembly 84
Figure 88 Left view of the seat before (A) and after (B) the crash, describing the working principle of the mechanism 85
Figure 89 Kinematic sketch of the quick forward anti-whiplash mechanism 87
Figure 90 θ_{13} vs. θ_{12} during the full cycle of the mechanism 89
Figure 91 s_{32} vs. θ_{12} during the full cycle of the mechanism 89
Figure 92 θ_{13} vs. θ_{12} in the working range of the mechanism 90

Figure 93 s_{32} vs. θ_{12} in the working range of the mechanism 90
Figure 94 A general view of the test facility (METU-BILTIR Center, 2013)..... 92
Figure 95 General flow chart of the Euro NCAP whiplash tests 93
Figure 96 Euro NCAP whiplash test sample 94
Figure 97 Origin of the coordinate system used 95
Figure 98 A general view of the seat and the dummy prior to test 96
Figure 99 Generic seat belt anchorage mounting (Euro NCAP whiplash testing protocol, 2011)..... 97
Figure 100 Seat belt anchorage fixture set-up 98
Figure 101 Use of HPM and HRMD 100
Figure 102 Torso angle measurement..... 102
Figure 103 H-point measurement with CMM 102
Figure 104 HRMD backset..... 103
Figure 105 HRMD height 103
Figure 106 The dummy weights used during the iteration of the parameters of the electronic control unit of the sled's accelerator for each pulse severity.. 105
Figure 107 The target sled pulse obtained for each test severity 105
Figure 108 Measurement foil application for determining the head restraint contact starting and ending times 108
Figure 109 Sled acceleration signals attained during the low severity tests of each seat type together with the associated target pulse..... 109
Figure 110 Sled acceleration signals attained during the medium severity tests of each seat type together with the associated target pulse 109
Figure 111 Sled acceleration signals attained during the high severity tests of each seat type together with the associated target pulse..... 110
Figure 112 Left side view of the dummy and seat prior to the test of the seat #2.3 .. 111
Figure 113 Front view of the dummy and seat prior to the test of the seat #2.3..... 111
Figure 114 Right side view of the dummy and seat prior to the test of the seat #2.3 112
Figure 115 Left side view of the dummy and seat after the test of the seat #2.3..... 112
Figure 116 Front view of the dummy and seat after the test of the seat #2.3 113
Figure 117 Right side view of the dummy and seat after the test of the seat #2.3..... 114
Figure 118 Required video tracking measurements (Euro NCAP whiplash testing protocol, 2011)..... 114
Figure 119 The response of the dummy in the low severity pulse test of the seat type #2 at (a) t =0 ms, (b) t= 25 ms, (c) t =50 ms, (d) t = 75 ms, (e) t = 100 ms, (f) t = 125 ms, (g) t= 150 ms, (h) t = 175 ms, (i) t = 200 ms, (j) t = 225 ms, (k) t = 250 ms, (l) t = 275 ms, (m) t = 300 ms 115
Figure 120 Required film target application to the sled, seat and dummy (Euro NCAP whiplash testing protocol, 2011)..... 125
Figure 121 RCAR-IIWPG head restraint rating scale (RCAR static evaluation protocol, 2008)..... 127

Figure 122 RCAR-IIWPG neck force classification scale (RCAR-IIWPG dynamic evaluation protocol, 2008).....130

LIST OF SYMBOLS AND ABBREVIATIONS

A_{mean}	Mean acceleration
ANCAP	Australasian New Car Assessment Program
b	Backset distance
c	Damping coefficient of the anti-whiplash seat suspension damper
CFC	Channel frequency class
CL	Capping limit
CMM	Coordinate measuring machine
d	Maximum sliding distance of the seat
dV	Velocity change
Euro NCAP	European New Car Assessment Program
F_b	Initial bias force of the anti-whiplash seat suspension spring
F_x	Upper neck shear force
F_z	Upper neck tension force
HPL	Higher performance limit
HPM	H-point manikin
HRMD	Head restraint measuring device
IIHS	Insurance Institute for Highway Safety
IIWPG	International Insurance Whiplash Prevention Group
JNCAP	Japan New Car Assessment Program
k	Stiffness of the anti-whiplash seat suspension spring
LPL	Lower performance limit
NIC	Neck Injury Criterion
RCAR	Research Council for Automobile Repairs
SRA	Swedish Road Administration
T1	Horizontal acceleration of the first thoracic vertebrae
T-HRC	Starting time of the contact of the head of the dummy with the head restraint
$T\text{-}HRC_{(end)}$	Ending time of the contact of the head of the dummy with the head restraint
$V_{rebound}$	Head rebound velocity
θ_{12}	Joint variable of the lower assembly of the quick forward anti-whiplash mechanism
θ_{13}	Joint variable of the upper assembly of the quick forward anti-whiplash mechanism

CHAPTER 1

INTRODUCTION

This chapter is devoted to introduce the definition and importance of whiplash injury. Based on a review of the related existing literature, the main factors that are affecting the likelihood of the injury occurrence and a summary of the basic guidelines for injury preventive design of vehicle seats are given in the following sections. The objective and scope of this thesis are also stated.

1.1 Motivation

Whiplash syndrome, which refers to neck injuries, although not life-threatening, is one of the most important types of injury when its longtime effects are considered (Jakobsson, Lundell, Norin, & Isaksson-Hellman, 2000). Neck and shoulder pains, headache, upper limb numbness, dizziness, vision blur, and tinnitus are the characteristic symptoms of this disorder that are enumerated by Bogduk (1986) (as cited in Minton, Murray, Stephenson, & Galasko, 2000). In some cases, these complaints may continue for long periods of time and become chronic (Olivegren, Jerkvall, Hagström, & Carlsson, 1999). Apart from being a health problem with long-lasting pain and disorder, whiplash becomes also more and more a serious socio-economic problem due to the increasing labor force losses and treatment costs in recent years (Cholewicki, et al., 1998).

These injuries are frequently seen in motor vehicle crashes; especially in low-speed rear-end collisions (Deans, McGalliard, & Rutherford, 1976; Hohl, 1990; Sturzenegger, DiStefano, Radanov, & Schnidrig, 1994, as cited in Hartling, Pickett, & Brison, 2002). Annually there are about 13 million car crashes worldwide and more or less 1 million of these result in whiplash injuries (Güzel, et al., 2000). As a result, this type of injuries, constituting half of all traffic injuries resulted in sustained consequences (Von Koch, Nygren, & Tingvall, 1994, as cited in Linder, 2000), makes

some precautions necessary for vehicle seat design (Krafft, Kullgren, Tingvall, Boström, & Fredriksson, 2000).

1.2 Occupant Motion during a Rear Crash and the Injury Mechanism

For a better understanding of whiplash phenomenon, it is required to examine the general nature of the motion of the occupant during rear crash. Motion of an occupant during a rear-end collision can be examined in the following four phases (Sendur, Thibodeau, Burge, & Tencer, 2005):

- Retraction phase
- Extension phase
- Rebound phase
- Protraction phase

When the vehicle is struck from behind, the occupant's upper torso resting on the seatback is forced forwards, whilst the occupant's head lags behind the torso and almost remains stationary due to its inertia. Thus, the upper cervical spine is brought into flexion, and the lower cervical spine into extension, resulting in an S-like shape of the cervical spine. This first phase of motion is called the retraction phase.

When the maximum retraction of the head is reached, i.e., the maximum rearward linear displacement of the head relative to the torso is reached, the extension phase begins wherein the head starts rotating backwards. As this happens, the upper cervical spine is also brought from flexion into extension as well as the lower cervical spine, and hence, the neck goes into hyperextension as shown in Figure 1.

Next comes the rebound phase. In this phase, the head contacts and rebounds from the headrest, leading to the highest translational accelerations of the head in addition to peak axial and shear forces.

After rebound, when differential motion between the head and torso is reversed, that is the direction of the motion of the head relative to the torso is reversed, the protraction phase arises. The importance of this phase increases dramatically when the seat belt stops the forward motion of the upper torso.

Unfortunately, the exact injury mechanism has not been completely revealed yet (Chen, Yang, & Wang, 2009; Maher, 2000; Panjabi, et al., 1998; Viano, & Gargan, 1996; Welcher, & Szabo, 2001; Yoganandan, Pintar, & Gennarelli, 2002). However, the main underlying cause is generally accepted to be the severe hyperextension of the cervical spine (Bring, & Westman, 1991; Watanabe, et al.,

2000). Limiting the motion of the neck during a rear impact is believed to significantly decrease the injury risk (Sekizuka, 1998; Young, Ragel, Su, Mann, & Frank, 2005).

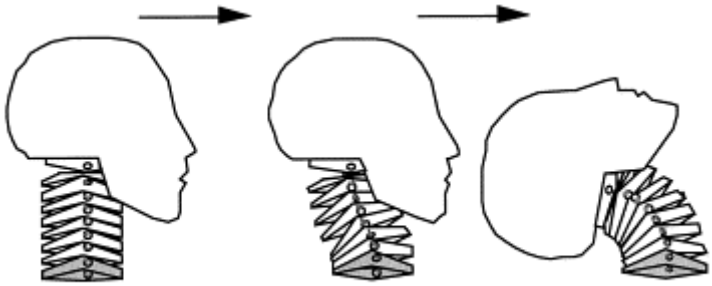

Figure 1 Hyperextension of the cervical spine (Svensson, et al., 2000)

1.3 Influence of Different Factors Regarding Vehicle Seat Design on Whiplash Injury Risk

Whiplash injuries are characteristically seen in low-speed rear crashes (Croft, 1996). For instance, a report compiling the German traffic accident data revealed that over 90 % of whiplash injuries in rear impact collisions occur at velocity changes less than 25 km/h (Eichberger, Geigl, Moser, Fachbach, & Steffan, 1996, as cited in Watanabe, et al., 2000).

The risk of whiplash injury is primarily related to the seat characteristics. One of the most important characteristics is the horizontal distance between the head and headrest or, as commonly known, backset (Figure 2). Olsson, et al. (1990) studied the rear-end collisions experienced by the Volvo cars and found out that backsets greater than 100 mm surely result in whiplash symptoms lasting more than a year (as cited in Minton, et al., 2000). In another study, Stemper, Yoganandan, & Pintar (2006) suggested that reducing the backset to a value less than 60 mm, passively or actively immediately after an impact, may eliminate the injury risk. Others also drew similar conclusions (Chapline, Ferguson, Lillis, Lund, & Williams, 2000; Eriksson, 2005; Farmer, Wells, & Lund, 2003; Göçmen, 2009; Ivancic, Sha, & Panjabi, 2009; Sendur, et al., 2005; Siegmund, Heinrichs, & Wheeler, 1999; Svensson, Lövsund, Haland, & Larsson, 1996; Viano, 2008).

For a complete description of the position of the headrest, the vertical distance between the top of the head restraint and the top of the head (Figure 2) should be considered as well (Chapline, et al., 2000; Eriksson, 2005; Farmer, Wells, & Lund, 2003; Göçmen, 2009; Siegmund, et al., 1999; Viano, 2008).

Some researchers, on the other hand, have proposed that the deformation of the seatback to absorb some of the crash energy in a low severity rear-impact should also be considered to prevent whiplash (Martinez, 1968; Parkin, Mackay, Hassan, & Graham, 1995, as cited in Maher, 2000). Raking characteristics of the seatback have been also found influential on the injury outcome (Golinski, & Gentle, 2001; Shin, Park, & Park, 2003; Svensson, et al., 1996; Viano, 2003a, c, 2008; Watanabe, et al., 2000)

However, Welcher & Szabo (2001) have revealed that the seatback constitutive properties such as stiffness and energy absorption are not as effective on the likelihood of the injury as the horizontal and vertical head-to-headrest distances. Similarly, backset and height were reported to be much more effectual on injury potential than the stiffness and energy absorbing of the seat foam (Szabo, Voss, & Welcher, 2003).

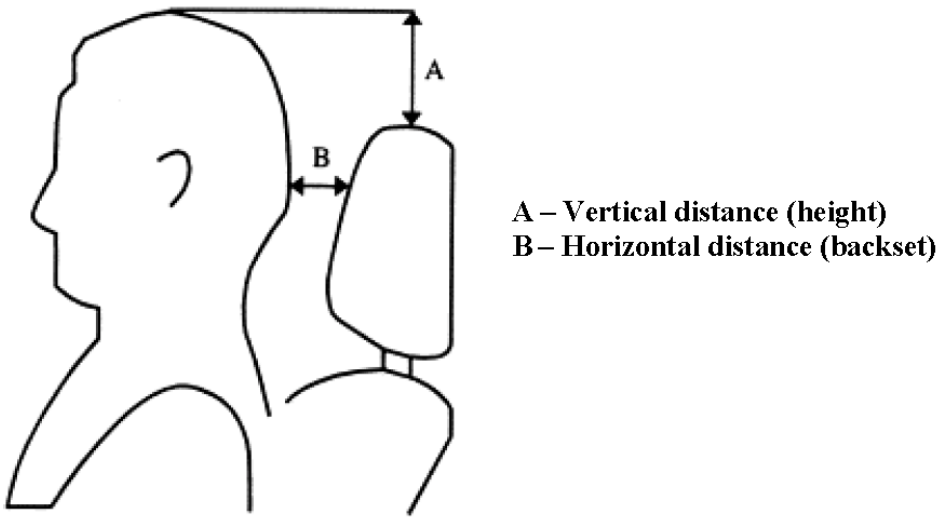

Figure 2 Backset and height (Chapline, et al., 2000)

Other than seat characteristics, gender-specific differences (Bring, Björnstig, & Westman, 1996; Viano, 2003b), occupant age (Farmer, Wells, & Werner, 1999), vehicle age (McCreesh, Arthurs, Horgan, Keane, & Meagher, 2012), awareness of the imminent crash (Kumar, Narayan, & Amell, 2000), vehicle stiffness (Sendur, et al., 2005), and variations in the crash pulse (Krafft, et al., 2000; Krafft, Kullgren, Ydenius, & Tingvall, 2002) have been also thought to have a role in the injury risk.

A seat design for avoiding whiplash injuries should ensure reduced occupant acceleration, minimum change in the curvature of the spine of the occupant, and decreased forward rebound of the occupant into the seat belt (Jakobsson, et al., 2000).

1.4 Objective and Scope of the Thesis

In this thesis, it is aimed to analyze the whiplash syndrome in low-speed rear-end impacts and develop a novel anti-whiplash vehicle seat mechanism that reduces the risk of whiplash injuries.

With this purpose, an overview of the current state of the art of the available anti-whiplash system patents is presented in Chapter 2. A classification of these systems is also given based on their working principles. Chapter 3 introduces a simplified finite element model for a standard vehicle seat. This model is developed for the preliminary evaluation of the functional design alternatives. Chapter 4 discusses two different design alternatives, namely the backset reducing design and the slidable seat concept. Chapter 5 proposes two novel anti-whiplash vehicle seat mechanisms. Both systems proposed in this chapter rely on the reduced backset principle.

For the assessment of one of the developed systems, namely the quick forward anti-whiplash vehicle seat mechanism, a series of sled tests is performed at the Vehicle Safety Unit of the METU-BILTIR Center, Ankara, Turkey as described in Chapter 6. Chapter 7 focuses on the Euro NCAP and the RCAR-IIWPG whiplash assessment systems, respectively. The ratings of the tested seats according to both of these evaluation systems are presented in Chapter 8. Finally, Chapter 9 outlines a summary of the thesis, discusses the findings of the conducted simulations and tests and suggests some recommendations for future work.

CHAPTER 2

CLASSIFICATION OF ANTI-WHIPLASH SYSTEMS: A PATENT SURVEY

This chapter presents a detailed patent survey of various anti-whiplash systems. Almost 50 patents are checked and classified into the following main groups according to their basic working principles:

- Systems where the head restraint is moved forward by an electrical control system
- Systems where the head restraint is moved forward by a mechanical trigger mechanism
- Systems where the backrest moves
- Systems where the entire seat moves
- Special-shaped backrest and head restraint designs made of special materials
- Air-bagged head restraints
- Other headrest forms
- Helmet and collar designs

These are explained in detail in the following sections.

2.1 Systems where the Head Restraint is Moved Forward by an Electrical Control System

Systems covered in this category have a control unit which can sense rear-end crash impacts and move the head restraint forward for the purpose of decreasing the distance between the head and head restraint.

GB Patent No. 2301906 and US Patent Nos. 6088640, 2006186713, and 2008042477 propose a system with a crash anticipatory sensor for rear impacts (Figure 3). When a rear crash is predicted, with the aid of sensors which determine the location of the occupant's head with respect to the headrest, servo motors 374 and 375

are driven by the control unit in order to move the headrest in the vertical and horizontal directions, respectively, as required to catch and support the occupant's head.

US Patent No. 6017086 teaches an anti-whiplash system where a pyrotechnic actuator 36 is activated by a crash acceleration sensor in order to push the displacement element 28 in the transverse direction of the seat (Figure 4). In this manner, the headrest-carrying elements 44 are forced to slide in the guide slots 40, causing the head restraint to move forward. The retaining curved end portions 50 of the respective slots 40 provide a stop and serve as a locking means for the head restraint at this limit position. US Patent No. 6149232 uses a very similar mechanism, with the only exception that electromagnetic or electromechanical means are preferred instead of a pyrotechnic actuator.

In the system suggested by US Patent No. 2002195846 there is a gas actuator 30 that is to be operated when an acceleration sensor measures an acceleration above a predetermined threshold value (Figure 5). This actuator moves the rod 43 forward while the pin 17 fixed to the rod 43 slides upwards along the guide slot 16a of the bracket 16 welded to the headrest frame 13, and thus the headrest frame 13 and the headrest 2 are pushed to rotate forwards around the shafts 14. To prevent malfunction of the gas actuator 30 due to a possible backwards motion of the rod 43 under forces applied to the headrest by the occupant, a ratchet-gear coupling is formed on this rod and its cylindrical case.

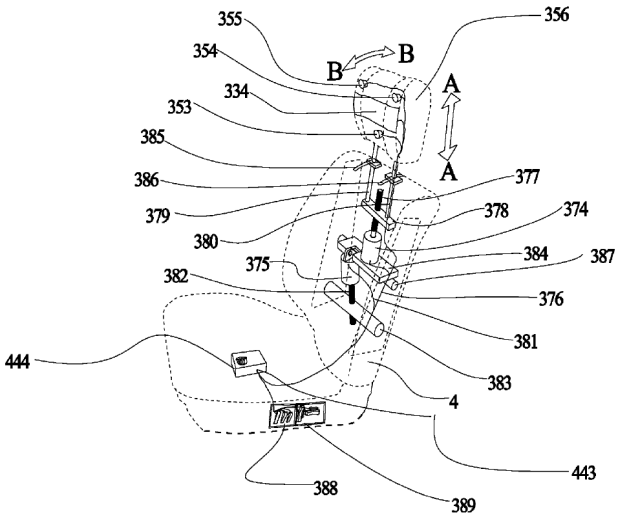

Figure 3 GB Patent No. 2301906 and US Patent Nos. 6088640, 2006186713, and 2008042477

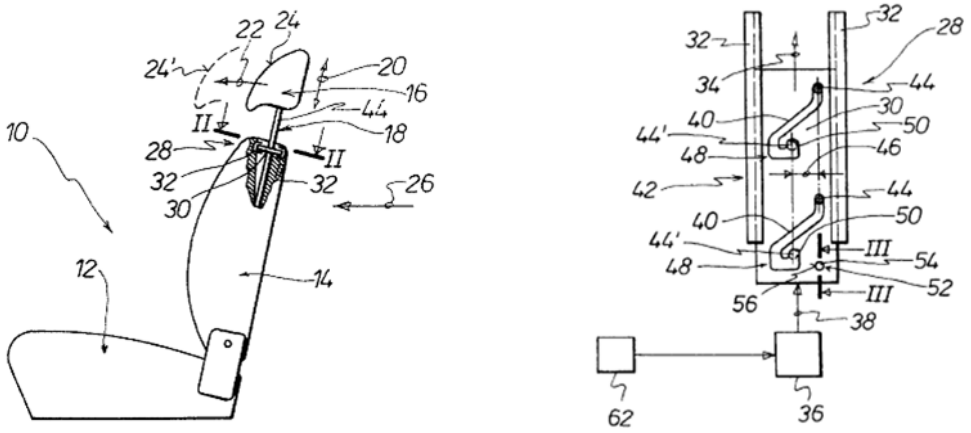

Figure 4 US Patent Nos. 6017086, and 6149232

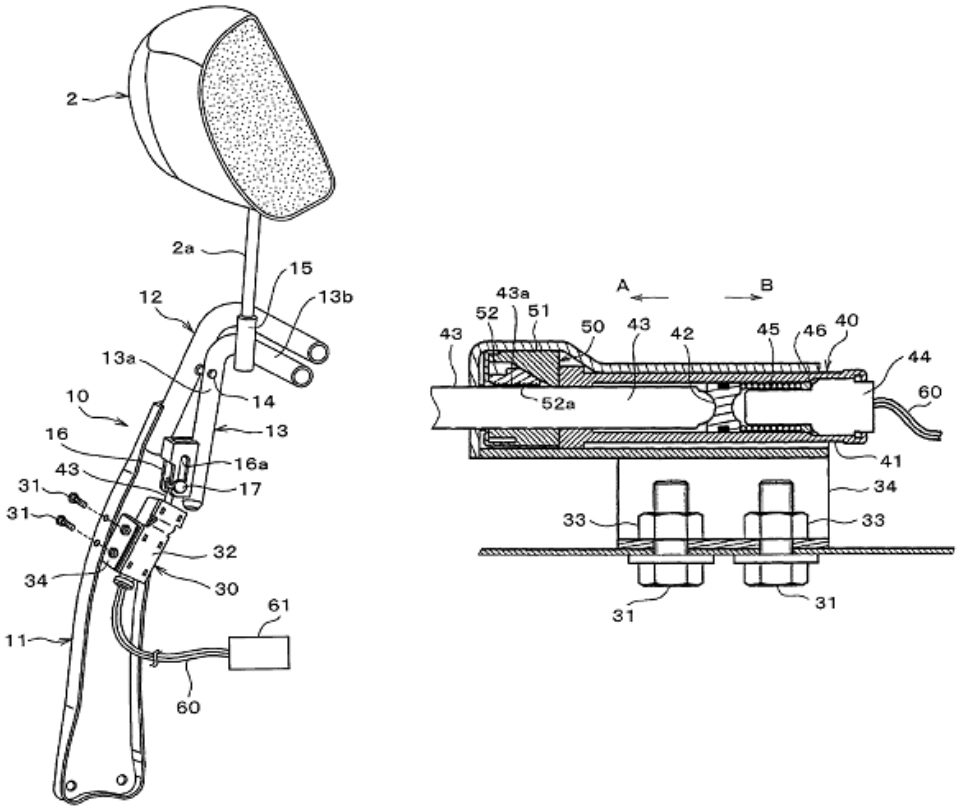

Figure 5 US Patent No. 2002195846

US Patent No. 2005280304 provides a two-piece head restraint assembly (Figure 6). When a collision impact is predicted or sensed by a sensor 92, an actuator 39 moves the front head support portion first vertically along path P1 through the first moving mechanism and then horizontally along path P2 through the second moving mechanism. A number of proximity sensors 60 may also be placed on the front portion so that the actuator 39 can be stopped when the head restraint becomes close enough to the head of the occupant for a safe support.

Yet another design where a bipartite head restraint is applied is WO Patent No. 0050258 (Figure 7). In the case of a rear impact collision, the sensor arrangement 15 senses this event and operates the Bowden cable 14 in order to unlock the lock 8. Hence, the spring 21 is released, causing the front portion of the head restraint to go forward. In the meantime, air is filled into the resilient concertina tube 22 through one-way valves 24 with the intention of obstructing the rearward motion of the head restraint.

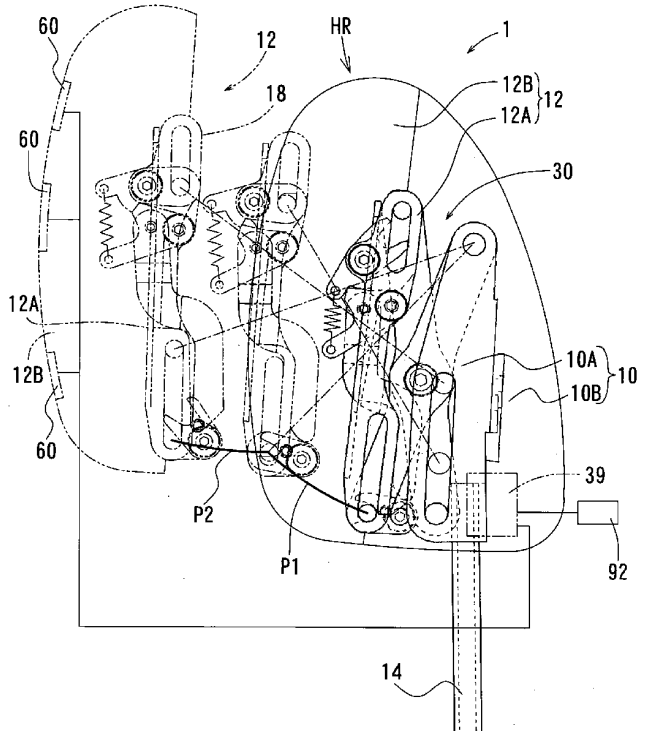

Figure 6 US Patent No. 2005280304

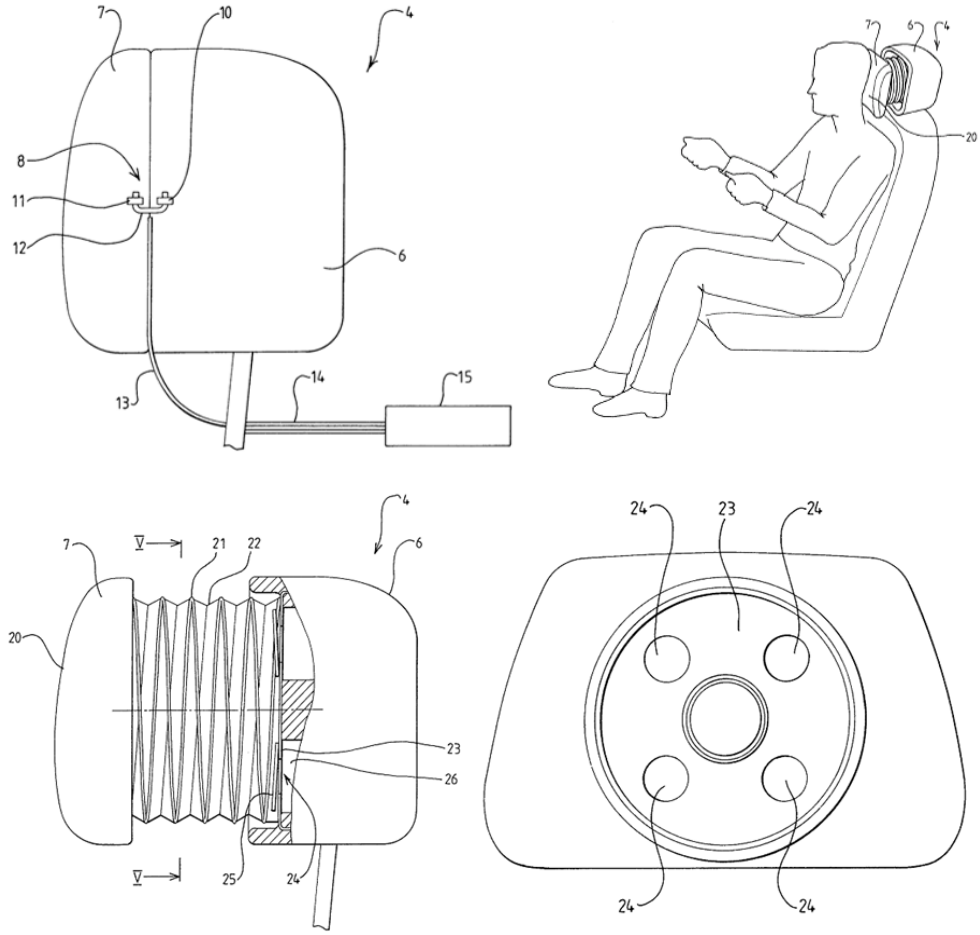

Figure 7 WO Patent No. 0050258

2.2 Systems where the Head Restraint is Moved Forward by a Mechanical Trigger Mechanism

From the point of working principle, patents classified under this group are pendulum-like systems. In these patents, head restraint is directly connected to a moving mechanism within the backrest.

GB Patent No. 2395114 recommends a spring-biased forwardly moving headrest to give a support to the head of the occupant (Figure 8). In a rear crash, the rod 11, due to its inertia, rotates rearward into engagement with the catch 24. The

occupant loading on the seatback moves the rod 11 upward, causing the catch 24 to disengage from the abutment face 23 and the plate 21 to free to rotate about the axis 20. Accordingly, the plate 16 mounting the headrest 2 starts rotating about the axis 15 with the aid of the biased spring 28 and hence moves forward. A prominent feature of this design is that the system is to be only activated in a rear-end collision and when the seat is occupied.

In the GB Patent No. 2403137, a very simple but efficient solution is described (Figure 9). When a rear-end crash has occurred to the vehicle, the force plate 18 is moved backwards by the occupant applying force to the seatback so that the portions 16, 17 of the link 16, 17, 19, 20, 21, 22 lying between the said force plate and the head restraint 4 start a backward movement along the guides 14, 15 and the head restraint pivots forward about the surface 13 on the base 12 while the portions 21, 22 of the said link deform to absorb some of the transmitted impact energy.

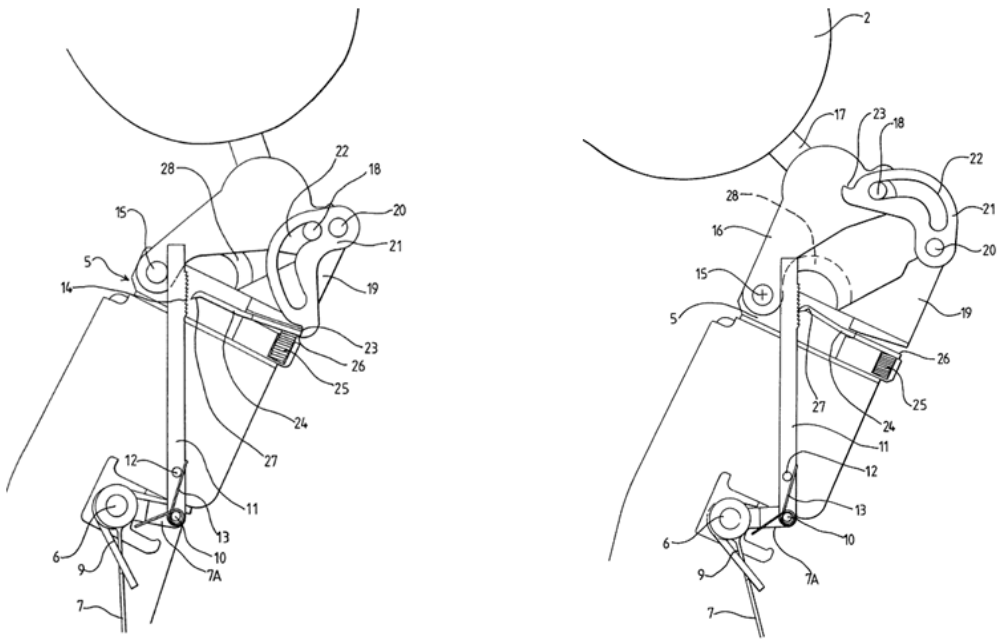

Figure 8 GB Patent No. 2395114

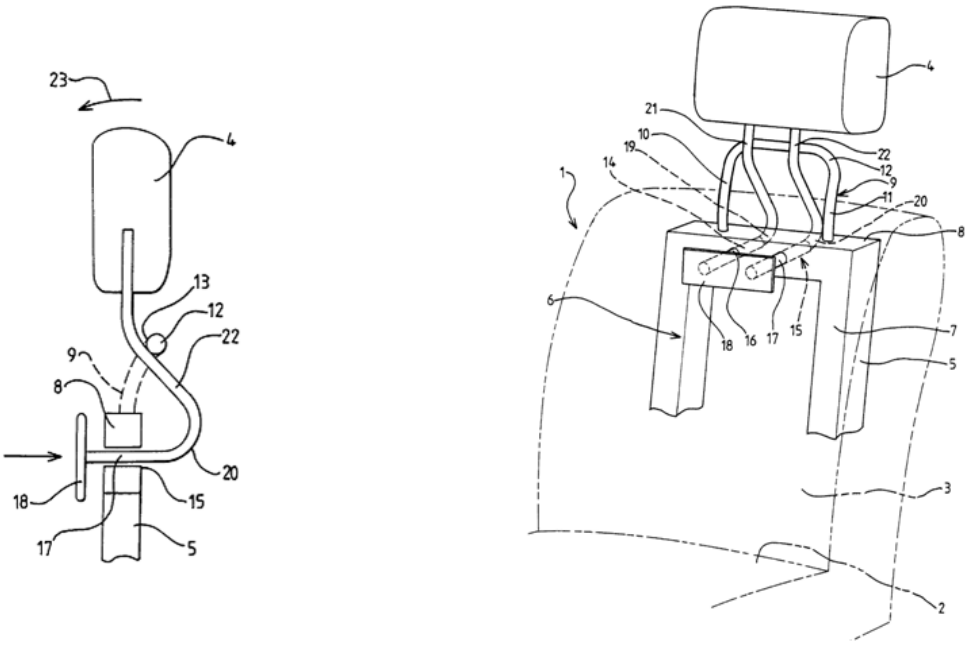

Figure 9 GB Patent No. 2403137

EP Patent No. 1842717 involves a force plate 31 attached to the seat springs 34(A), 34(B) and a mechanism that transmits the backward motion of the said force plate and the said seat spring under occupant loading on the backrest happened during rear crash to the headrest, causing it to move forward (Figure 10). A similar system is proposed by US Patent No. 2008129092 (Figure 11).

Finally, in the system protected by US Patent No. 2004061362, when the vehicle is struck from behind, the head restraint is moved forward by a swinging block mechanism incorporated within the seatback to reduce the backset (Figure 12). The headrest moving mechanism is driven by the force being applied on the seatback by the occupant.

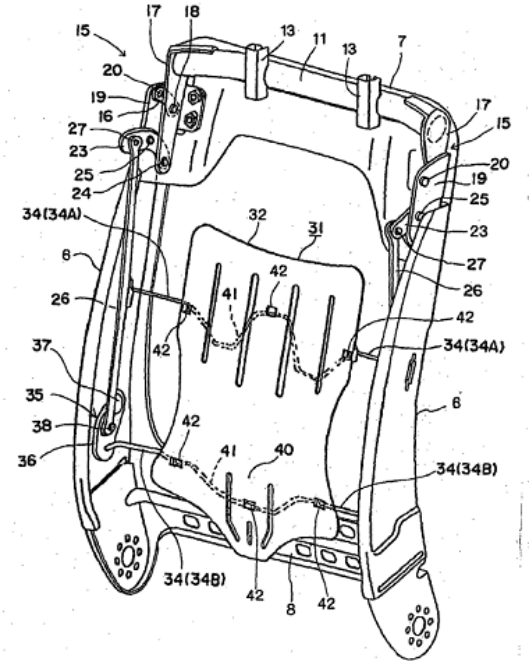

Figure 10 EP Patent No. 1842717

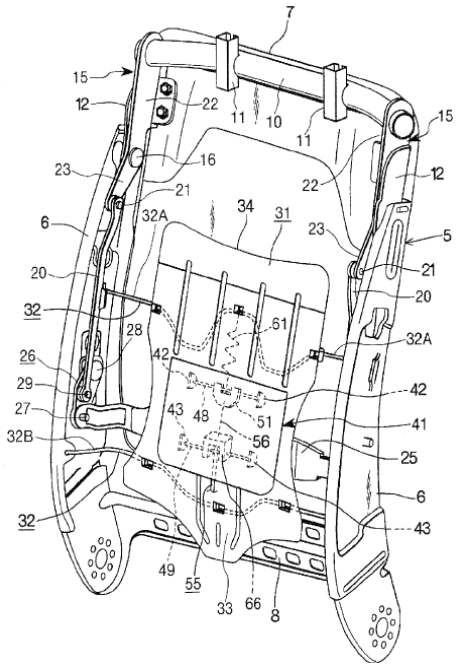

Figure 11 US Patent No. 2008129092

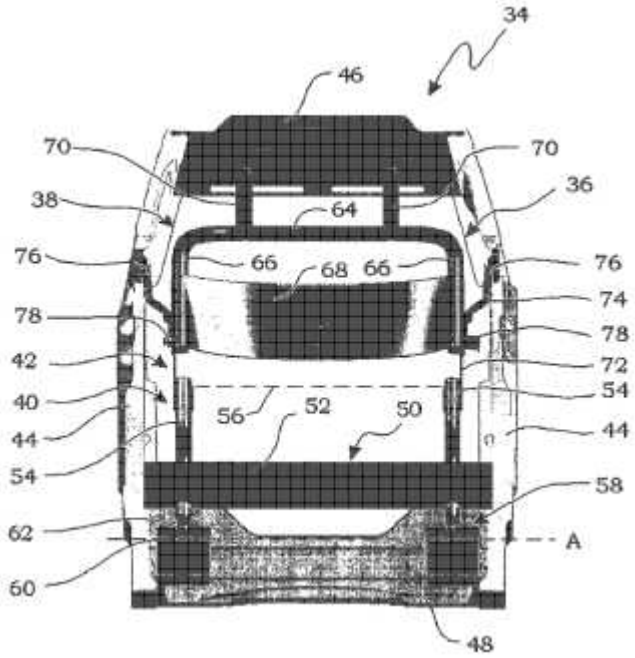

Figure 12 US Patent No. 2004061362

2.3 Systems where the Backrest Moves

One of the patents in this category is GB Patent No. 2311212 wherein the backrest 5, due to the force being applied onto it by the occupant during rear crash, entirely rotates rearward against a force limiter 7 which presents a relatively low resistance over a distance of d_1 and a relatively high resistance over a distance of d_2 (Figure 13). A stop limit 8 is provided to limit this movement after a total distance of d_1+d_2 is travelled by the backrest. In an alternative design of this patent, it is thought to slide the backrest 5' backwards instead of rotating (Figure 14). Figure 15 shows a force limiter 7, in the form of a piston-cylinder arrangement. The force limiter7 comprises a cylinder 60 being provided with two outlet orifices 61, 62 and filled with a compressible material 64 such as lead or plastic, and a piston 63 being attached to the backrest and inserted into the said cylinder. As the backrest moves backward, the piston moves along the cylinder. Initially, both orifices are open to eject the compressible material. However, after the piston moves a distance corresponding to the distance, d_1, travelled by the backrest, the piston passes the orifice 62; thus there

remains only the orifice 61 available for ejection and, hence, the force that has to be applied to the piston to move it within the cylinder is increased considerably throughout the distance the piston moves hereafter, which corresponds to the distance, d_2, travelled by the backrest.

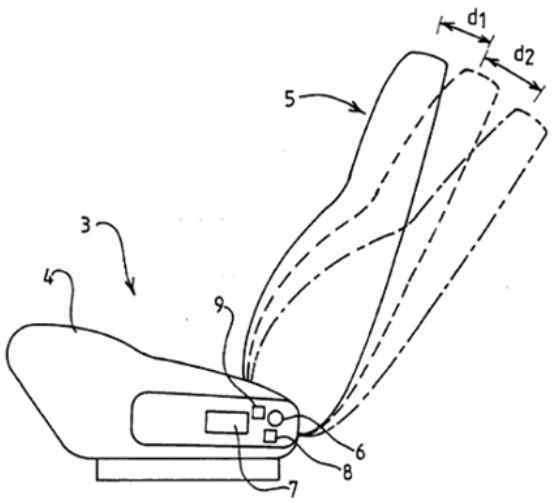

Figure 13 GB Patent No. 2311212

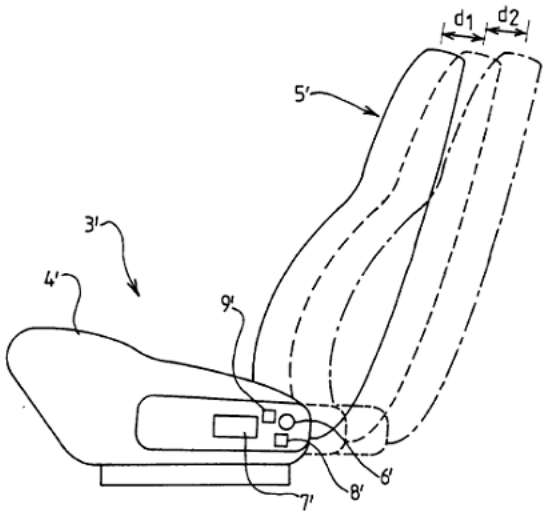

Figure 14 An alternative embodiment in GB Patent No. 2311212

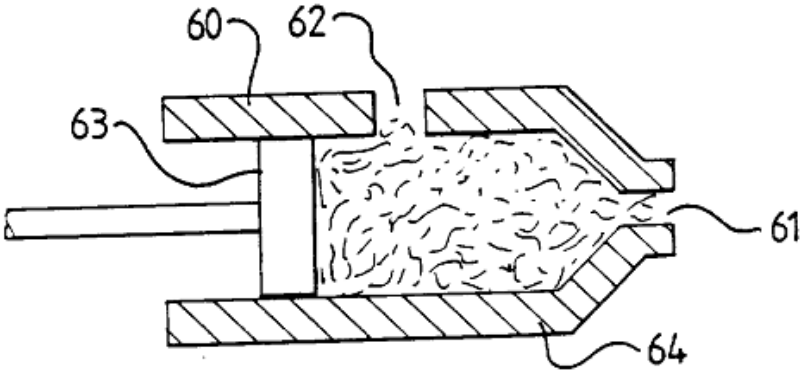

Figure 15 The force limiter of the design of GB Patent No. 2311212

The design taught in the EP Patent No. 1084901 basically relies on an idea that the entire seatback 3 rotates by virtue of the force applied on it by the occupant in the event of a rear-end accident about its instantaneous center which is indeed located above the point of application of the force, and thereby the headrest 4 moves forward and upward (Figure 16). For this purpose, there is constructed a seatback supporting mechanism 5 which moves the instantaneous center of the seatback 3 forward and upward while the seatback 3 rotates.

The last patent in this category, US Patent No. 6179379 proposes a seatback recliner mechanism 8 provided with an arm 10 (Figure 17). In the normal use of the recliner mechanism 8, the arm 10 rotates together with the seatback 4. But, besides this, the recliner mechanism 8 also embodies a mechanism allowing the seatback 4 to rotate rearward with the substantial force applied thereto by the occupant of the seat as a result of rear-end collision without the recliner mechanism 8 being operated manually. Meanwhile, the arm 10 remains unmoving, causing the link 12 to pivot about its pivot point 13. Hence, the link 14 is forced to move upwardly, and because of the curved shape of the link 14 and the presence of the guiding rollers 15, 16, the head restraint 5 undergoes a forward and upward movement with respect to the seatback 4 in the direction 21. Figure 18 illustrates another alternative embodiment of the invention where a four-link mechanism is used, the support plate 106 being the fixed link.

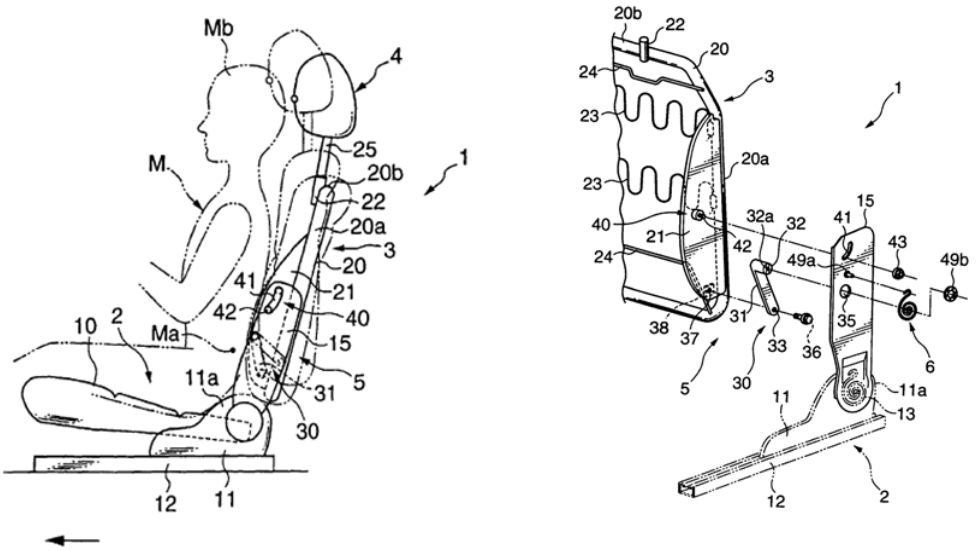

Figure 16 EP Patent No. 1084901

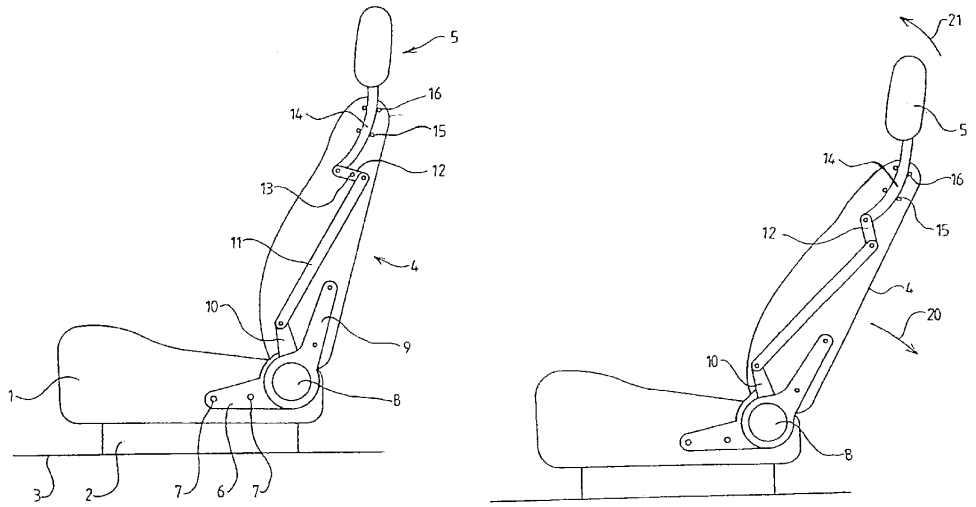

Figure 17 US Patent No. 6179379

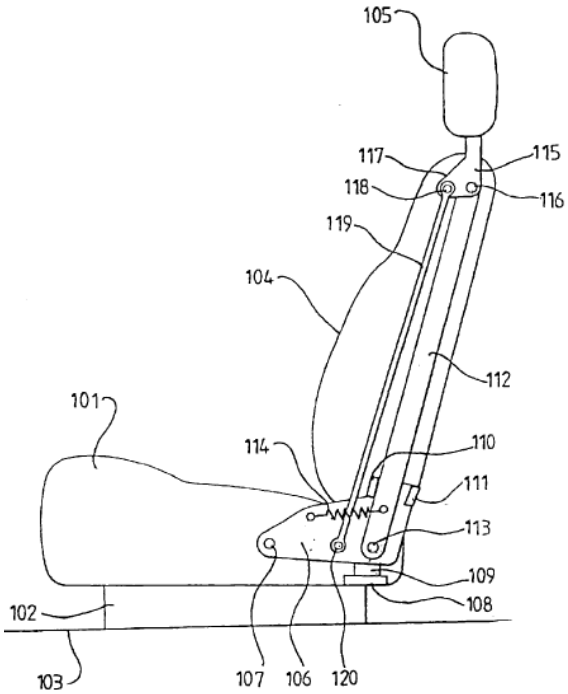

Figure 18 An alternative embodiment in US Patent No. 6179379

2.4 Systems where the Entire Seat Moves

Patents in this group consider that backward translational motion or rearward rotation of the entire seat during a rear crash situation may decrease the risk of whiplash injuries.

In EP Patent No. 1551664 and US Patent No. 2005253408, there is described a seat slide 3 which, in the case of a rear crash, is released to allow the seat 1 to move backward relative to the vehicle 2 (Figure 19). The seat apparatus 10 devised for this purpose is shown in Figure 20. The said apparatus is mounted under the seat. Upon the rear-end impact, the mass 19 moves backward on the shaft 20 and opens the release mechanism 14 to enable the said backward motion of the seat. The said backward motion of the mass 19 also frees the plastically deformable element 17 being rotatably mounted on the slide 16 by releasing the engagement element 21 of the rod 15. During the said backward motion of the seat relative to the vehicle, the deformable element 17 is deformed plastically to damp this movement.

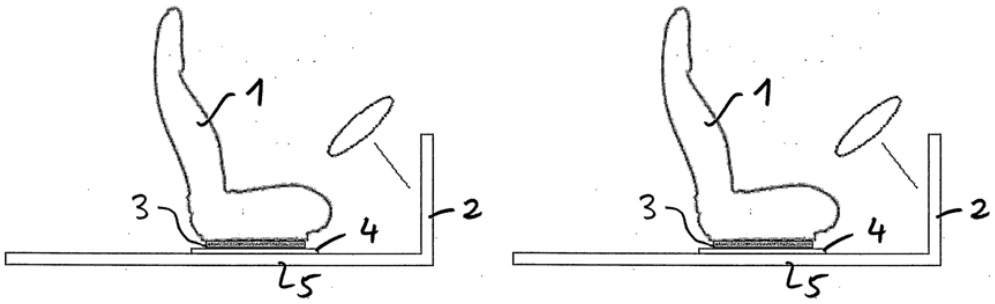

Figure 19 EP Patent No. 1551664 and US Patent No. 2005253408

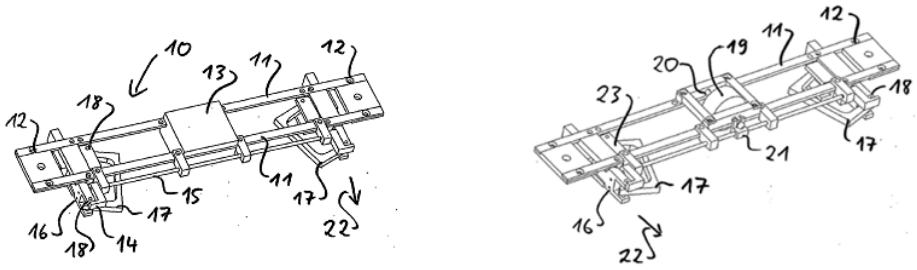

Figure 20 The seat apparatus devised in EP Patent No. 1551664 and US Patent No. 2005253408

In GB Patent No. 2354936, there is provided a catch mechanism which, in normal driving conditions, retains the tab 13 in its undeformed position (Figure 21). However, as the seat moves forward together with the vehicle in response to a rear impact, the inertia 20 maintains its position and the retainer plate 34 moves forward (Figure 22). Hence, the catch releases the tab 13. Thus, under the rearward loading of the seatback by the occupant, the tab 13 deforms so that the seat rotates backwards, as shown in Figure 23. Similarly, in GB Patent No. 2359482, when the occupant forces the back of the seat backwards in the course of a rear-end collision; the seat entirely pivots rearward about the roller 4, deforming the tab 29 (Figure 24). By this means, some of the energy transmitted during collision is absorbed.

Lastly, the invention in US Patent Nos. 6435591 and 2001011830 is intended to slide the entire seat linearly or curvilinearly backwards on the rollers 5 along the track rails 6 after a rear-end crash while the dampers 8 damp this movement (Figure 25).

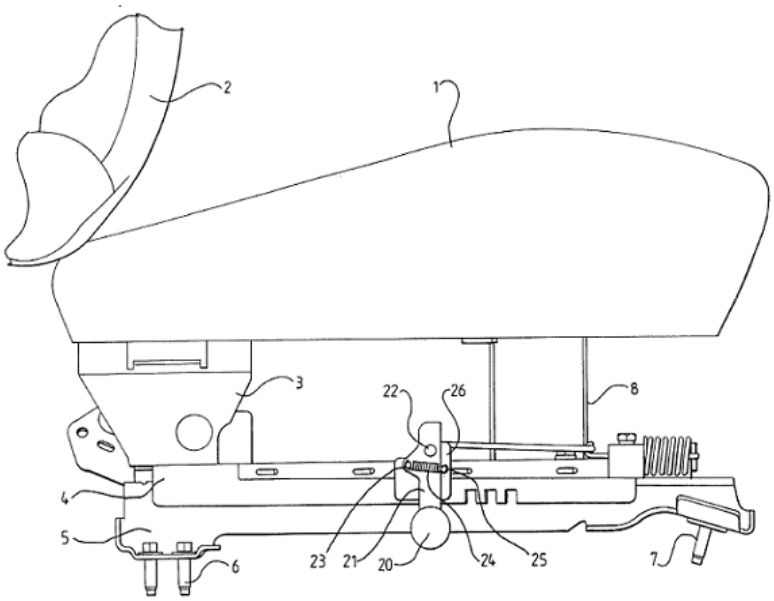

Figure 21 The invention in GB Patent No. 2354936 in an initial position

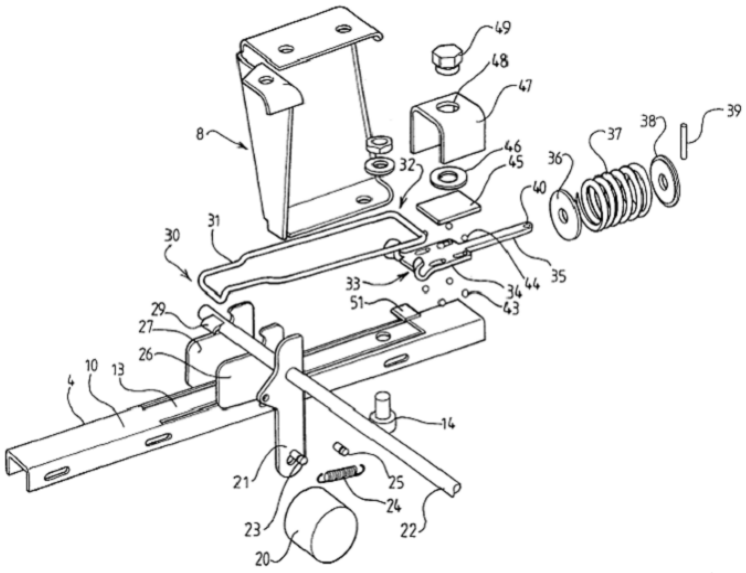

Figure 22 The catch mechanism used in GB Patent No. 2354936

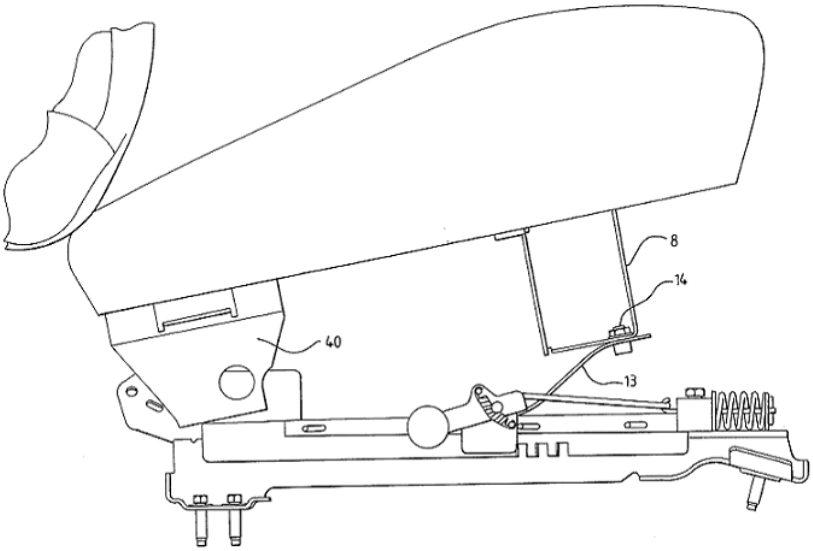

Figure 23 The invention in GB Patent No. 2354936 after a crash

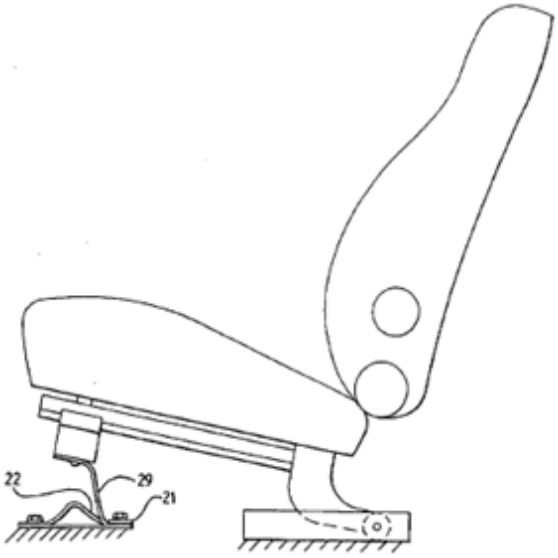

Figure 24 GB Patent No. 2359482

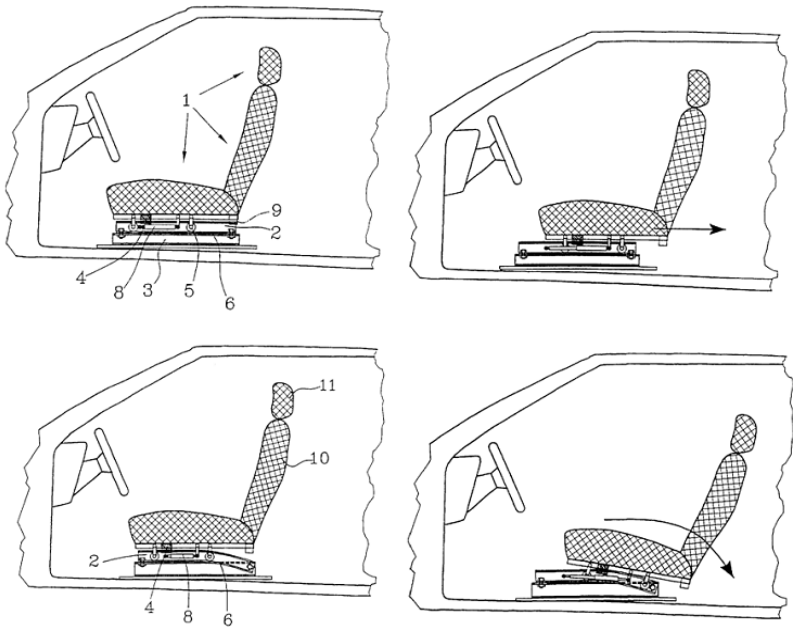

Figure 25 US Patent Nos. 6435591 and 2001011830

2.5 Special-Shaped Backrest and Head Restraint Designs Made of Special Materials

Patents in this category provide different backrest and/or head restraint designs with special profiles and shapes suitable for corresponding body parts and/or with high energy absorption ability.

WO Patent No. 9204847 and US Patent Nos. 5181763, and 5290091 offer an adjustable headrest having an outer surface contour that matches the posterior contour of the occupant's head and neck (Figure 26). In a rear impact, when the occupant's head rotates back and meets the headrest, the headrest rotates back towards the seatback, causing the headrest contour to engage the respective head and neck portions. Thus, a proper support for the head and neck is provided to prevent whiplash injury.

US Patent No. 5580124 provides a backrest with an integral headrest of which the outer surface is such formed that it has a contour fitting the posterior contour of the head and neck (Figure 27). This apparatus is arranged so that there is an outer layer of resilient material lying on an inflexible support shell. Underneath this shell comes a

crush zone which is made of a deformable material that deforms under substantial rearward occupant load due to rear crash, and thereby absorbs some of the impact energy to avoid whiplash injuries.

Likewise, WO Patent No. 9743142 suggests a seatback having a section incorporating a solidifiable material 4 which can easily take the shape of the posterior contour of the back, head and neck of the occupant being pushed backward against the seatback when a rear-end impact occurs and solidify in that shape (Figure 28).

Further, WO Patent No. 0156830 offers a backrest with variable rigidity (Figure 29). The backrest is designed to be less rigid in the neighborhood of the seat part 2. Another patent, WO Patent No. 9511818, advises a support net 4 within the seatback frame (Figure 30). The said net is plastically deformed backward by the occupant's torso pushing the seatback rearward in a rear-end crash, allowing the head of the occupant to contact the head restraint.

Other than these patents, a headrest 20 including a frame which permanently deforms when subjected to the force applied by the occupant's head being whipped back during a rear-end crash is proposed in US Patent No. 2003001413 (Figure 31). Thereby, the exerted reaction force in the forward direction that is believed to yield whiplash syndrome is significantly decreased.

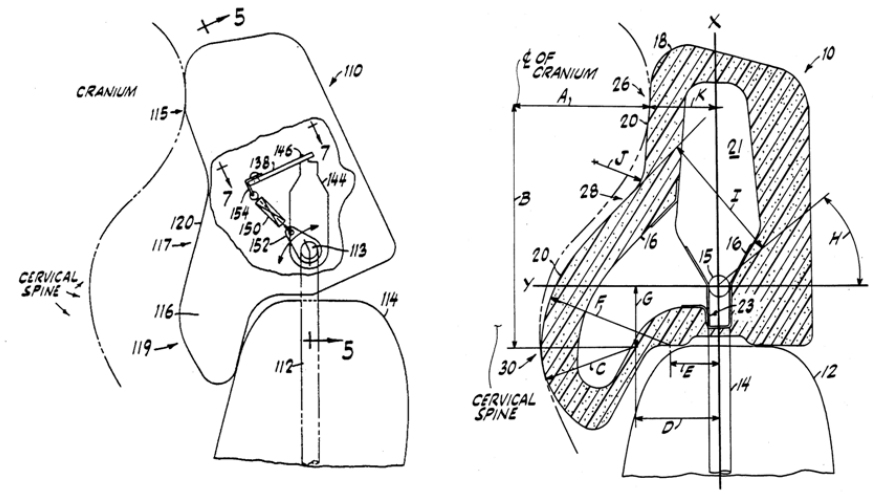

Figure 26 WO Patent No. 9204847 and US Patent Nos. 5181763, and 5290091

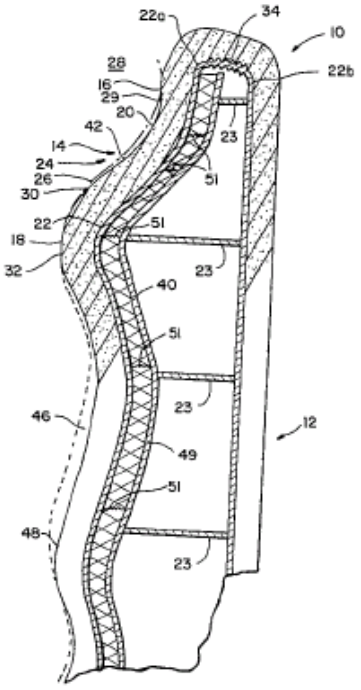

Figure 27 US Patent No. 5580124

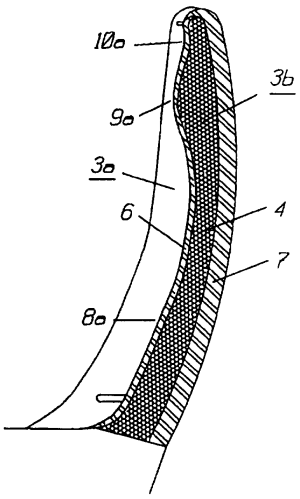

Figure 28 WO Patent No. 9743142

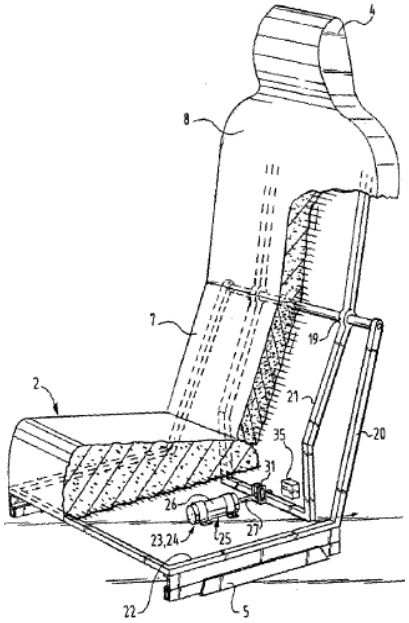

Figure 29 WO Patent No. 0156830

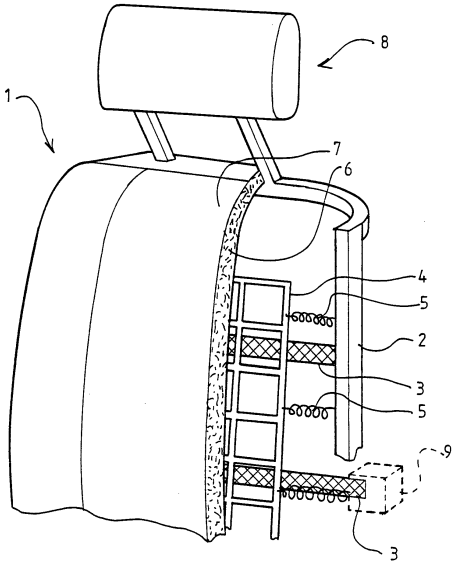

Figure 30 WO Patent No. 9511818

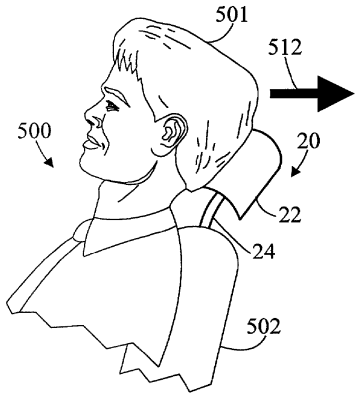

Figure 31 US Patent No. 2003001413

2.6 Air-Bagged Head Restraints

The patents of this group share a common characteristics in that they all use an inflatable airbag to prevent whiplash injury in the case of a rear-end collision.

US Patent No. 2002014760 uses an airbag which is inflated to protrude from the seat in such a way that it lays between the occupant's head and the head restraint during a rear collision (Figure 32). In a similar manner, in US Patent No. 2004075252, there is provided a headrest airbag that is to be deployed into a U-shape in order to support the occupant's head and neck properly when a rear impact occurs to the vehicle (Figure 33).

Another patent, US Patent No. 2008073886, affords a headrest airbag such that, when inflated upon a vehicle collision from behind, the distance that the occupant's head is thrown away rearward before meeting the headrest is dramatically decreased (Figure 34).

Still another patent, US Patent No. 2007158933, provides a backrest with an airbag placed at its uppermost part (Figure 35). Such an airbag is to be deployed upwardly in a rear-end accident situation to constitute a headrest for the occupant.

A further US Patent No. 5833312 discloses a seatback 3 being comprised of a seatback pocket 11 full of air 4a and an empty canvas pocket 13 being connected to the said seatback pocket 11 through passageways 12 (Figure 36). When the occupant's torso is forced against the seatback 3 due to a rear-end collision, the seatback 11 is compressed so that the air 4a thereof is transferred through the passageways 12 into

the canvas pocket 13. The resulting canvas surface 13' creates a support for the head and neck of the occupant.

Finally, US Patent No. 2004070239 proposes a head restraint which incorporates an air bladder 113, the walls of which define a contour corresponding to the posterior contour of the occupant's head and neck (Figure 37). A pump 117 is provided to pressurize the said bladder 113 by pumping air into it through the non-return valve 118.

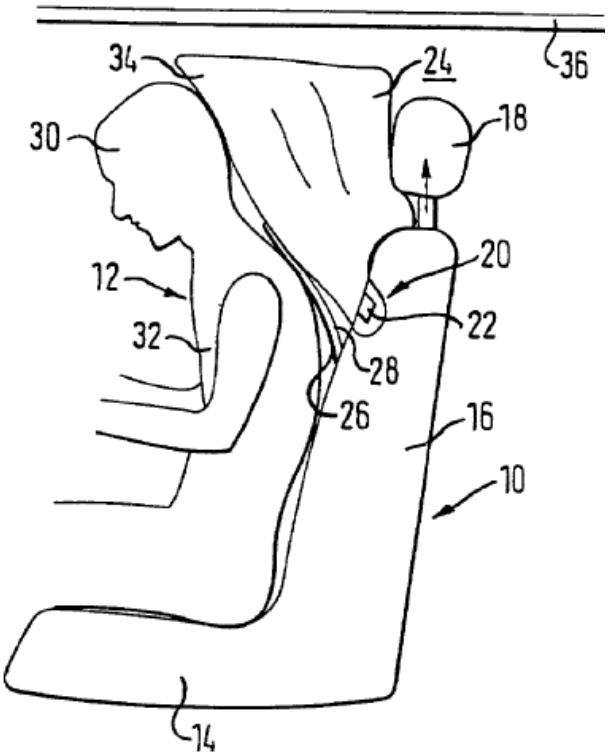

Figure 32 US Patent No. 2002014760

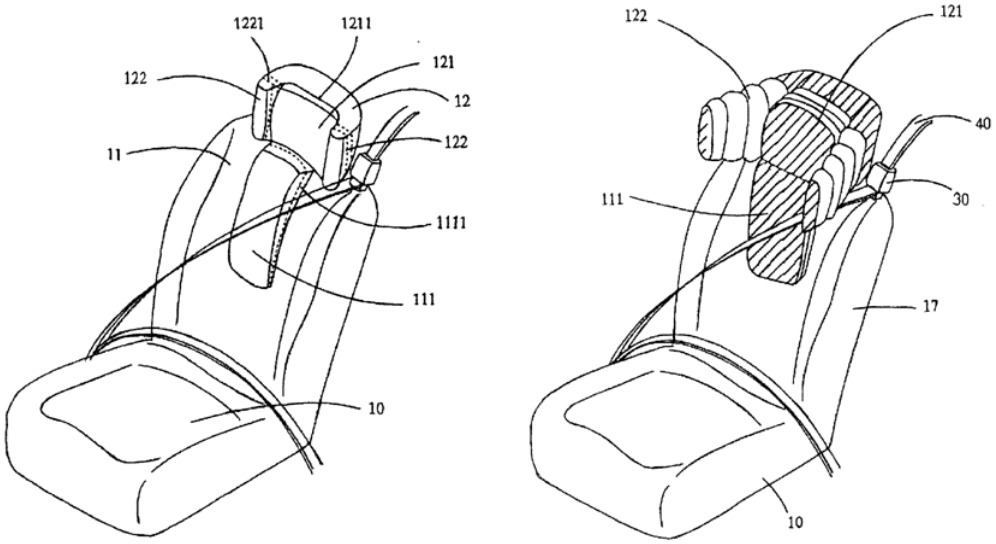

Figure 33 US Patent No. 2004075252

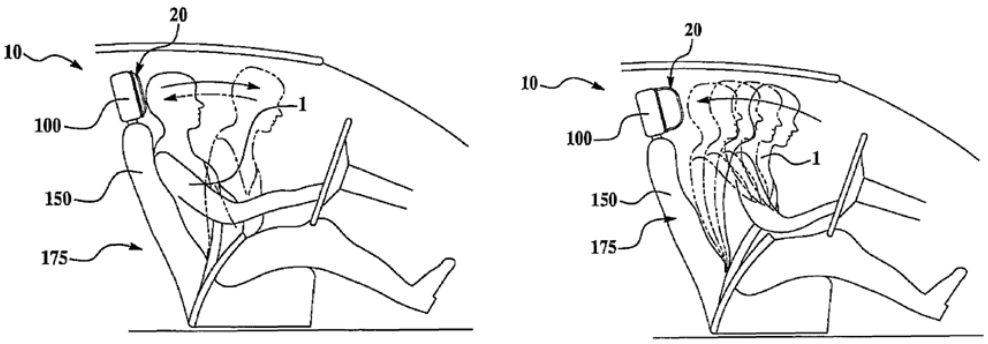

Figure 34 US Patent No. 2008073886

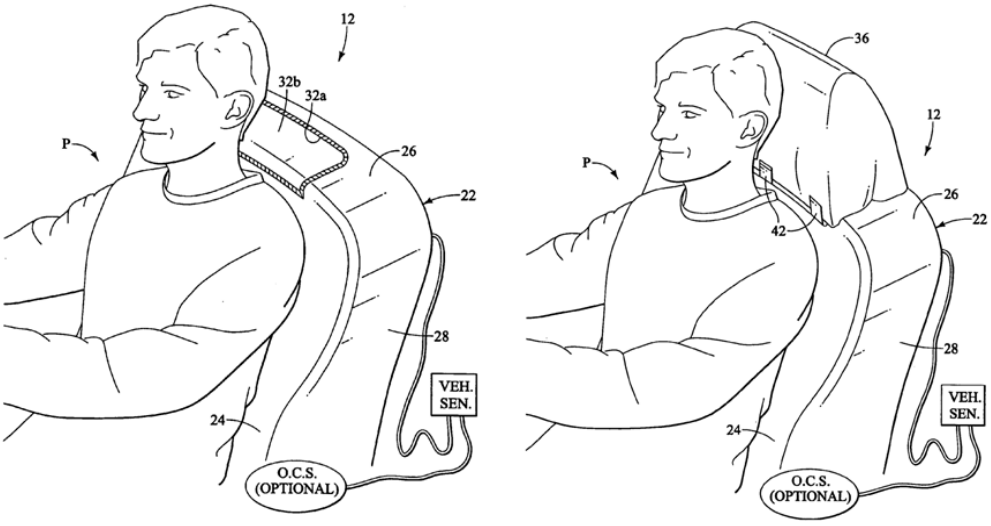

Figure 35 US Patent No. 2007158933

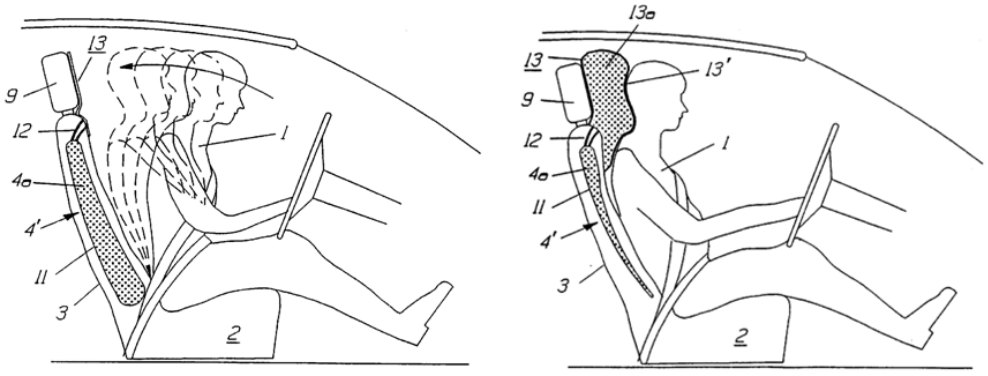

Figure 36 US Patent No. 5833312

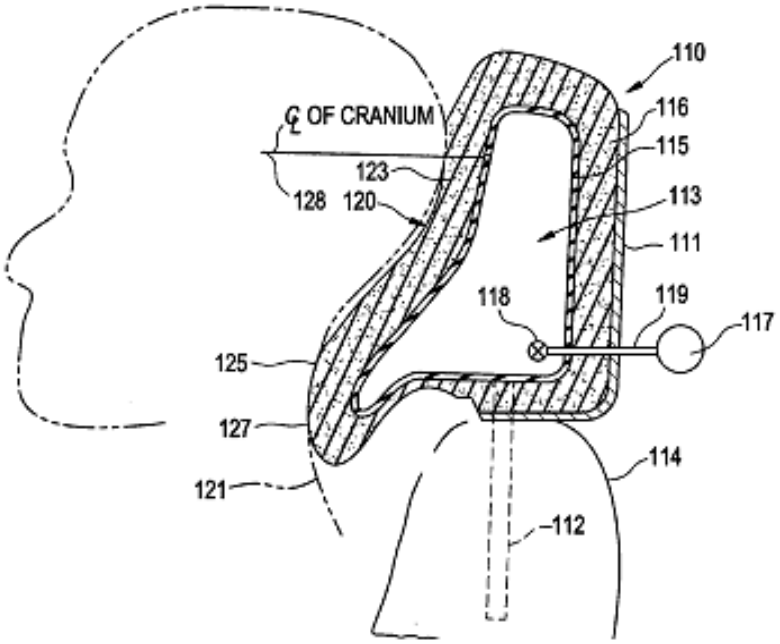

Figure 37 US Patent No. 2004070239

2.7 Other Headrest Forms

This group of patents encompasses apparatuses that function similarly with the headrest. For this reason, one can say that they are aimed to replace the headrest. For instance, in CA Patent No. 1273375, a head stop suitable for vans and trucks is developed to restrict the backward motion of the head of the occupant when the vehicle is run into from behind (Figure 38). The said stop is mounted to the ceiling of the driver's cab.

Besides, US Patent Nos. 2002056980 and 2002180197 recommend an occupant safety network located between the front and rear seats, as shown in Figure 39. Likewise, in US Patent No. 3643972, there is provided a yieldable, transparent safety shield for shock-absorbing purposes (Figure 40).

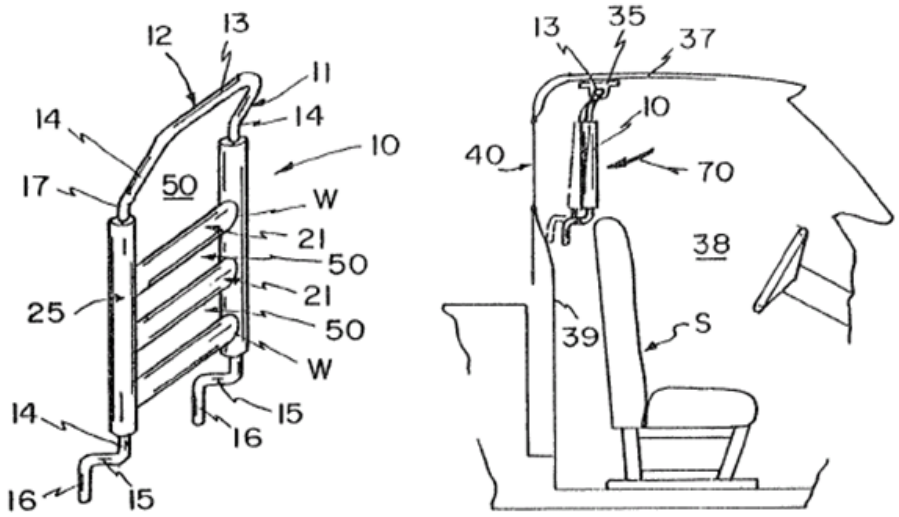

Figure 38 CA Patent No. 1273375

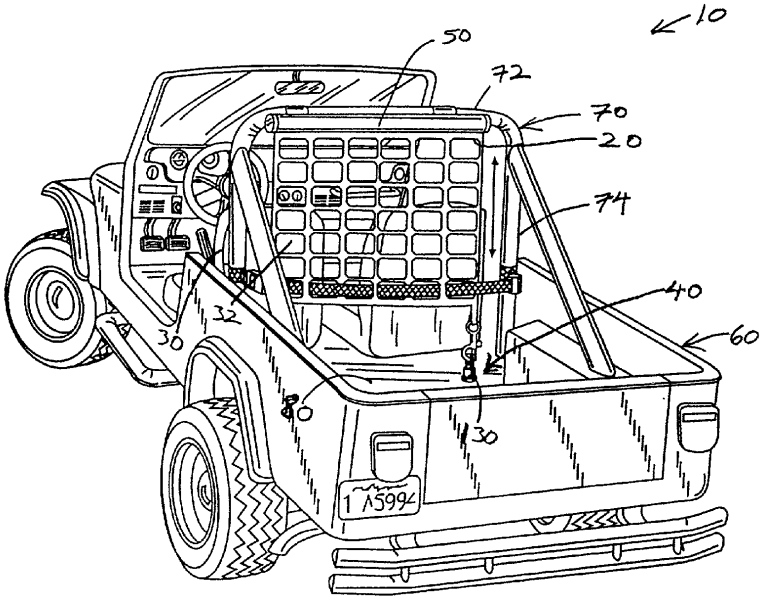

Figure 39 US Patent Nos. 2002056980 and 2002180197

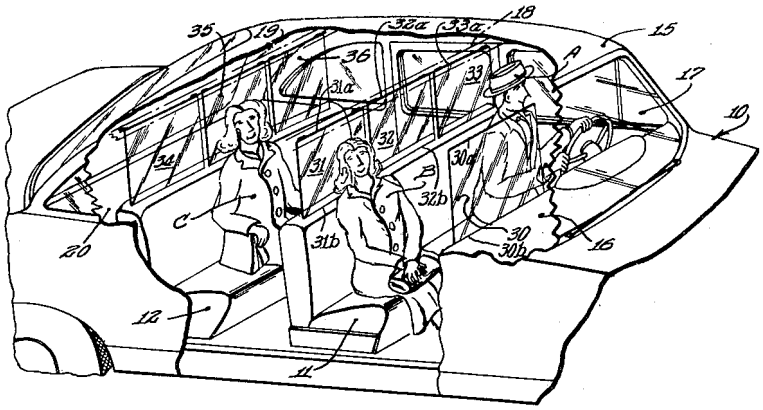

Figure 40 US Patent No. 3643972

Another patent, US Patent No. 3151911, develops an easily applicable and detachable headrest for various types of seatbacks (Figure 41). Said headrest is designed to be both vertically and laterally adjustable.

Yet another patent of this group is US Patent No. 3222084 (Figure 42). In this patent a non-elastic, webbed-strap is disclosed to be mounted between two members of the chassis frame.

Moreover, US Patent No. 2007241594 claims a device attachable to the existing head restraints (Figure 43). In this way, the distance between the occupant's head and the head restraint is significantly reduced in normal driving conditions. Hence, the distance that the head of the occupant travels backwards before striking the head restraint during a rear crash is greatly lessened. In addition, shock absorbing pads are provided inside the said device.

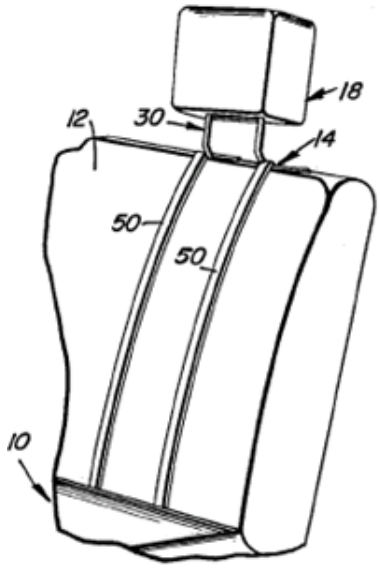

Figure 41 US Patent No. 3151911

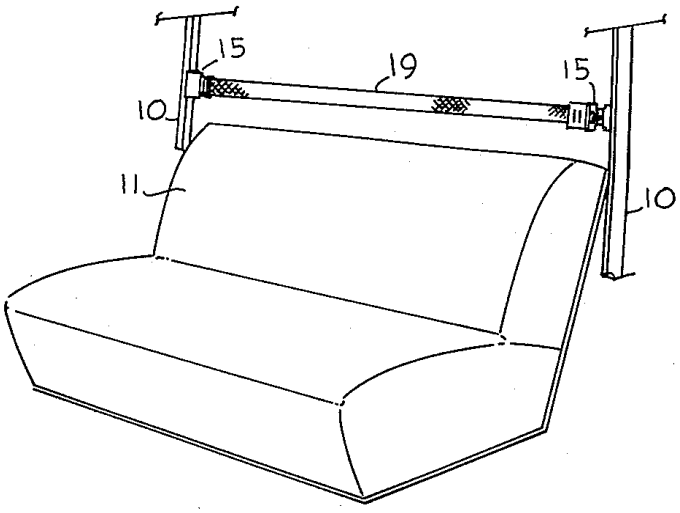

Figure 42 US Patent No. 3222084

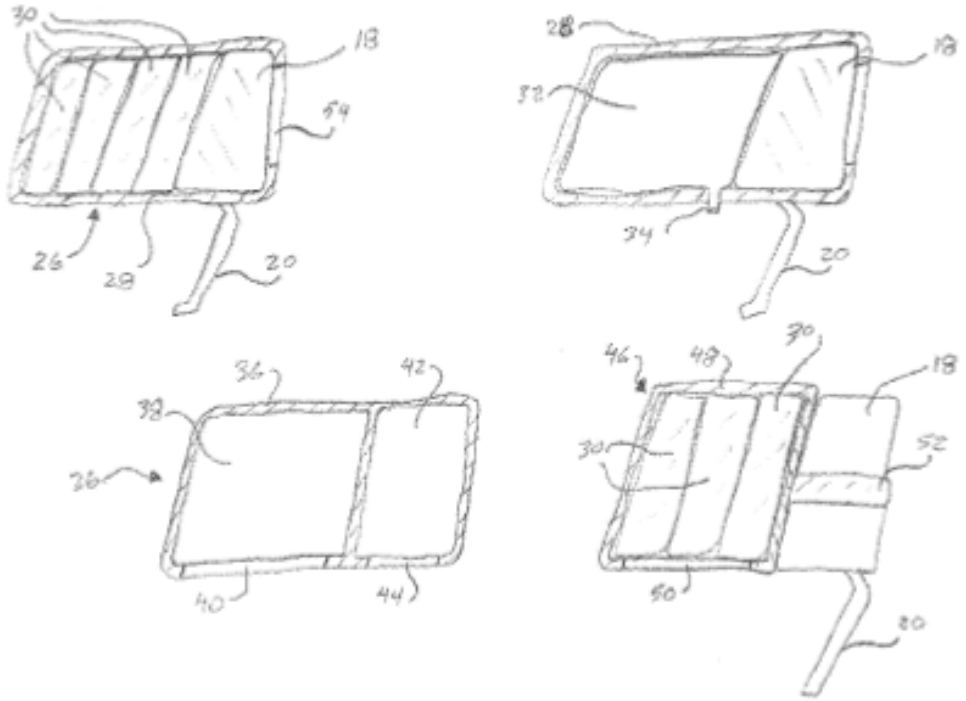

Figure 43 US Patent No. 2007241594

2.8 Helmet and Collar Designs

Apparatuses developed in this group of patents do not seem applicable in everyday driving as far as the driving comfort is concerned. However, the author believes that these inventions may find applications themselves in racing cars to provide high safety.

One patent in this category, GB Patent No. 1348239, declares an inflatable appliance that is to be worn by the occupant (Figure 44). The said invention inflates automatically upon an impact to the vehicle to ensure reduced rotational displacement of the occupant's head and neck. A similar apparatus is devised in GB Patent No. 2296855 (Figure 45). In another patent, WO Patent No. 9818356, there is similarly described a cylindrical ring-shaped device, which is made of a rigid, but deformable, material (Figure 46). The occupant wears the said device around her/his neck.

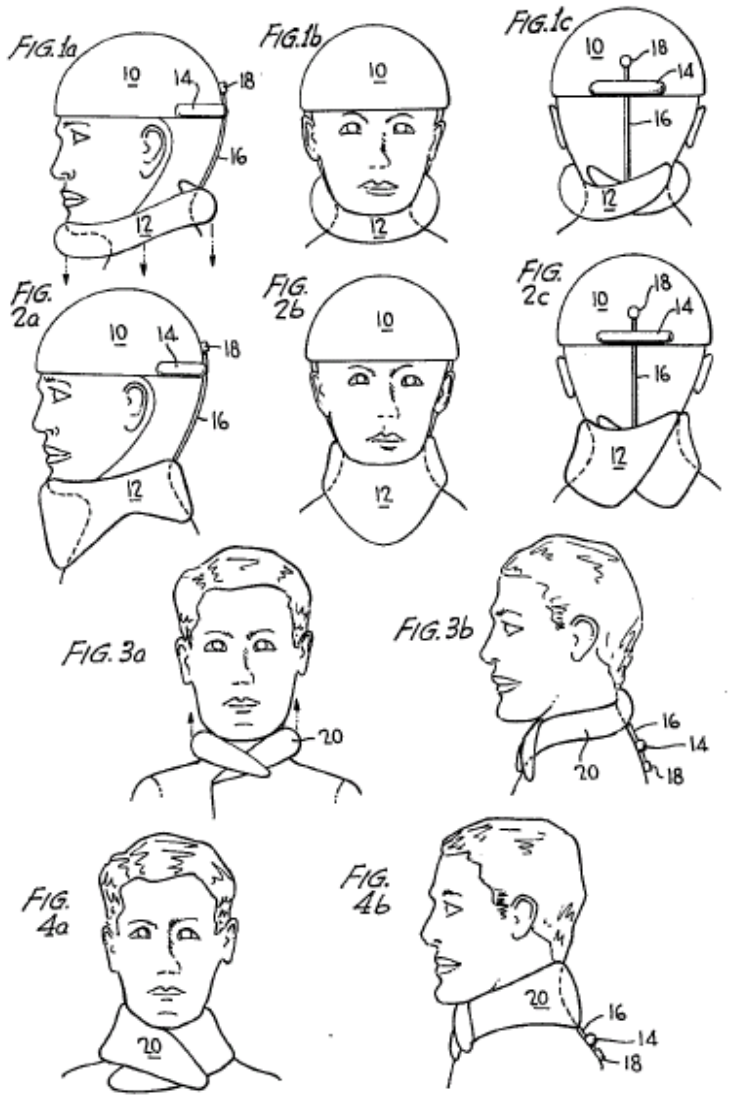

Figure 44 GB Patent No. 1348239

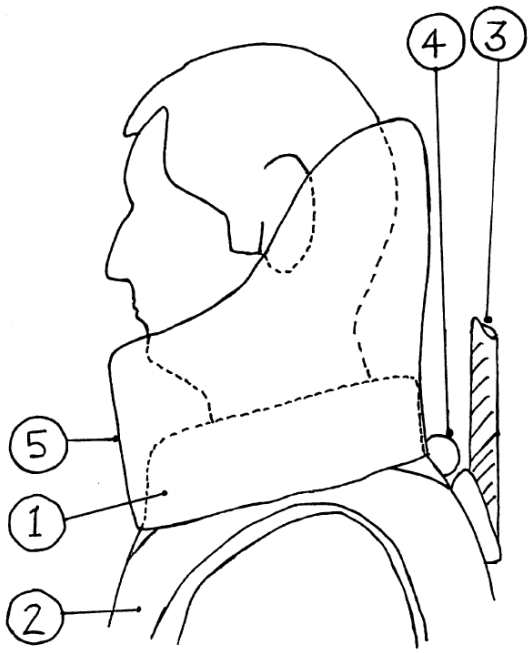

Figure 45 GB Patent No. 2296855

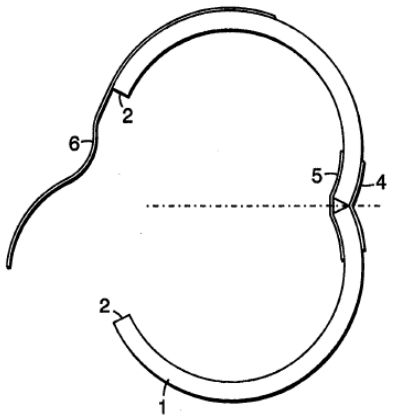

Figure 46 WO Patent No. 9818356

The last patent in this group, US Patent No. 2007209667, suggests a helmet-like device, which is attached to a shock-absorber by a joint giving necessary motion freedom to the occupant's head (Figure 47). The shock-absorber is detachably fastened to the seatback.

Figure 47 US Patent No. 2007209667

CHAPTER 3

WHIPLASH SIMULATION WITH SIMPLIFIED VEHICLE SEAT MODEL

In this chapter, a simplified model for a standard vehicle seat that is developed in LS-DYNA® environment is introduced, and the rear-end collision is simulated with this model. In these simulations, the commercially available finite element model of the BioRID II test dummy is used. The selected seat model parameters are verified by comparing the simulation results yielded by the model with the associated sled test and simulation results available in the literature.

3.1 Finite Element Model Development

Since vehicle seats differ in a wide range of shapes and characteristics, a simplified seat, the so-called Chalmers seat, was utilized during the development of the BioRID crash dummy (Figure 48) (Deter, Malczyk, & Kuehn, 2007; Stahlschmidt, Keding, Franz, & Hirth, 2006a; Stahlschmidt, Keding, Witowski, Müllerschön, & Franz, 2006b). This seat comprises a rigid seat bottom, a seatback frame with four movable elements and a movable headrest. All the seatback elements and the head restraint are separately adjustable (Deter, et al., 2007). Similarly, in this study, a simplified seat model is needed to evaluate the functional design alternatives. The model developed for this purpose is shown in Figure 49. In this model, the seat construction is represented by three rigid plates, namely the seat bottom plate, the seatback plate and the headrest plate. Other than these, there is a rigid horizontal floor plate and a rigid toe board plate which makes an angle of 45° with the floor plate. The surfaces of the seat bottom plate, the seatback plate and the headrest plate that are facing the dummy are all covered with 70 mm-thick prismatic layers of foam. This thickness value is adopted as the average thickness of the seat foam.

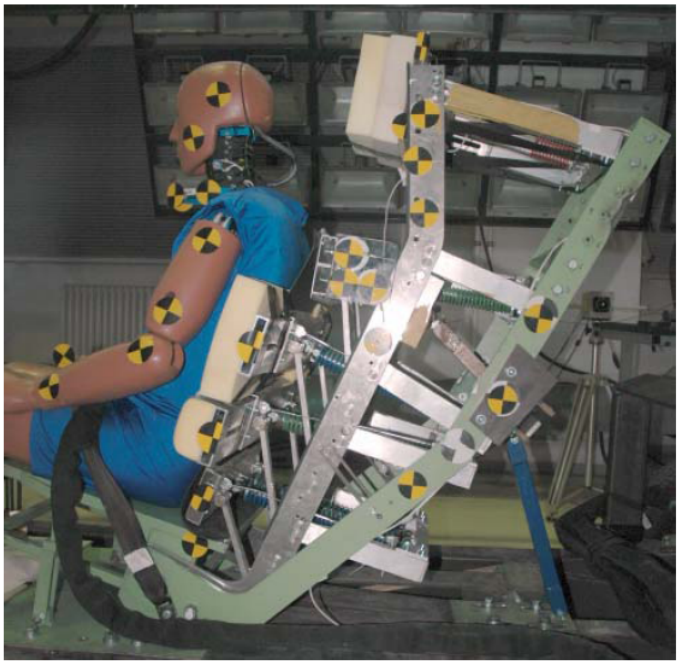

Figure 48 Chalmers seat (Deter, et al., 2007)

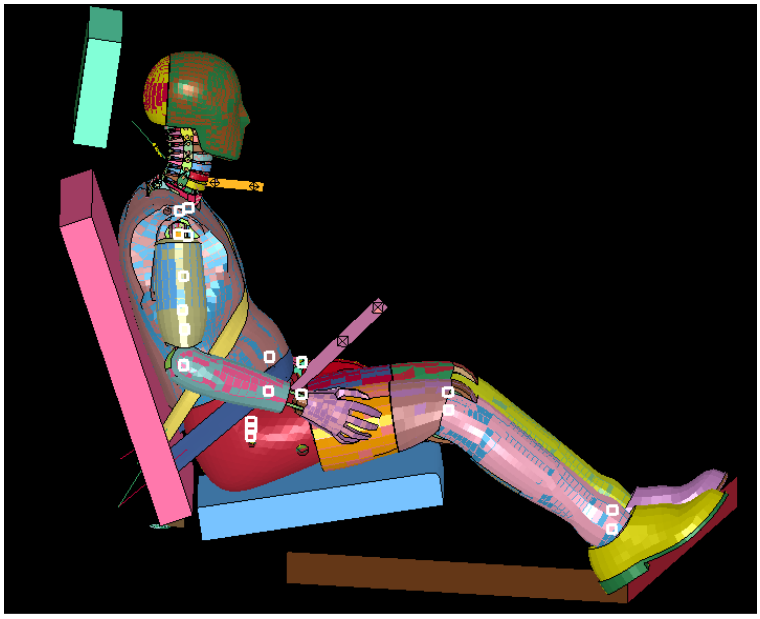

Figure 49 The simplified standard seat model

The plates are all meshed with shell elements, and the foam parts are meshed with solid brick elements and tied to their underlying plates. The material parameters used for the foam layers are taken from the work of Tabiei, & Nilakantan (2007) and are summarized in Table 1. The nominal stress strain plot of the foam material is shown in Figure 50. All potential contacts between the BioRID II dummy and seat models are included in the automatic contact definition wherein the static and dynamic friction coefficients are taken as 0.5. The lap and shoulder seat belts are also employed in the model.

The seat bottom plate and the toe board plate are rigidly connected to the floor plate whereas the headrest plate is rigidly connected to the seatback plate. Since the seat construction is represented by using rigid plates in the model, a revolute joint is defined between the seat bottom plate and the seatback plate, and a torsional spring and a torsional damper are placed on both sides of this joint to represent raking characteristics of the seatback. Here, raking characteristics refer to the backward inclining of the backrest frame about its pivot point at its bottom, when leaned by the occupant (See Figure 51 for the pivot center of the Chalmers seat, which is shown in red circle). Hence, the contribution of the parts of the physical seat frame that are not modeled in the simplified seat model is taken into consideration.

Table 1 The foam material parameters (Tabiei, et al., 2007)

Mass density	1.22E-7 kg/mm^3
Young's modulus	0.794 N/mm^2
Tension cut-off stress	1 MPa
Hysteretic unloading factor between 0 and 1	0.7
Decay constant to model creep in unloading	0.0

The BioRID II model is given an initial position according to the European New Car Assessment Program (Euro NCAP) whiplash testing protocol (2008) as much as the simplified seat model allows. In this sense, the pelvis angle and the head plane angle are adjusted to be 26.5° and 0°, respectively. In each simulation conducted with the developed model, as suggested in the work of Stahlschmidt, et al. (2006a), a 100-ms pre-simulation is run before the application of the acceleration pulse in order to close the small gaps between the seat and the test dummy by gravity rather than generating the initial posture roughly using the LS-PrePost® pre and post-processor.

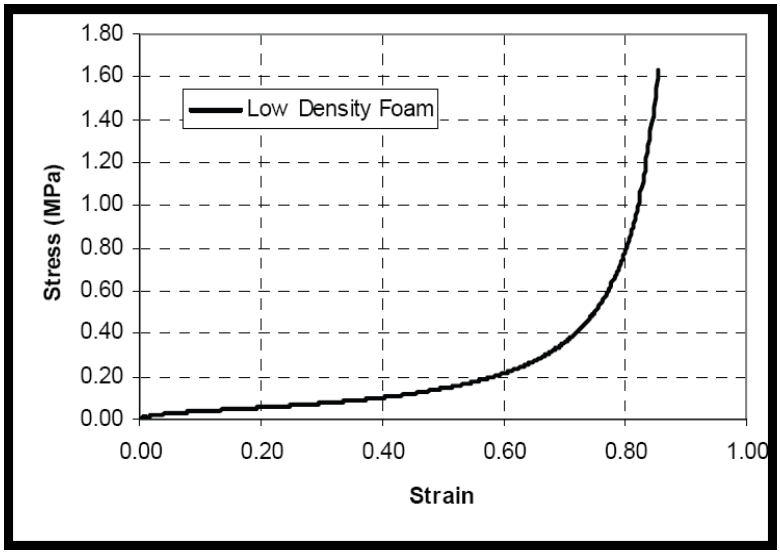

Figure 50 The nominal stress strain plot of the foam (Tabiei, et al., 2007)

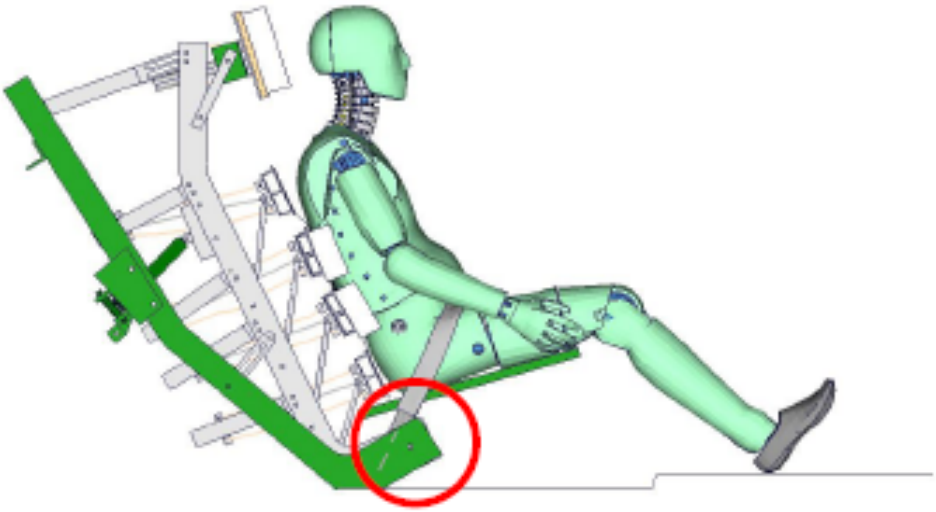

Figure 51 The pivot point of the seatback (Stahlschmidt, et al., 2006a)

3.2 Selection and Validation of the Seat Model Parameters

With the seat modeled as described in the previous section, the two model parameters to be determined are the equivalent rake stiffness coefficient and the equivalent rake damping coefficient. Since these will determine the deflection of the seatback during a whiplash simulation, they have direct effects on the position change of the head restraint relative to the head of the dummy. Therefore, the results yielded by the introduced seat model will highly depend on the values selected for each of them.

When the literature is searched for the specific values of these parameters, it is seen that the rake stiffness coefficient varies greatly in a range of about 2.5 kN·m/rad to 40 kN·m/rad depending on the vehicle model (Golinski, & Gentle, 2005). Apart from this, Himmetoglu, Acar, Bouazza-Marouf, & Taylor (2008) used in their multi-body seat model a damping coefficient of 1 N·m·s/deg for the rearward deflection of the seatback about its pivot point as a representative value for a typical seat reclining mechanism. However, similar to the rake stiffness coefficient, this value will also depend on the particular vehicle model of interest. For this reason, a trial-and-error process is followed in this study for the selection of the rake parameters.

During this process, Neck Injury Criterion (NIC) is considered as a comparison and validation measure. It is given according to the following formula (Euro NCAP whiplash testing protocol, 2011):

$$\mathrm{NIC}(t) = a_{rel}(t) \cdot 0.2 + v_{rel}^2(t) \tag{3.1}$$

where

$$a_{rel}(t) = a_x^{T1}(t) - a_x^{Head}(t) \tag{3.2}$$

$$v_{rel}(t) = \int a_{rel}(t)\,dt \tag{3.3}$$

Here, t designates the time, $a_x^{T1}(t)$ and $a_x^{Head}(t)$ are the horizontal accelerations of the first thoracic vertebrae (T1) and the center of gravity of the head, respectively. Before substituting into the given formula, both $a_x^{T1}(t)$ and $a_x^{Head}(t)$ should be converted to be in [m/s^2], and then filtered at channel frequency class (CFC) 60. Only the positive peak value of NIC(t), i.e., NIC_{max} is considered, whereas the negative values attained by the head-to-headrest contact are not of interest (Boström, et al., 2000). It might be worth to mention that the constant 0.2 appearing in Eq. (3.1) stands for a

representative length of the human neck in [m] (Croft, Herring, Freeman, & Haneline, 2002).

The reason for this criterion to be selected among the many others, which are presented in Chapter 7, is due to the fact that it is one of the mostly used in the literature (Schmitt, Muser, Walz, & Niederer, 2002) and has been validated to a great extent (Boström, et al., 2000; Eichberger, et al., 1998).

Two studies are used in this thesis for model verification. One of them is the study of Stahlschmitd, et al., (2006b) where they performed simulations and tests during the development of the BioRID dummy using the low severity Euro NCAP sled pulse (Figure 52). Their results are shown in Figure 53 and Figure 54.

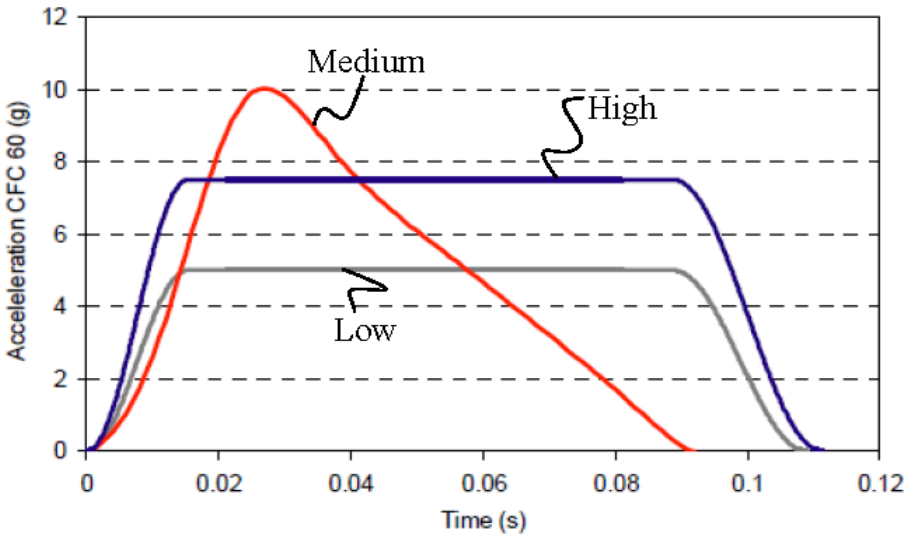

Figure 52 Low, medium and high severity Euro NCAP sled pulses (Van Ratingen, et al., 2009)

Although it is not explicitly given in the original work, the NIC curve is also calculated using the results presented in Figure 53 and Figure 54, and it is given in Figure 55. The NIC_{max} value here is 25.2 m^2/s^2, and it is attained at 76 ms.

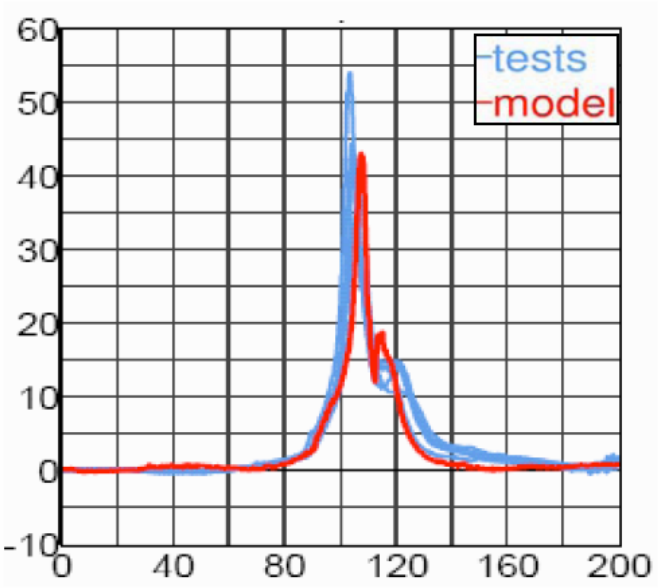

Figure 53 Head x-acceleration [g] vs. time [ms] (Stahlschmitd, et al., 2006b)

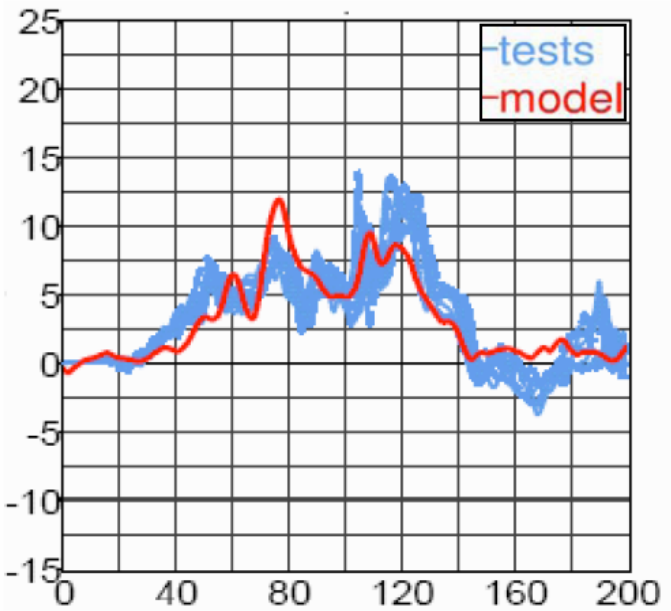

Figure 54 T1 x-acceleration [g] vs. time [ms] (Stahlschmitd, et al., 2006b)

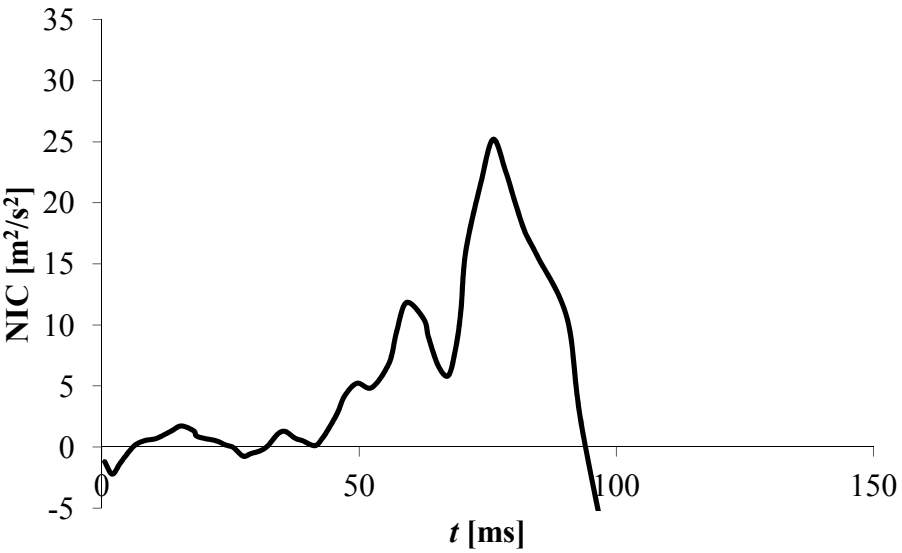

Figure 55 NIC vs. time calculated with the results given by Stahlschmitd, et al., (2006b)

The other study that is used to verify the selected model parameters is that of Yuen, & Bilston (2004) who performed a series of crash tests by using the BioRID dummy. Their test set-up is shown in Figure 56. In one of these tests, the sled pulse given in Figure 57 was used for a standard seat to simulate a rear crash where whiplash may occur. The NIC curve they obtained for this test is presented in Figure 58. Here, the obtained NIC_{max} value is 29.8 m^2/s^2 and this value is reached at 102 ms.

In order to select the rake stiffness coefficient and the rake damping coefficient of the simplified seat model, they are varied iteratively in each simulation until both of the above two NIC curves from the literature are fairly reproduced by the model when the associated acceleration pulse is used. As a result of this trial-and-error simulations conducted, the equivalent rake stiffness coefficient and the equivalent rake damping coefficient are selected as 4000 N·m/rad and 112 N·m·s/rad, respectively, and distributed equally among each pivot point.

With these selected values and the same acceleration pulse with that of Stahlschmitd, et al., (2006b), the simplified seat model yields the results shown in Figure 59 and Figure 60. The NIC curve obtained in this simulation is presented in Figure 61. The NIC_{max} value is found to be 21.0 m^2/s^2 and it occurs at 70 ms.

It can be seen that the results obtained by the simplified model introduced here are in well agreement with the results given by Stahlschmitd, et al., (2006b) in terms

of the general trend of the corresponding curves, the maximum values attained and the times at which they occur.

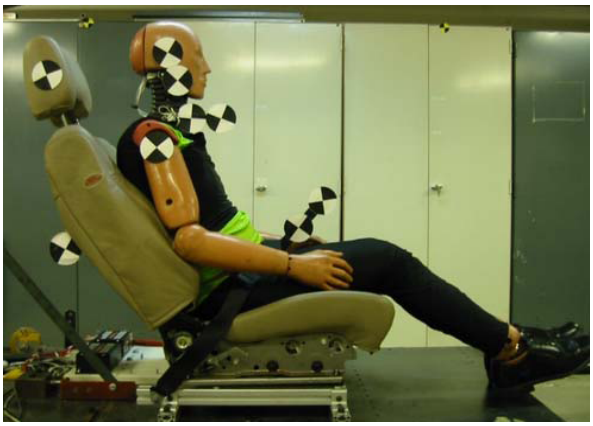

Figure 56 The test set-up of Yuen, et al. (2004)

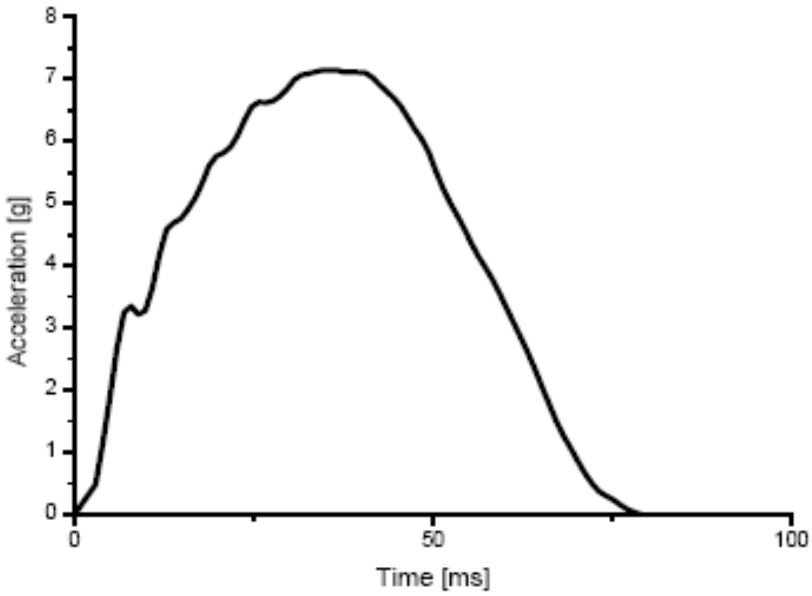

Figure 57 The sled pulse used by Yuen, et al. (2004) to simulate a rear crash where whiplash may occur

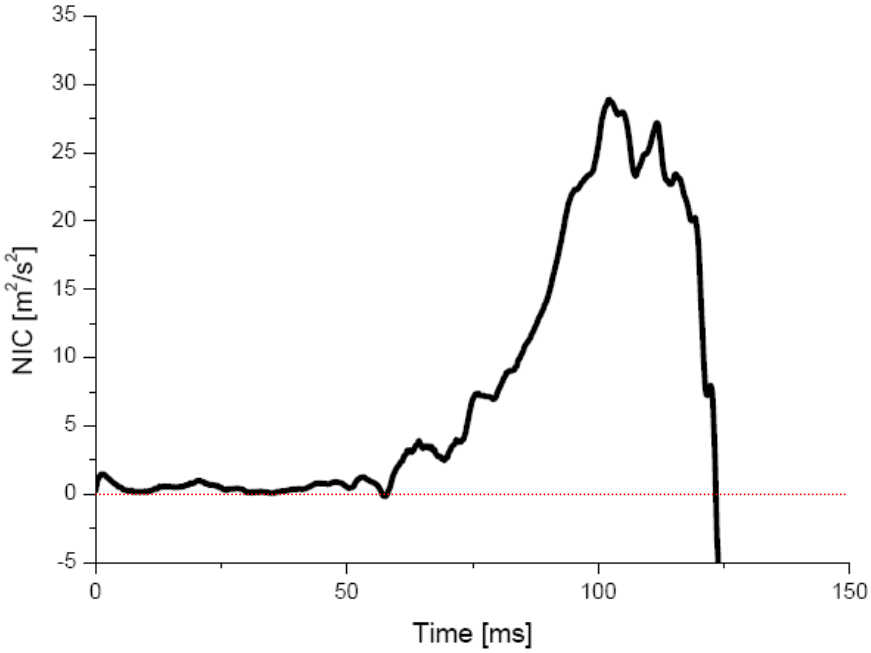

Figure 58 The NIC curve obtained by Yuen, et al. (2004)

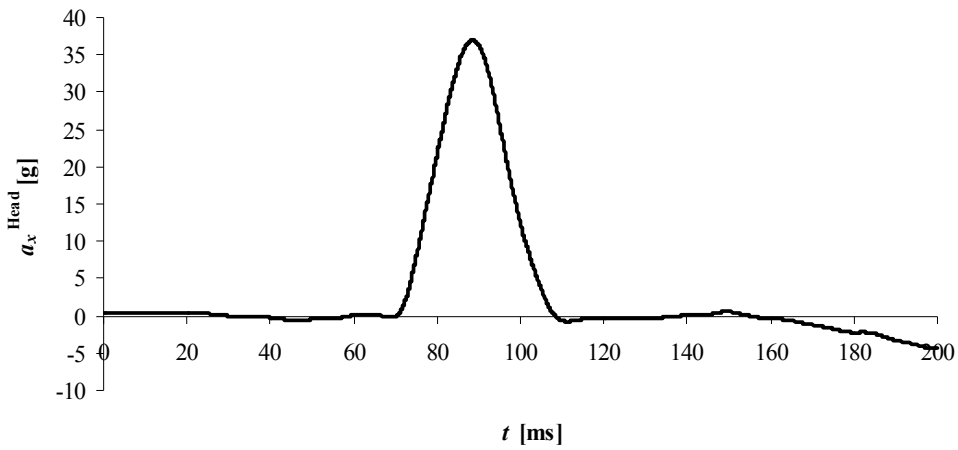

Figure 59 Head x-acceleration vs. time result obtained with the developed model when the same acceleration pulse with that of Stahlschmitd, et al., (2006b) is used

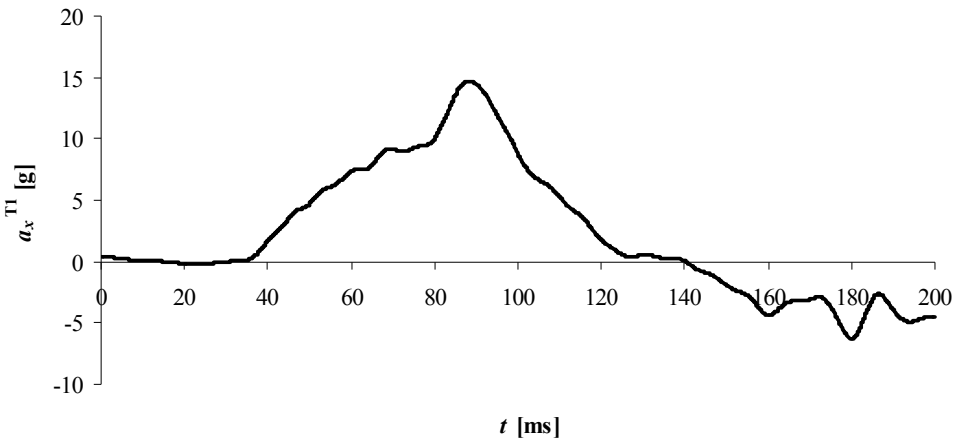

Figure 60 T1 x-acceleration vs. time result obtained with the developed model when the same acceleration pulse with that of Stahlschmitd, et al., (2006b) is used

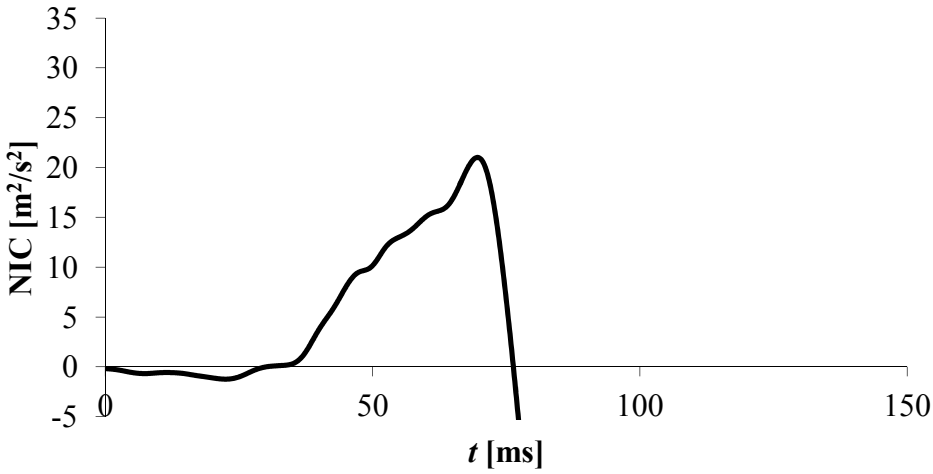

Figure 61 NIC vs. time result obtained with the developed model when the same acceleration pulse with that of Stahlschmitd, et al., (2006b) is used

When the test pulse of Yuen, et al. (2004) is used with the proposed simplified seat model, the NIC curve is obtained as shown in Figure 62. Here, the NIC_{max} value is

found out to be 27.9 m^2/s^2 at time t = 72 ms. This curve is again in well agreement with the curve given in Figure 58 except a phase difference in the time axis. The 30-ms time difference that exists between these two results is most probably due to the difference between the time at which the data-acquisition system is started and the time at which the sled pulse is started to be applied during the sled test.

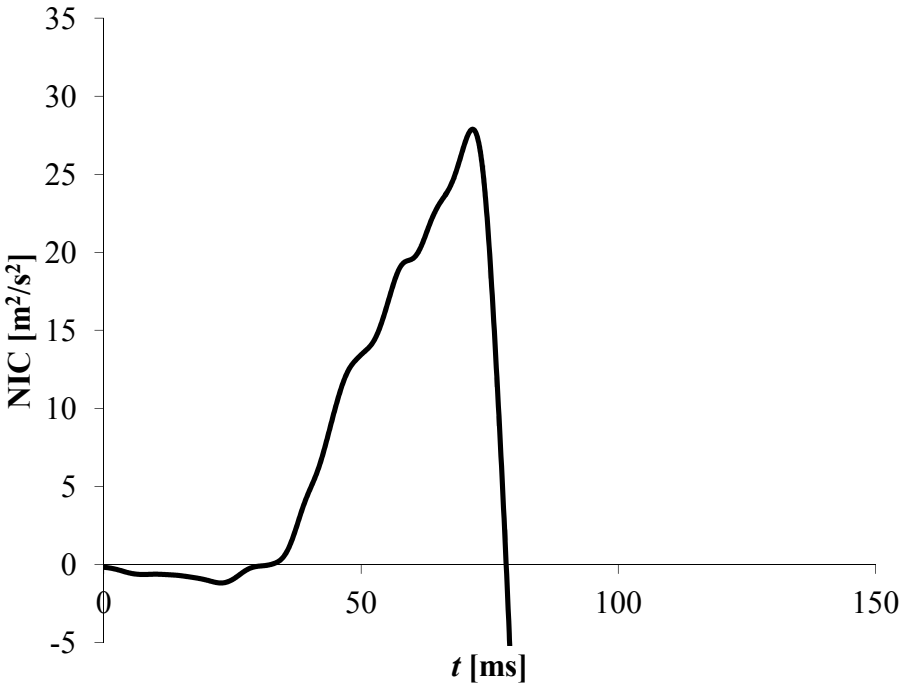

Figure 62 NIC vs. time result obtained with the developed model when the same acceleration pulse with that of Yuen, et al. (2004) is used

CHAPTER 4

EVALUATION OF ALTERNATIVE FUNCTIONAL DESIGNS

In this chapter, two alternative functional designs are introduced and discussed. An evaluation of each alternative is made based on simulations carried out by modifying the simplified seat model introduced in the previous chapter.

4.1 Alternative Functional Designs

The first alternative is to move the headrest in the forward direction by an enough distance (about 30 mm) to support the head and the neck of the occupant in a sufficiently short time immediately after a rear end crash.

A second alternative is to allow the entire seat to move, being guided in a pair of rails, backwards relative to the car under the force applied by the occupant during a rear crash. During this movement of the seat, it is thought to compress a spring and a damper lying within the rails to further decrease the negative effects of the crash on the passenger. The spring may be given a bias so that the seat will be prevented from moving back under the forces that may be applied during normal driving conditions since the bias force on the spring acts against these forces.

It should be mentioned that both alternative designs considered in this chapter assume that the headrest height is properly adjusted by the occupant according to his/her height. Another point that should be remarked is that, while considering the second alternative, the backward movement of the entire seat should be limited in order not to hurt the passengers sitting on the rear seats.

4.2 Effect of Backset Distance on Whiplash Syndrome

In order to investigate the effect of backset on whiplash syndrome, a finite element analysis is performed in LS-DYNA® environment.

For this purpose, four different backsets of 60, 40, 30 and 10 mm are examined, and for each, the simulation is repeated three times by using the low, medium and high severity Euro NCAP pulses (see Figure 52). Table 2 summarizes the performed simulations. In all of these simulations, the developed simplified seat model is used together with the finite element model of the BioRID II test dummy.

Table 2 Simulations performed

Simulation No	Backset [mm]	Acceleration Pulse
1	60	Euro NCAP Low Severity
2	40	Euro NCAP Low Severity
3	30	Euro NCAP Low Severity
4	10	Euro NCAP Low Severity
5	60	Euro NCAP Medium Severity
6	40	Euro NCAP Medium Severity
7	30	Euro NCAP Medium Severity
8	10	Euro NCAP Medium Severity
9	60	Euro NCAP High Severity
10	40	Euro NCAP High Severity
11	30	Euro NCAP High Severity
12	10	Euro NCAP High Severity

Before each simulation, the backset distance is adjusted to its target value by simply moving the headrest backwards and forwards with the LS-PrePost®. However, since in each simulation, a 100-ms pre-simulation is run before the acceleration pulse is applied as described in Section 3.1 and during these sitting pre-simulations the backsets values change with respect to the backset values adjusted using the pre-processor prior to the pre-simulation, these changes are also estimated and considered while presetting the headrest. Hence, in each simulation, the backset distance appeared at the end of its pre-simulation is close to the targeted backset of that simulation with an error of less than 1 mm.

Each simulation is evaluated by calculating the NIC_{max} value. These results are given in Table 3. It has to be mentioned that these results are most useful for comparisons among themselves rather than for the exact numerical values because of the following error sources: First, the seat model used is a simplified model which includes some errors due to the approximations made during the model development phase. A similar situation also exists for the BioRID II crash dummy model as well. In addition, as said before, the rake characteristics vary greatly from vehicle model to model in a wide range. Since these characteristics determine how much the seatback rotates backwards in a rear crash, they have a direct effect on the effective dynamic backset distance, and the results will also change greatly depending on the vehicle model.

Table 3 Simulation results

Simulation No	**NIC_{max} [m^2/s^2]**
1	21.02
2	16.43
3	14.91
4	9.64
5	30.71
6	23.14
7	20.84
8	16.17
9	28.65
10	20.97
11	18.18
12	13.03

Keeping in mind the above-mentioned annotations, when the results are examined, one can clearly see the decreasing trend of the whiplash injury risk with decreasing backset. This finding confirms the literature findings presented in the previous chapters.

Another conclusion that can be drawn from the results is that for a given backset, the lowest and highest NIC_{max} values are attained for the low and medium severity Euro NCAP pulses, respectively. This is in well agreement with the fact that, in the Euro NCAP whiplash assessment protocol (2008), the lowest and highest lower

performance and capping limits for NIC_{max} are assigned to the low and medium severity pulses, respectively.

4.3 Parametric Analysis of an Anti-whiplash Seat Suspension

There has not been much work on the preventive potential of a slidable vehicle seat during rear crash. Studies of Schmitt, Muser, Heggendorn, Niederer, & Walz (2003) and Luo, & Zhou (2010) focused on vehicle seats that can slide backwards during a rear-end crash and showed promising results for this seat design concept to be considered as an efficient way of preventing whiplash injuries. However, both of the said works have proposed to use deformation elements within the system in order to absorb some of the crash energy. But such deformation elements should necessarily be replaced with new ones after the accident since the deformation is plastic, and this would bring an additional difficulty and cost to the consumers.

This section of the study considers a vehicle seat that slides backwards relative to the vehicle during a rear end impact with the occupant pressed onto the backrest due to the inertial effects. To ensure a controlled sliding of the seat, a horizontal suspension arrangement composed of a spring and a damper is proposed to be incorporated within a pair of rails along which the seat slides backwards. It should be made clear that this pair of rails is different than the one used for the back and forth adjustment of the seat. Figure 63 describes this design concept. At the top of this figure, the seat is shown at its normal driving position, whereas at the bottom, the situation after the vehicle is struck from behind is illustrated. Since the force applied by the occupant on the backrest is used as the driving input to the system, sliding of the seat under forces that can arise during normal driving conditions, such as forces due to leaning back of the occupant or pressing the breaking pedal, should be eliminated. For this purpose, a sufficient amount of initial bias can be given to the seat spring.

A plurality of deformable pins which secure the seat to the rails and deform plastically to release this attachment under forces that can be applied onto the backrest only during a rear crash may also be used for the same purpose. However, in this case the deformed pins should be replaced with the new ones after the accident, and that will bring an additional cost to the consumers. For this reason, initial bias application is preferred in this study, rather than using deformation pins. The damper within the suspension, on the other hand, absorbs some of the crash energy. In this way, no

deformation element, and hence no replacement after the accident is needed without any sacrifice from its functions in the system.

Another advantage of a system as described here is its ease of re-setup for reuse. The seat will be restored to its normal driving position by the biased spring automatically after the accident. Surely, there should be a stop to prevent further forward travel of the seat when its normal driving position is reached.

In such a system, once the initial seat spring bias force (F_b) is predetermined to avoid any undesired backward motion of the seat under everyday driving conditions, the design parameters to be considered are the seat spring stiffness (k) and the seat damping coefficient (c), and these two together determine the maximum sliding distance of the seat (d) in the backward direction. Since relatively large seat sliding distances may lead to undesired problems for the rear-seat occupants, the suspension parameters should be carefully selected in this respect, while attempting to reduce the likelihood of whiplash injuries.

A parametric analysis of this system is performed in LS-DYNA® environment for the purpose of investigating the effects of the corresponding suspension parameters and the maximum distance that the seat slides back, on reducing the risk of whiplash injury by using the commercially available BioRID II dummy model and a simplified sliding seat model (Figure 64). The slidable seat model used is a modification of the previously introduced simplified standard seat model. In this study, it is aimed to identify any potential improvements in injury prevention obtained by tuning the previously mentioned seat parameters in question using comparative means. Therefore, a simplified seat model with uniquely selected raking characteristics would still suffice for drawing quantitative conclusions about the effect of the addressed parameters on injury risk when the raking characteristics are kept the same in all simulations.

The modifications which are made to the simplified standard seat model in order to transform it to a slidable seat include addition of a translational spring and a translational damper between a first spring bracket which is rigidly connected to the seat bottom plate and a second spring bracket which is rigidly connected to the floor plate. By this way the seat is made free to slide back and forth on the floor plate while it is subjected to spring and damper forces. In addition, a limiter bracket, which is also rigidly connected to the floor plate, is used to prevent the forward movement of the seat from its normal driving position due to the biased seat spring. Details regarding this suspension arrangement are given in Figure 65.

a)

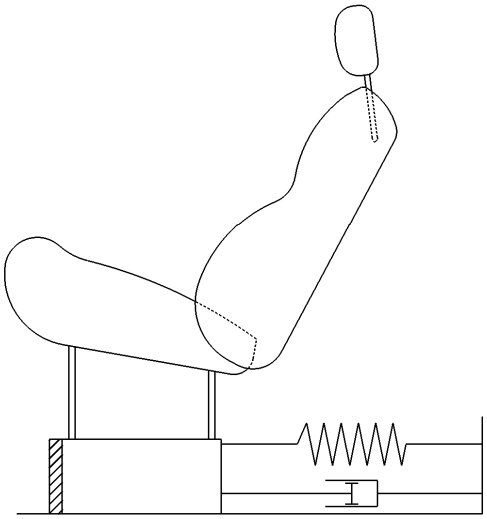

b)

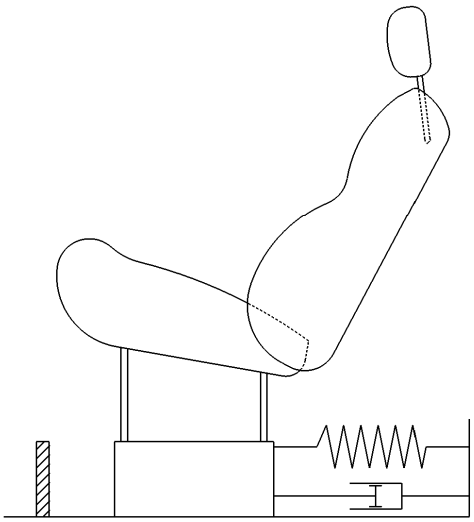

Figure 63 A sketch of the slidable vehicle seat and the horizontal anti-whiplash seat suspension arrangement (a) during normal driving and (b) during crash.

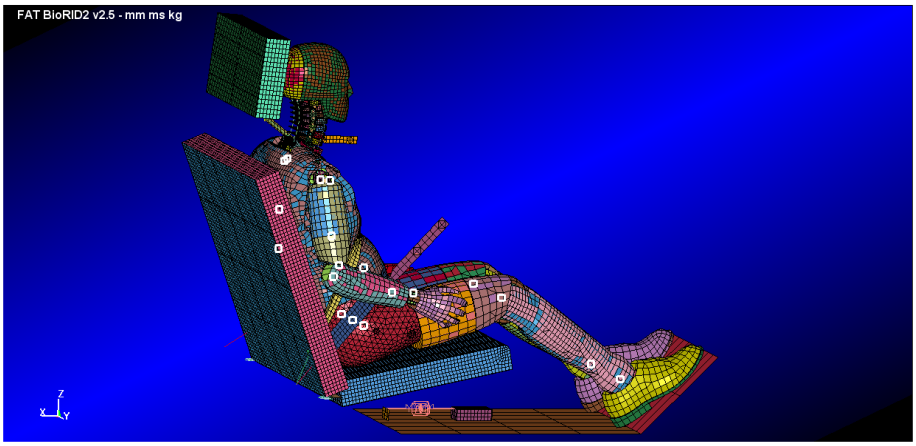

Figure 64 A general view of the finite element model of the conceptual slidable vehicle seat and the BioRID II dummy

Before attempting any simulations, it is convenient to determine F_b. As a threshold recommendation for this purpose, it can be selected to be in the order of magnitude of the inertia force acting on a mass of 100 kg, which is approximately the typical total weight of a vehicle seat and an occupant sitting on it, while accelerating from 0 to 100 km/h in 9 s with constant acceleration. The inertia force in such a case is 309 N, and an F_b value in this order of magnitude is believed to be easily realizable during the assembly of the seat.

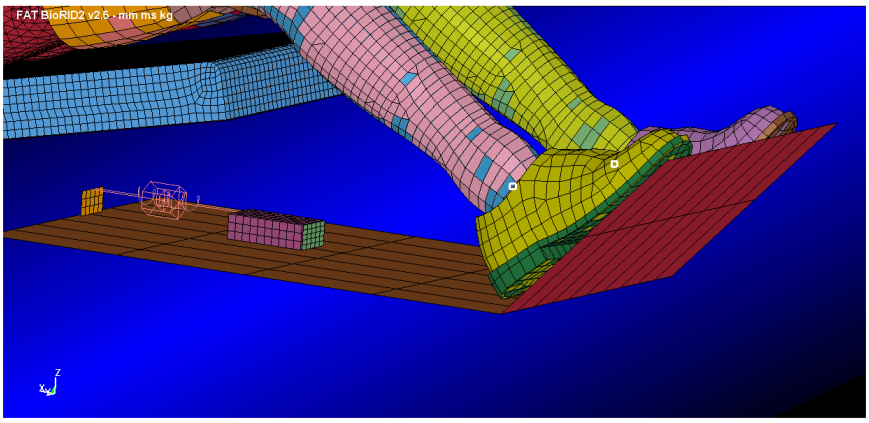

Figure 65 A view showing the details of the suspension arrangement used in the finite element model

In the first seven simulations, k and c are varied arbitrarily while the initial seat spring bias (x) is given such that the seat spring produces an F_b value of 320 N in each case. In all of these simulations, the acceleration pulse shown in Figure 57 is used as a crash pulse and the backset distance (b) is recorded as 59 mm. NIC_{max} results are tabulated together with associated d values in Table 4. It is clearly seen from these results that NIC_{max} decreases significantly with increasing d. Furthermore, although d values are obtained using different suspension parameters in each simulation, NIC_{max} decreases almost linearly with increasing d (see Figure 66). The best line fit of the NIC_{max} vs. d data with a very high R^2 value of 0.99 justifies this linear inverse unique correlation observed between NIC_{max} and d. It should be mentioned here that R^2 denotes the coefficient of determination. By definition, it can only take values between 0 and 1, and as its value gets closer to 1, it means that the model fits to the data better (Gujarati, 2003). Furthermore, a unique relationship implies one-to-one relation between NIC_{max} and d. It should be noted that the equation of this best line fit depend on the raking characteristics of the seat back, the b and F_b values, and the crash pulse used in the simulations.

Table 4 The effect of k and c on the NIC_{max} (F_b=320 N, b=59 mm)

k (N/m)	c (Ns/m)	x (mm)	d (mm)	NIC_{max} (m^2/s^2)
2000	179	160	47	17.8
2000	89	160	59	15.6
2000	45	160	68	14.5
1500	77	213	63	15.0
1000	316	320	38	19.0
1500	39	213	73	13.8
1000	126	320	57	16.5

Following the above set of simulations, a new set of two simulations are performed to simulate the performances of the seats having different k and c values, but almost the same d value. In these two simulations, x is given to the seat spring such that F_b is 309 N in each case, and the high severity Euro NCAP pulse shown in Figure 52 is taken as the crash pulse, while b is kept the same with the previous runs. A trial and error process is used in order to obtain the d values to be almost equal. The resulting NIC_{max} values are presented in Table 5. The results obtained with the standard seat model using the same crash pulse and b value are also provided in this table as a baseline for comparison. From these results, it is found that once d is fixed,

NIC_{max} remains almost the same, verifying the one-to-one relationship obtained between NIC_{max} and *d* in Figure 66. In fact, the small difference in the NIC_{max} values of the two slidable seats is believed to be mainly due to the small difference in their *d* values. Assuming that the high severity Euro NCAP pulse is a good representative of the highest possible severity of the acceleration pulses that can be encountered in real life crashes where whiplash is the main concern, another remark is that when compared to the standard seat, a slidable seat with an F_b value in the order of 309 N and a *d* value of about 100 mm would significantly reduce the risk of whiplash injury. These values are believed to be reasonable for industrial use. However, the final decision on the selected parameters should be made through sled tests.

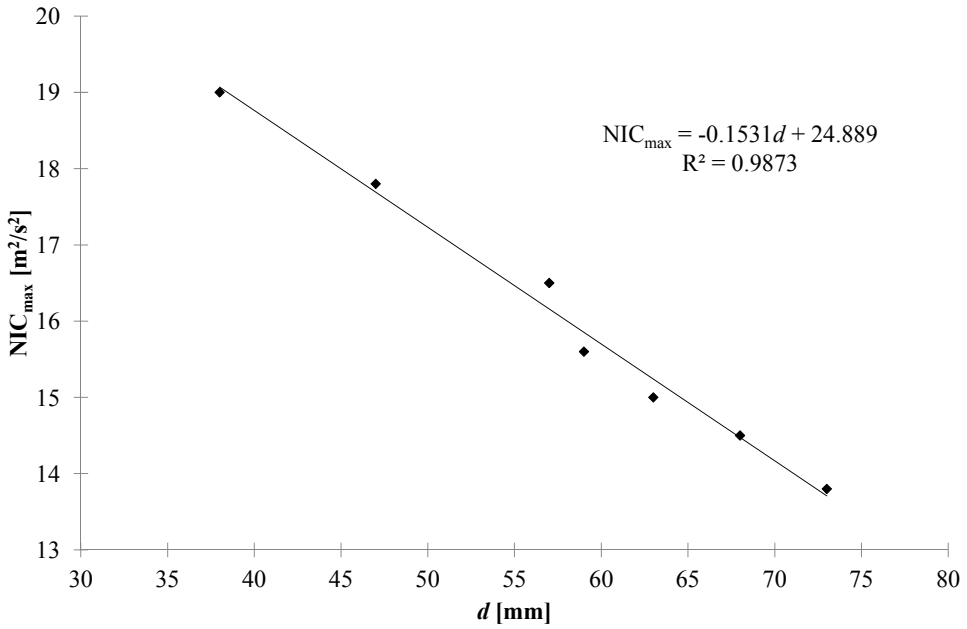

Figure 66 NIC_{max} vs. the seat's maximum sliding distance, *d* (F_b=320 N, *b*=59 mm)

These conclusions are important, especially due to the fact that a slidable seat may cause some unwanted side effects for the occupants sitting in the seats behind it, or, to remedy this problem, may require relatively larger vehicle interior volumes. For this reason the *d* value should be limited. However, the trade-off of this limitation is shown to be an increase in the NIC_{max} value, hence the injury risk. Therefore, a compromise should be found between *d* and the injury risk.

Table 5 The performances of slidable seats that have different *k* and *c* values, but same *d* value (F_b=309 N, *b*=59 mm)

k (N/m)	*c* (Ns/m)	*x* (mm)	*d* (mm)	NIC_{max} (m^2/s^2)
3000	296	103	102	21.88
4000	253	77	103	21.77
	Standard seat			28.65

4.4 Selection of the System

Although the second alternative promises good performance in the sense of avoiding whiplash injuries, the backward movement of the seat may bring out adverse effects on the passengers sitting on the rear seat. For this reason, such a system may not be preferable. In the rest of this thesis, the first alternative will be investigated in detail.

CHAPTER 5

TWO NOVEL ANTI-WHIPLASH VEHICLE SEAT MECHANISMS BASED ON REDUCING BACKSET

In this chapter, two different and novel vehicle seat mechanisms are proposed for preventing whiplash injury. Both systems rely on the principle of reduced backset, and can be considered under the group of systems where the head restraint is moved forward by a mechanical trigger mechanism.

5.1 An Anti-whiplash Vehicle Seat Mechanism Having a Lock

In systems where the head restraint is moved forward by a mechanical trigger mechanism, the force applied to the back rest by the occupant as a result of the crash is used as the system input. However, since the performance of these systems in general directly depends on the force applied by the occupant on the back rest and the maximum value of the force applied on the back rest may be reached before the time that the head should be supported by the headrest, the headrest may be in backward return motion during the time that the head should be supported by the headrest, and might not provide the required support. Besides, the force acting on the back rest may not wholly fall on the upper back region, which is generally foreseen, but instead, a fraction of this force may fall also on the lumbar region, as a result of that some of these systems may not function properly. Furthermore, in these systems, after the headrest is brought to its forwardmost position, it is desired to be kept at this position with the aid of the force being applied by the occupant on the back rest. Nevertheless, under the forces caused as a result of the head hitting the headrest, in cases wherein the forces applied on the back rest by the occupant are not sufficient, the headrest may move backwards again, and the head and the neck of the occupant cannot be supported sufficiently.

However, the performance of the system proposed in this section does not directly depend on the force applied by the occupant on the back rest with the effect of the rear end collision, but the system operates independently from the magnitude of the said force or its change in time and provides the same support to the occupant's head under all conditions after this force exceeds the threshold value that is predetermined to activate the system. This is achieved with the accomplishment of a lock release action within the system.

The proposed vehicle seat (K) with an anti-whiplash mechanism having a lock (1) comprises (referring to Figure 67 through Figure 77)

- at least one back rest (2) of the seat (K) which supports the back of the occupant,
- at least two side sheet members (21) which are located at the left and right of the back rest (2) construction,
- at least one upper traverse (22) which is located between the side sheet members (21) of the back rest (2) construction and connects the side sheet members (21) from their upper sides to each other,
- at least one headrest (3) which supports the head and neck of the occupant at the top of the back rest (2),
- at least one lower assembly (4) which is present within the back rest (2) and pivoted to the side sheet members (21) of the back rest (2) construction,
- at least one back plate (41), which is one of the members forming the lower assembly (4), on which the force applied by the occupant on the back rest (2) falls,
- at least one back plate tube (42) to which the back plate (41) is fixed, preferably with screws,
- at least one cable connection bracket (43) which is fixed, preferably welded, to the back plate tube (42),
- at least two back plate brackets (44), being one on the left and one on the right, which are fixed to the back plate (41) and the back plate tube (42), preferably with screws and nuts, which form the lower assembly (4) together with the back plate (41), back plate tube (42) and the cable connection bracket (43), and enable the lower assembly (4) to be pivoted to the side sheet members (21) of the back rest (2) construction by being rotatably mounted on the side sheet members (21) of the back rest (2) construction,
- at least two back plate springs (5), being on each side between the back plate brackets (44) and the spring lower connection points present on the side sheet members (21) of the back rest (2) construction, which have a pre-tension that will allow the lower assembly (4) to rotate backwards upon the application of a threshold force that is predetermined to occur as a result of only a rear impact to the back rest (2) by the occupant,

- at least two stopper pins (6), being one on each side, which are fixed, preferably welded, to the side sheet members (21) of the back rest (2) construction, on which the back plate brackets (44) bear under normal driving conditions and by this means enable the lower assembly (4) to rest at its nominal position despite the pre-tensioned back plate springs (5),
- at least one stopper shaft (7) on which lower assembly (4) bears and stops after it rotates backwards a predetermined sufficient amount with the effect of the force applied on the back rest by the occupant as a result of the rear-end collision, and which is fixed, preferably welded, to both of the side sheet members (21) of the back rest (2) construction,
- at least one upper assembly (8) which carries the headrest (3) and which is pivoted to the side sheet members (21) of the back rest (2) construction,
- at least two headrest support tubes (81) which are on left and right, and to which the headrest (3) is mounted,
- at least one headrest tube (82) to which the headrest support tubes (81), amongst the components forming the upper assembly (8), are fixed, preferably welded,
- at least one lock bracket (83) which is fixed, preferably welded, to the headrest tube (82),
- at least two headrest tube brackets (84), being one on the left and one on the right, which are fixed, preferably welded, to the headrest tube (82), which form the upper assembly (8) together with the headrest support tubes (81), headrest tube (82) and the lock bracket (83), and enable the upper assembly (8) to be pivoted the side sheet members (21) of the back rest (2) construction by being mounted rotatably to the side sheet members (21) of the back rest (2) construction,
- at least two headrest springs (9) which have enough pre-tension to rotate the upper assembly (8) and the headrest (3) it carries forward when the trigger lock (10) is released, and hold the headrest (3) at this forwardmost position when the predetermined forward movement amount is acquired under the forces that will occur as a result of the contact of the head with the headrest (3), and which are located on both sides between the headrest tube (82) spring connection points and the upper traverse (22) spring connection points,
- at least one trigger lock (10) which enables the upper assembly (8) and the headrest (3) it carries to rest at their nominal position under normal driving conditions despite the pre-tensioned headrest springs (9), and by being released allows the upper assembly (8) and the headrest (3) it carries to be rotated forward by the headrest springs (9) after the lower assembly (4) rotates backwards a predetermined sufficient amount with the effect of the force applied by the occupant on the back rest as a result of the rear-end collision,

- at least one lock guide bracket (101), being one of the members forming the trigger lock (10), which is fixed to the upper traverse (22), preferably with screws and nuts,
- at least one lock guide (102) which is fixed, preferably welded, to the lock guide bracket (101),
- at least one lock pin (103) which enables the trigger lock (10) to have locking function by being grabbed by the lock bracket (83) under normal driving conditions, and enables the trigger lock (10) to be released by being pulled inside the lock guide (102) after the lower assembly (4) rotates backward a predetermined sufficient amount with the effect of the force applied by the occupant on the back rest (2) as a result of the rear-end collision,
- at least one lock spring (104) which brings the lock pin (103) again to the locking position after the lock pin (103) is brought to the released position by being pulled inside the lock guide (102), and which has a sufficient amount of pre-compression to compensate the losses resulting from the friction,
- at least one cable upper holder (105) which is fixed to the end of the lock guide (102),
- at least two headrest housings (11) which are fixed on the upper traverse (22) and have such a form which will allow the upper assembly (8) to rotate forward a predetermined amount when it is operated, and through which the headrest support tubes (81) pass,
- at least one Bowden cable (12) the one end of the inner wire of which is fixed to the cable connection bracket (43), the other end of the inner wire of which is fixed to the lock pin (103), and the outer cable of which is fixed to the cable lower holder (121) and the cable upper holder (105), by this means which enables the trigger lock (10) to be released by the lower assembly (4) pulling the lock pin (103) inside the lock guide (102) while rotating backwards with the effect of the force applied by the occupant as a result of the rear-end collision,
- at least one cable lower holder (121) which is fixed, preferably welded, to at least one of the side sheet members (21) and to which the outer cable of the Bowden cable (12) is fixed.

When the force applied by the occupant to the back rest (2) as a result of the crash exceeds a predetermined threshold value and overcomes the pre-tension forces of the back plate springs (5), the lower assembly (4) rotates backwards around an axis passing through the points at which it is pivoted to the side sheet members (21) of the back rest (2) construction. While the end of the inner wire of the Bowden cable (12) attached to the cable connection bracket (43) is pulled backwards, the lock pin (103) to which the other end is attached is pulled inside the lock guide (102) with this backward rotation of the lower assembly (4). By this means the trigger lock (10) is released and the upper assembly (8) and the headrest (3) it carries rotate forward

around an axis passing through the points at which they are pivoted to the side sheet members (21) of the back rest (2) construction via the pre-tensioned headrest springs (9) until the headrest support tubes (81) bear on the front walls of the headrest housings (11). The lock bracket (83) is designed such that it blocks the front of the lock guide (102) in this position of the mechanism (1) and will not allow the lock pin (103), which is being pushed by the lock spring (104) to its former position before the accident, to be swept off. With a sufficient amount of pre-tension given to the headrest springs (9), the headrest (3) does not move backward with the effect of the forces it is subjected to as a result of its contact with the head in its forwardmost position, and maintains this position.

A sufficient amount of pre-tension is given to the back plate springs (5) in order to avoid the operation of the mechanism (1) with the forces applied by the occupant on the back rest (2) under normal conditions.

The mechanism (1) can be made ready to operate again by the occupant pushing the headrest (3) backwards after the accident until the headrest support tubes (81) again bear on the back walls of the headrest housings (11). After the headrest (3) and the upper assembly (8) are pushed to their nominal position in this manner, the front of the lock guide (102) is unblocked, and the lock pin (103) pushed out of the guide (102) by the lock spring (104) is grabbed by the lock bracket (83), and the trigger lock (10) is locked again. The back plate springs (5) bring the lower assembly (4) to its nominal position before the accident by rotating it forward until the back plate brackets (44) again bear on the stopper pins (6).

Since no component that is plastically deformed is used within the mechanism (1), the mechanism (1) can be made ready to use again after the accident without requiring any additional cost.

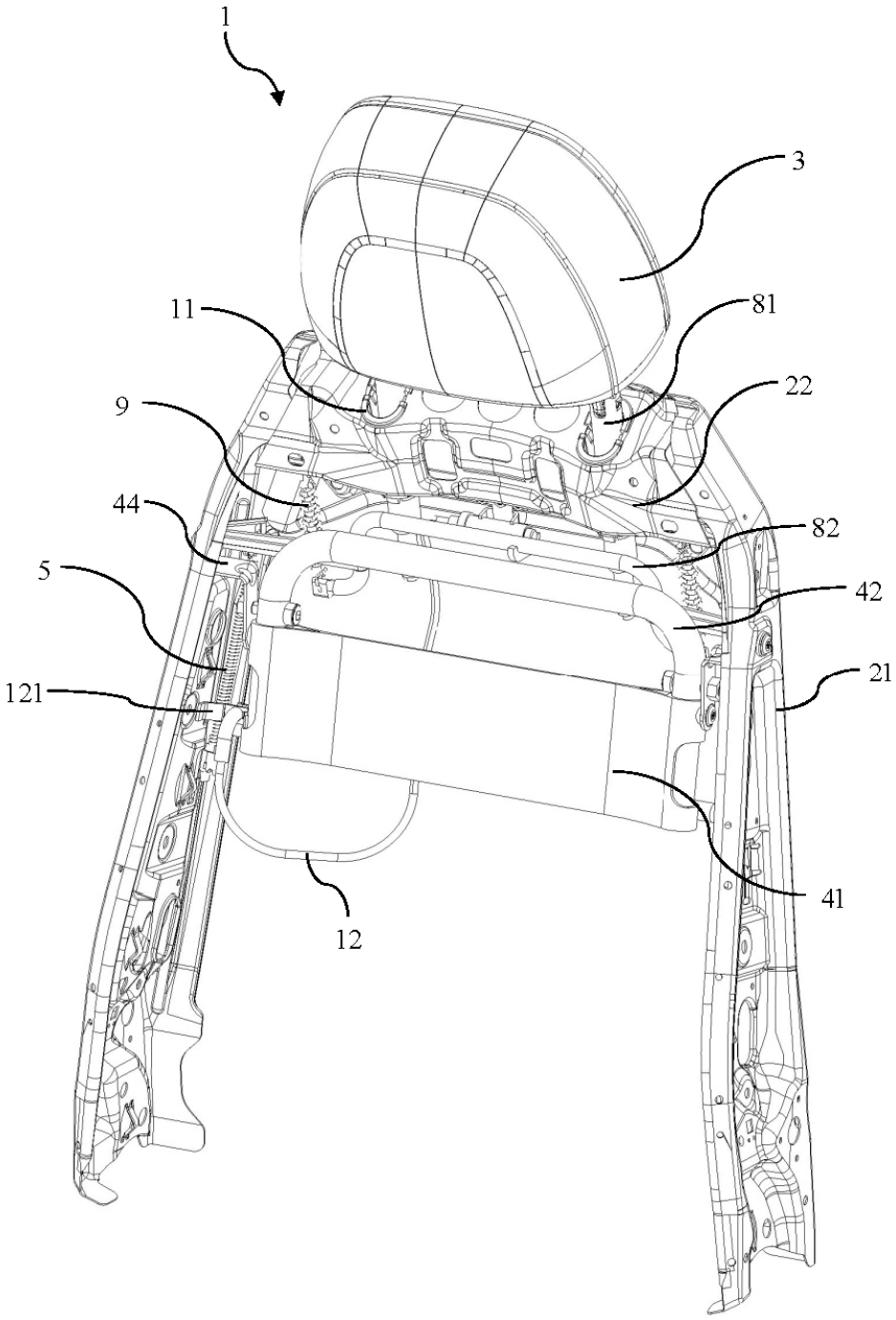

Figure 67 Front perspective view of the vehicle seat mechanism

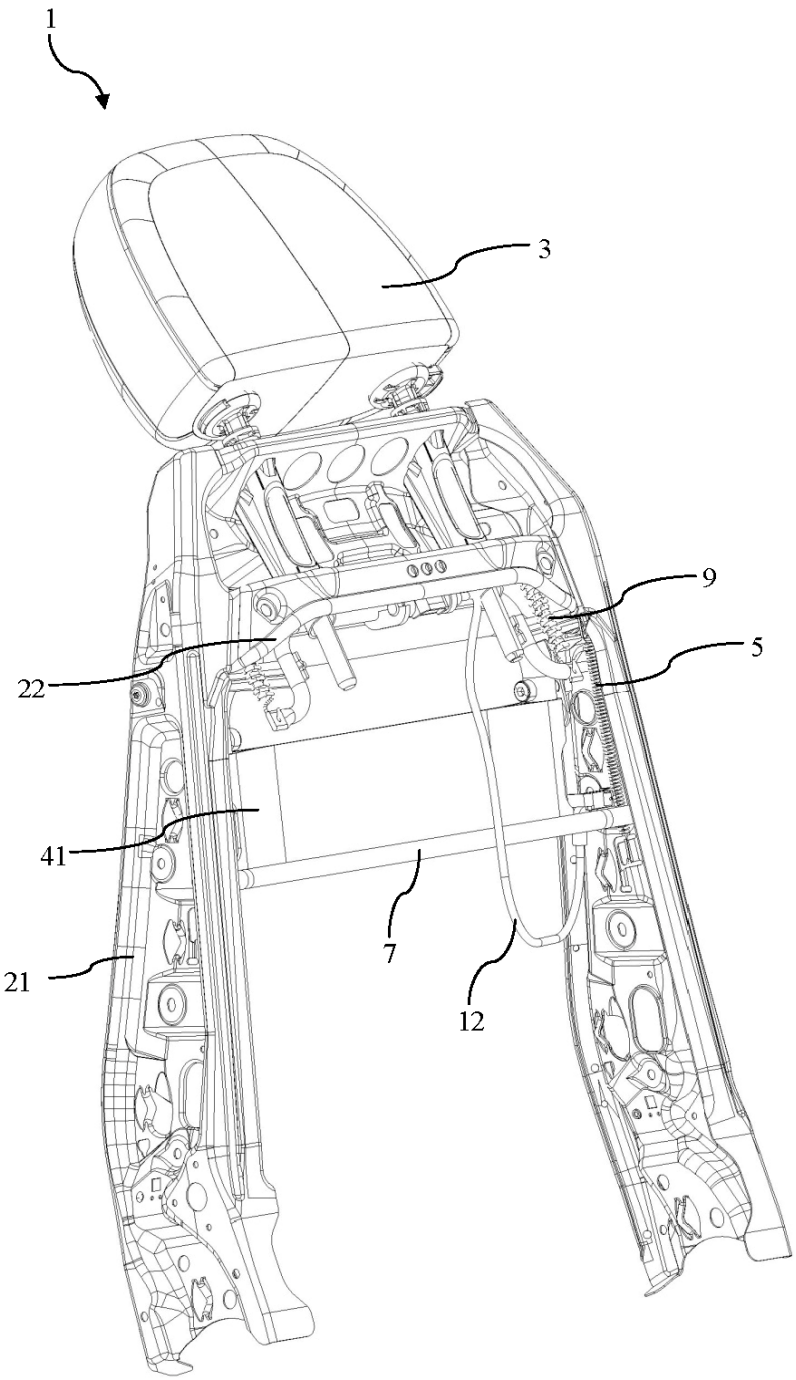

Figure 68 Rear perspective view of the vehicle seat mechanism

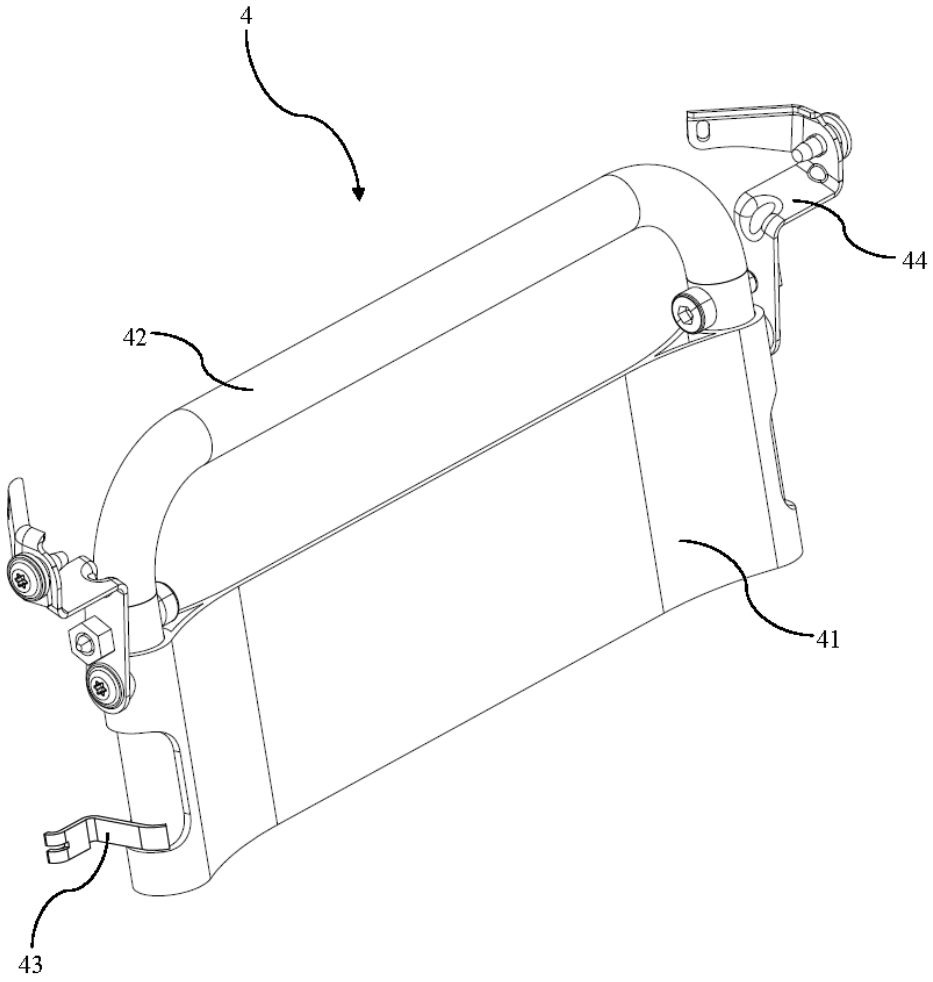

Figure 69 Perspective view of the lower assembly

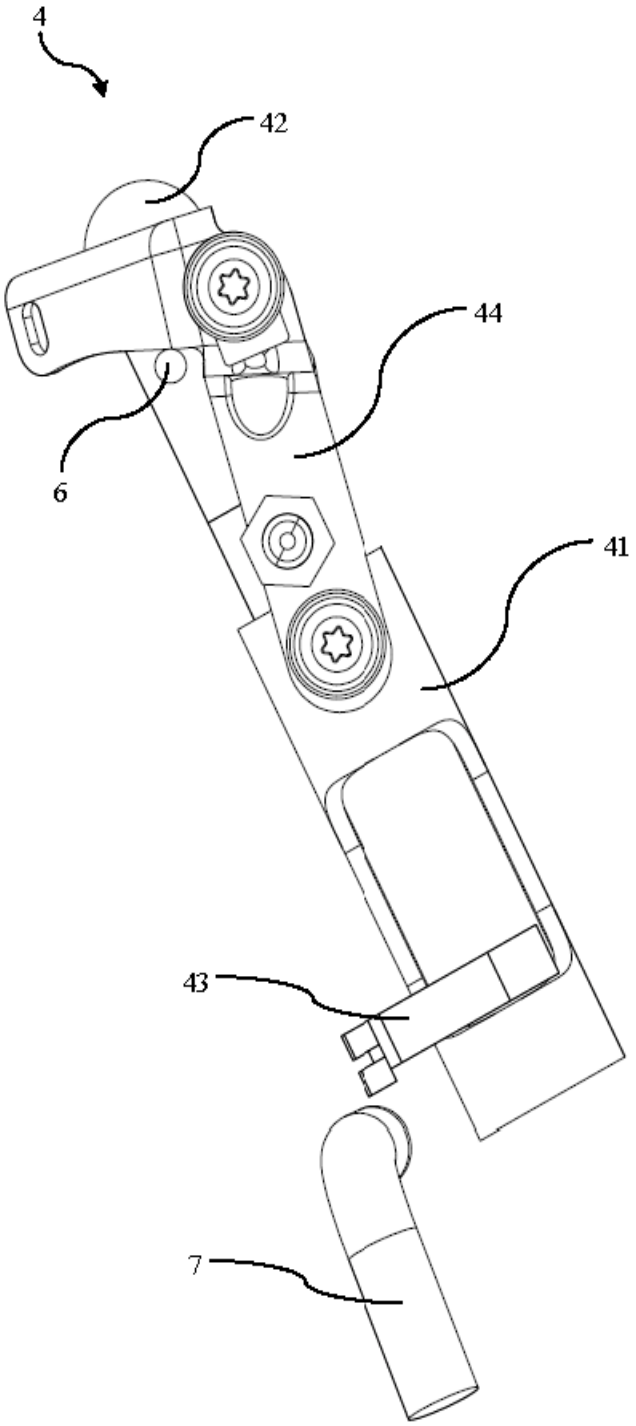

Figure 70 Right side view of the lower assembly before accident

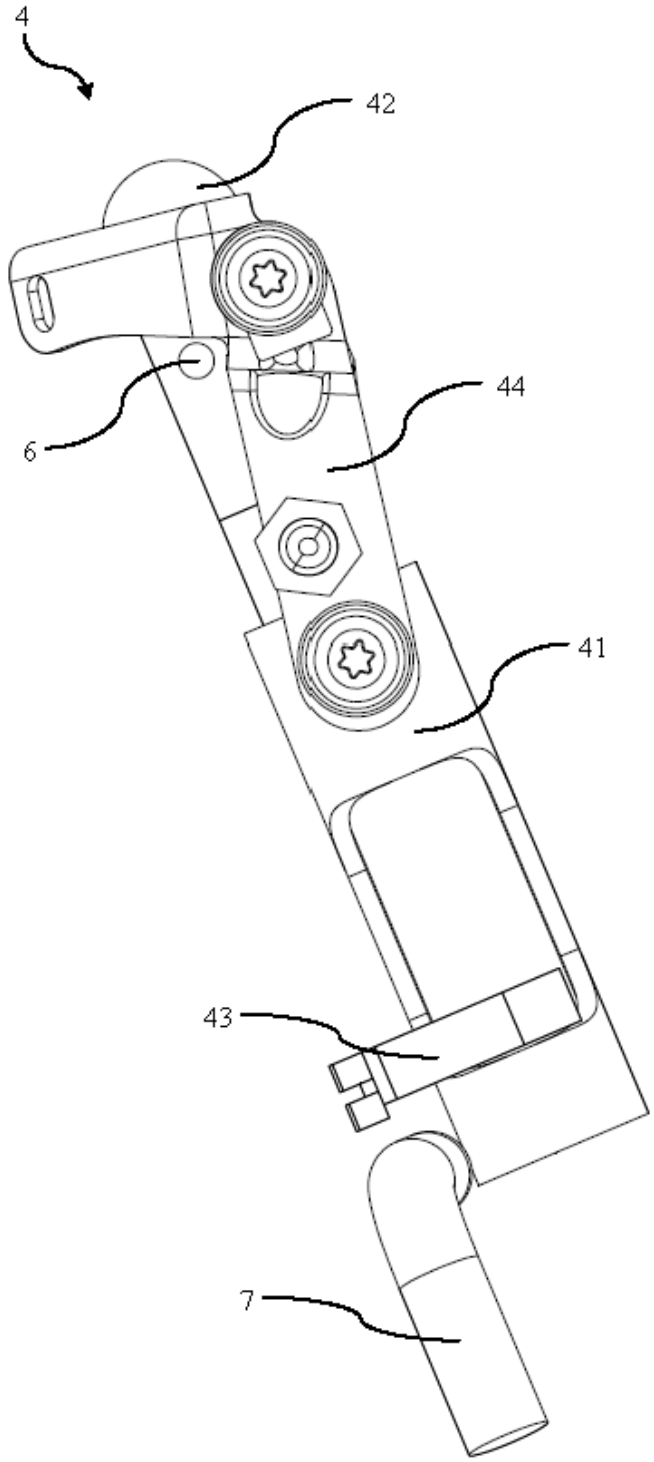

Figure 71 Right side view of the lower assembly after accident

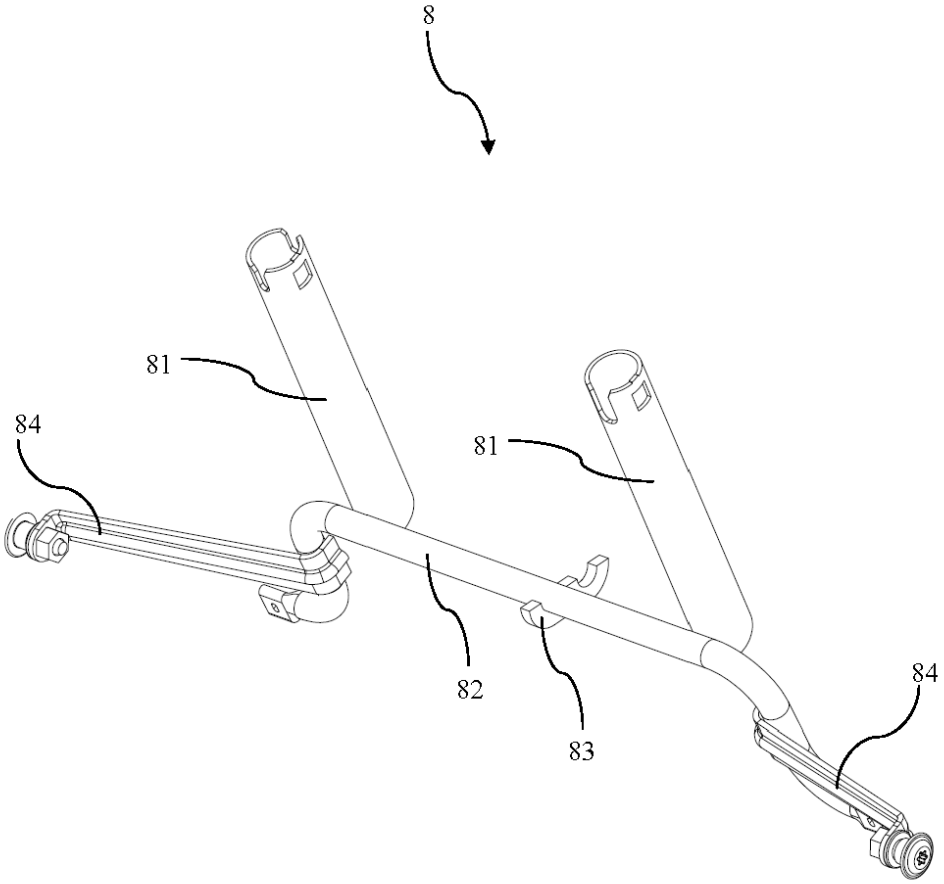

Figure 72 Perspective view of the upper assembly

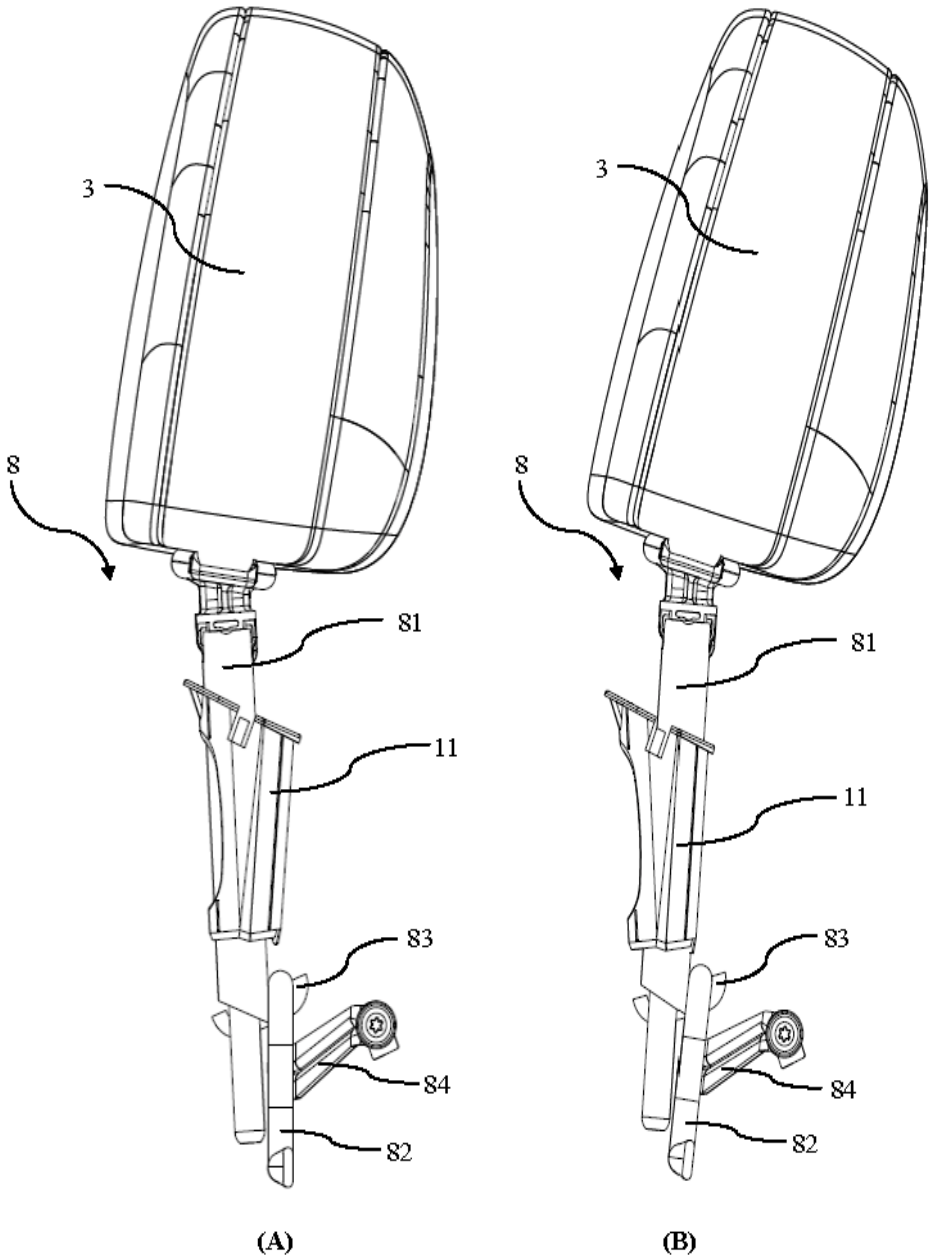

Figure 73 Right side view of the upper assembly before accident (A) and after accident (B)

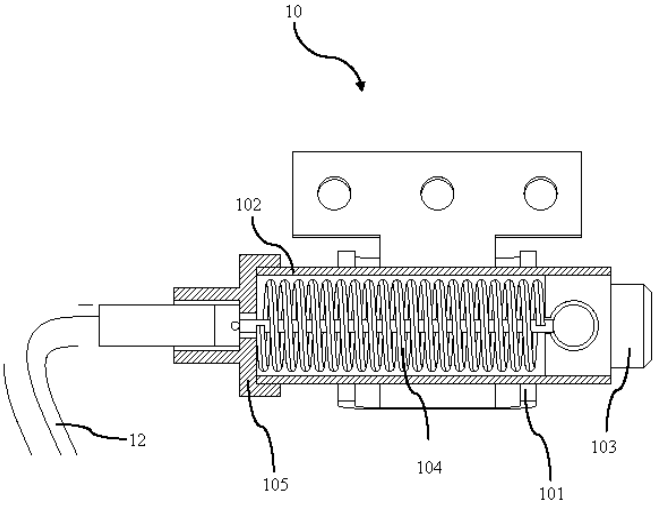

Figure 74 Detailed front view of the trigger lock

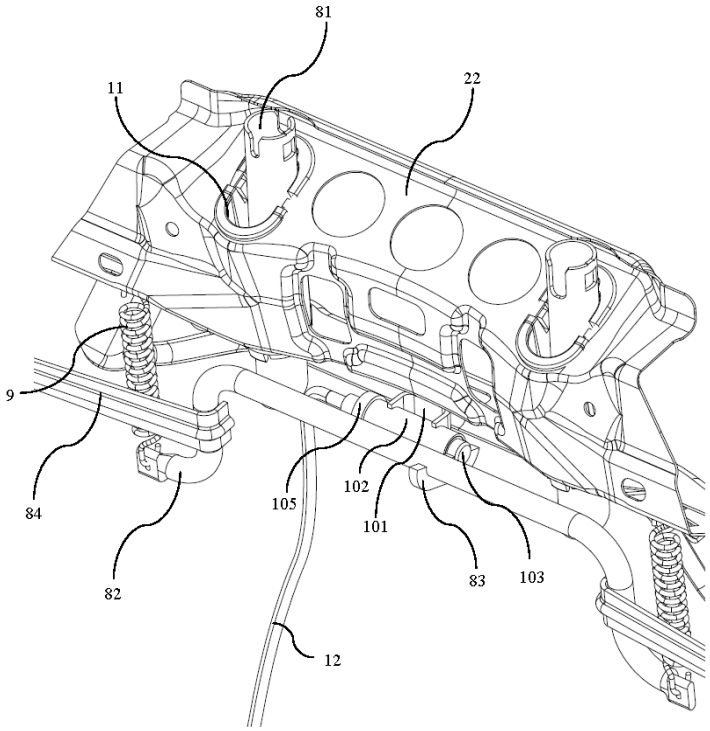

Figure 75 View of the trigger lock holding the upper assembly in its nominal position under normal driving conditions

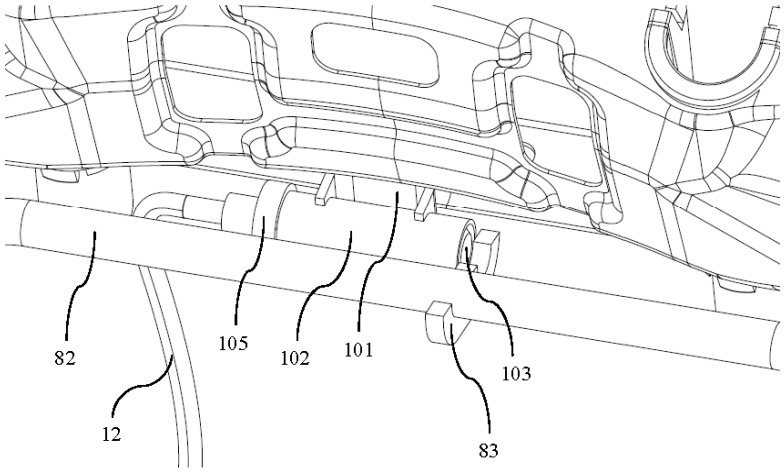

Figure 76 View of the trigger lock at the moment when it is released by the Bowden cable after the lower assembly moves backwards

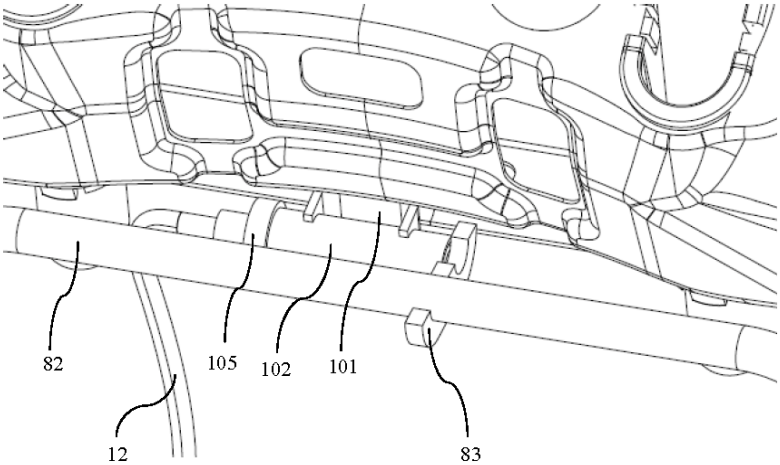

Figure 77 View of the trigger lock after the released upper assembly is rotated forward by the headrest springs

An alternative embodiment (100) of the anti-whiplash vehicle seat mechanism (1), in addition to the components forming the mechanism (1), comprises (referring to Figure 78 through Figure 83)

- at least one secondary lock bracket (13) which is fixed, preferably welded, to the headrest tube (82) in addition to the lock bracket (83) (two of them are shown in the accompanied figures),
- at least one secondary lock (14) which is locked to maintain the position of the headrest (3) when the upper assembly (8) and the headrest (3) are brought to their frontmost position by being rotated forward by the headrest springs (9) upon the rear-end collision,
- at least one secondary lock guide bracket (141), being one of the components forming the secondary lock (14), which is fixed, preferably with screws and nuts, to the upper traverse (22) in addition to the lock guide bracket (101),
- at least one secondary lock guide (142) (two of them are shown in the accompanied figures) which forms a prismatic joint with the secondary lock pin (143), which is fixed, preferably welded, to the secondary lock guide bracket (141), and to one end of which secondary lock guide cap (145) is fixed and on the other end of which the secondary lock pin (143) is present,
- at least one secondary lock pin (143) (two of them are shown in the accompanied figures) which lies inside the secondary lock guide (142) under normal driving conditions, and which is forced out of the secondary lock guide (142) by the secondary lock spring (144) when the upper assembly (8) and the headrest (3) arrive at their frontmost position during accident,
- at least one secondary lock spring (144) (two of them are shown in the accompanied figures) which has a sufficient amount of pre-compression to push the secondary lock pin (143) out of the secondary lock guide (142) when the upper assembly (8) and the headrest (3) arrive at their frontmost position, and which lies inside the secondary lock guide (142) between the secondary lock guide cap (145) and the secondary lock pin (143),
- at least one secondary lock guide cap (145) (two of them are shown in the accompanied figures) which is fixed to one end of the secondary lock guide (142) and through the hole on which (preferably at its center) the secondary lock reset wire (146) passes,
- at least one secondary lock reset wire (146) (two of them are shown in the accompanied figures) which is fixed to the secondary lock pin (143) from one end, and the other end of which extends out of the seat (K) such that the occupant can pull it for resetting the mechanism (100).

In the alternative vehicle seat mechanism (100), being different from the vehicle seat mechanism (1), after the headrest (3) arrives at its frontmost position, it is not kept at this position by the pre-tensioned headrest springs (9), but by the locking of

the secondary lock (14). The pre-tension is given to the headrest springs (9) only for the purpose of moving the headrest (3) forward after the trigger lock (10) is released.

In normal driving conditions, secondary lock pin (143) lies inside the secondary lock guide (142) such that it is being forced out of the secondary lock guide (142) by the pre-compressed secondary lock spring (144). In order to enable the secondary lock pin (143) to remain in its guide (142), the secondary lock bracket (13) is designed such that it is positioned in front of the secondary lock pin (143) in nominal position of the mechanism (100).

When the trigger lock (10) is released upon the rear-end collision and the upper assembly (8) and the headrest (3) are brought to the frontmost position by the pre-tensioned headrest springs (9), the front of the secondary lock pin (143) becomes free, and the secondary lock pin (143) is pushed out of the secondary lock guide (142) by the pre-compressed secondary lock spring (144). The secondary lock pin (143) pushed out of its guide (142) is grabbed by the secondary lock bracket (13), and the upper assembly (8) and the headrest (3) are locked in this frontmost position against rotating backwards under the forces resulted from the contact of the head.

For making the alternative vehicle seat mechanism (100) operable again after the accident, being different from the vehicle seat mechanism (1), first, the secondary lock reset wire (146) is pulled by the occupant before pushing the headrest (3) backwards in order to enable the secondary lock pin (143) to be pulled inside the secondary lock guide (142), then the headrest (3) is pushed backwards while the secondary lock reset wire (146) is being pulled.

The alternative mechanism (100) also does not comprise a component which is plastically deformed.

Both design alternatives presented in this section are on-off systems and preparing both of them for re-use necessitates user effort. If the user cannot re-set-up the system properly, this will deteriorate the driving comfort.

For this reason, it is believed to be very beneficial to eliminate the lock(s) from the system in order to have a continuous system that autonomously re-sets-up itself for reuse. Such a continuous system is proposed in the following section.

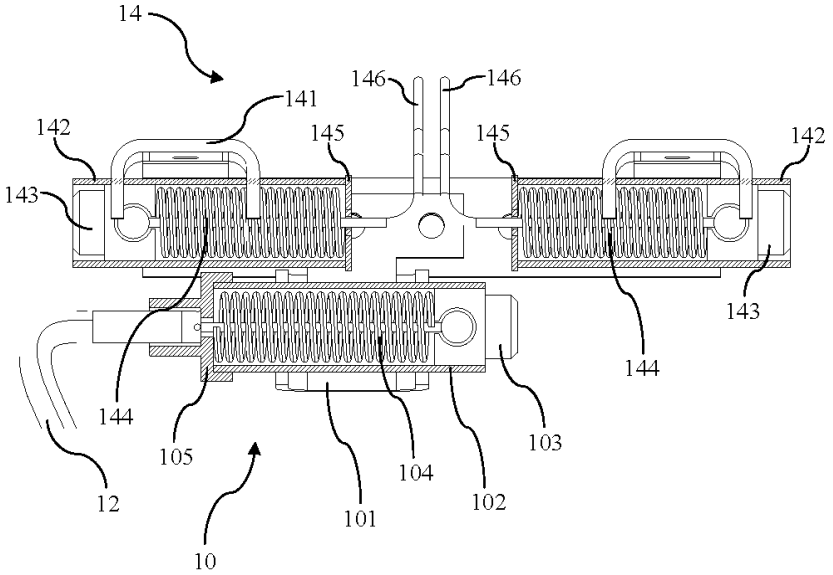

Figure 78 Detailed front view of the alternative secondary lock

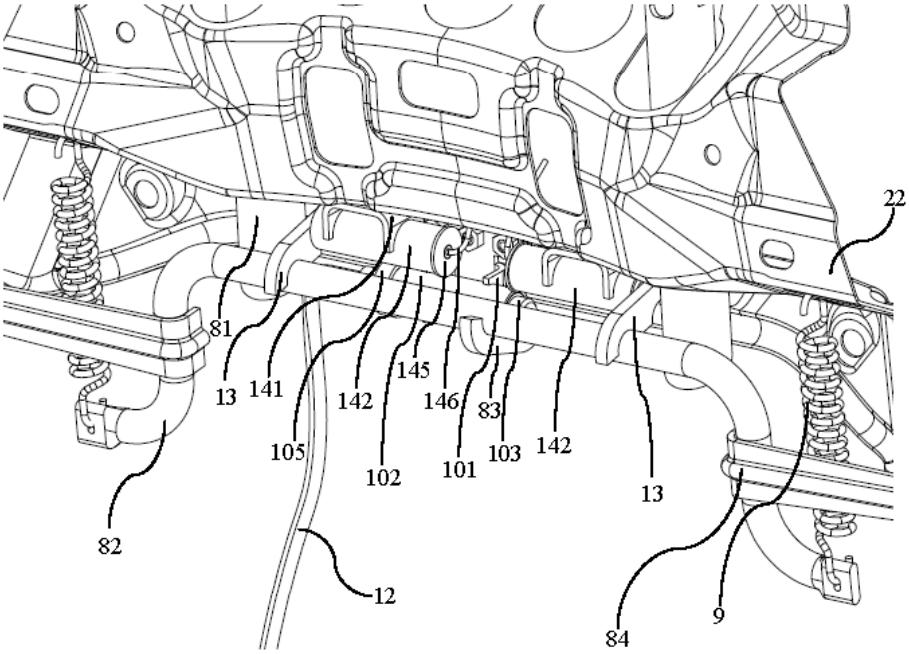

Figure 79 Front perspective view of the alternative secondary lock

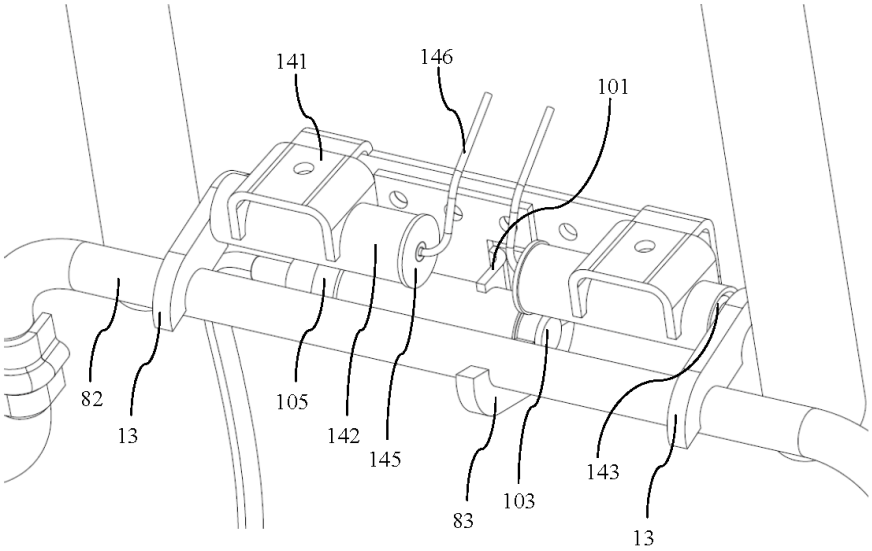

Figure 80 View of the alternative secondary lock at its nominal configuration under normal driving conditions

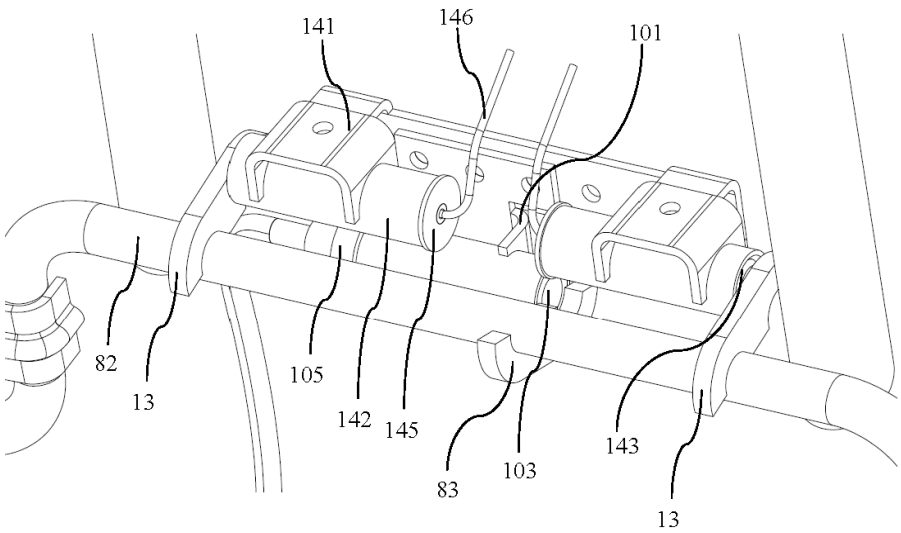

Figure 81 View of the alternative secondary lock at the moment when the trigger lock is released by the Bowden cable after the lower assembly rotates backwards

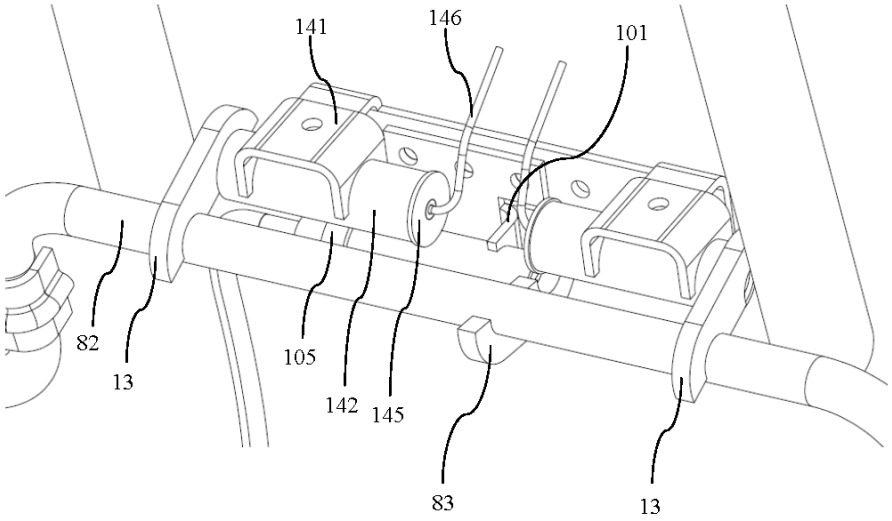

Figure 82 View of the alternative secondary lock after the released upper assembly is rotated forward by the headrest springs

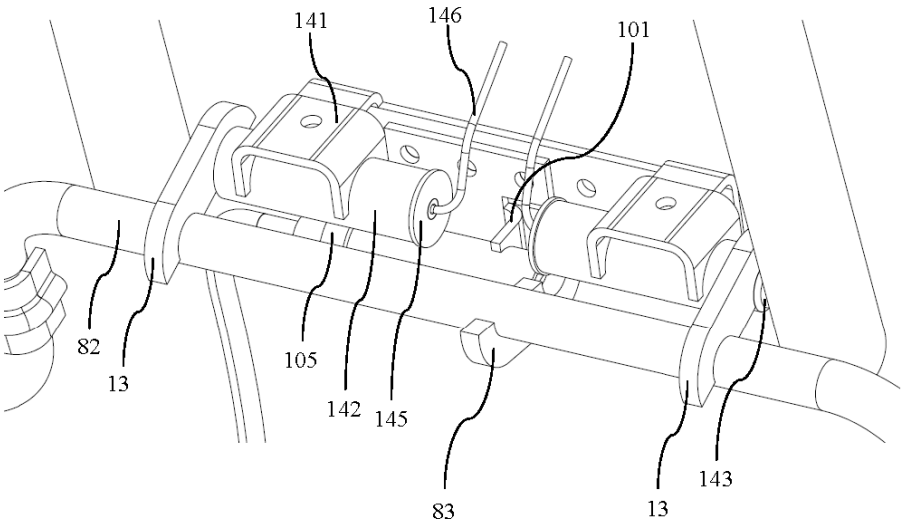

Figure 83 View wherein the alternative secondary lock locks the upper assembly at its frontmost position brought by the headrest springs

5.2 An Anti-whiplash Vehicle Seat with a Quick Forward Anti-whiplash Mechanism

In systems where the head restraint is moved forward by a mechanical trigger mechanism, the force applied to the back rest by the occupant as a result of the crash is usually used as the system input. In this kind of systems, usually a back plate lying underneath the back rest cushion is pushed backwards upon leaning of the occupant into the back rest as a result of the crash, and with the aid of a mechanism (a simple lever, four-bar mechanism, inverted slider-crank mechanism, etc.), this backwards movement gained by the back plate is transmitted to the headrest, thus the headrest is enabled to move forward. However, the time it takes for the headrest to complete this forward movement and support the head and neck of the occupant has a crucial importance on preventing whiplash syndrome. Reducing this time, which is determined by the kinematics and the dynamics of the mechanism used to move the headrest forward, will increase the performance of the system and provide an important advantage for avoidance of possible neck injuries. In the proposed system presented in this section, this is achieved by the use of a quick forward mechanism in vehicle seats in order to rotate the headrest forward during rear impact with appropriately chosen link dimensions and joint types.

Quick return mechanisms are commonly used in shaping machines. This mechanism converts the rotary motion of the disc to a reciprocating motion of the arm (Figure 84). As the drive disc rotates, the output arm moves back and forth. However, these forward and backward motions of the arm are at different rates. Through the full cycle of the mechanism, the amount of the rotation of the disc required to make the arm rotate backwards is relatively much smaller than the amount of the rotation of the disc required for the forward rotation of the arm. A quick return mechanism may easily be converted into a quick forward mechanism by simply reversing the direction of the rotation of the drive disc.

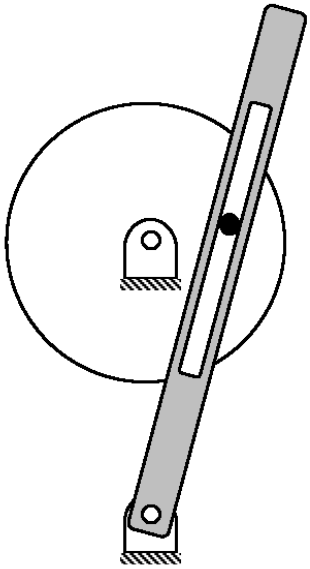

Figure 84 A quick return mechanisms

Referring to Figure 85 through Figure 88, the proposed vehicle seat with a quick forward anti-whiplash mechanism (1) comprises

- at least one back rest (2) at its back which supports the back of the occupant,
- at least two side sheet members (21) which are located at the left and right of the back rest (2),
- at least one upper traverse (22) which forms the upper skeleton of the back rest (2),
- at least one headrest (3) which is present on the upper part and supports the head and neck of the occupant,
- at least one lower assembly (4) which is present within the back rest (2) and pivoted to the side sheet members (21) of the back rest (2) construction,
- at least one back plate (41) which is one of the members forming the lower assembly (4) on which the force applied by the occupant on the back rest (2) falls,
- at least one back plate tube (42) on which the back plate (41) is fixed,
- at least two back plate brackets (43) being one on the left and one on the right which compose the lower assembly (4) together with the back plate (41) and the back plate tube (42), and enable the lower assembly (4) to be mounted pivotally on the side sheet members (21) of the back rest (2) construction,

- at least two joint pins (44), each of which is fixed on one of the back plate brackets (43),
- at least one upper assembly (5) on which the headrest (3) is mounted,
- at least two headrest support tubes (51) on the left and right which are supporting the headrest (3),
- at least one headrest tube (52) on which the headrest support tubes (51) are fixed,
- at least two spring upper connection brackets (53) which are fixed on the left and right of the headrest tube (52),
- at least two headrest tube brackets (54) being one on the left and one on the right which comprise the upper assembly (5) together with the headrest support tubes (51), headrest tube (52) and the spring upper connection brackets (53), and enable the upper assembly (5) to be pivotally mounted on the side sheet members (21) of the back rest (2) construction, each of which is fixed to the headrest tube (52), and which has a pivotally-sliding connection with the joint pins (44) fixed on the back plate brackets (43) via the slots present thereon,
- at least two springs (6) being on each side between the spring upper connection brackets (53) and the spring lower connection points present on the side sheet members (21) of the back rest (2) construction, which have a pre-tension that will allow the lower assembly (4) to rotate backwards upon the application of a threshold force that is predetermined to occur as a result of only a rear impact to the back rest (2) by the occupant,
- at least two headrest support tube housings (7) which are fixed on the upper traverse (22) of the back rest (2) construction and have such a form which will allow the upper assembly (5) to rotate forward a predetermined amount when it is operated, and through which the headrest support tubes (51) pass.

When the force applied by the occupant to the back rest (2) as a result of the crash exceeds a predetermined threshold value and overcomes the pre-tension forces of the springs (6), the lower assembly (4) rotates backwards (in direction of the arrow shown from A to B) around an axis passing through the points at which it is pivoted to side sheet members (21) of the back rest (2) construction. This backward movement is transmitted to the upper assembly (5) via the two degrees of freedom cylinder in slot joint between the slots present on the headrest tube brackets (54) and the joint pins (44) fixed on the back plate bracket (43), and the upper assembly (5) rotates forward around the axis (in direction of the arrow shown from C to D) passing through the points wherein it is pivoted to the side sheet members (21) of the back rest (2) construction. By this means, the headrest (3) supported by the headrest support tubes (51) also moves forward.

The mechanism is operated in the working range wherein the output link rotates faster than the input link so that the angle rotated by the output link /the angle

rotated by the input link ratio is achieved as high as required. Here, the input and output links refer to lower and upper assemblies (4, 5), respectively. After the crash, the mechanism is reversely operated by the springs (6), and it becomes ready to work again automatically without requiring any interference of the user.

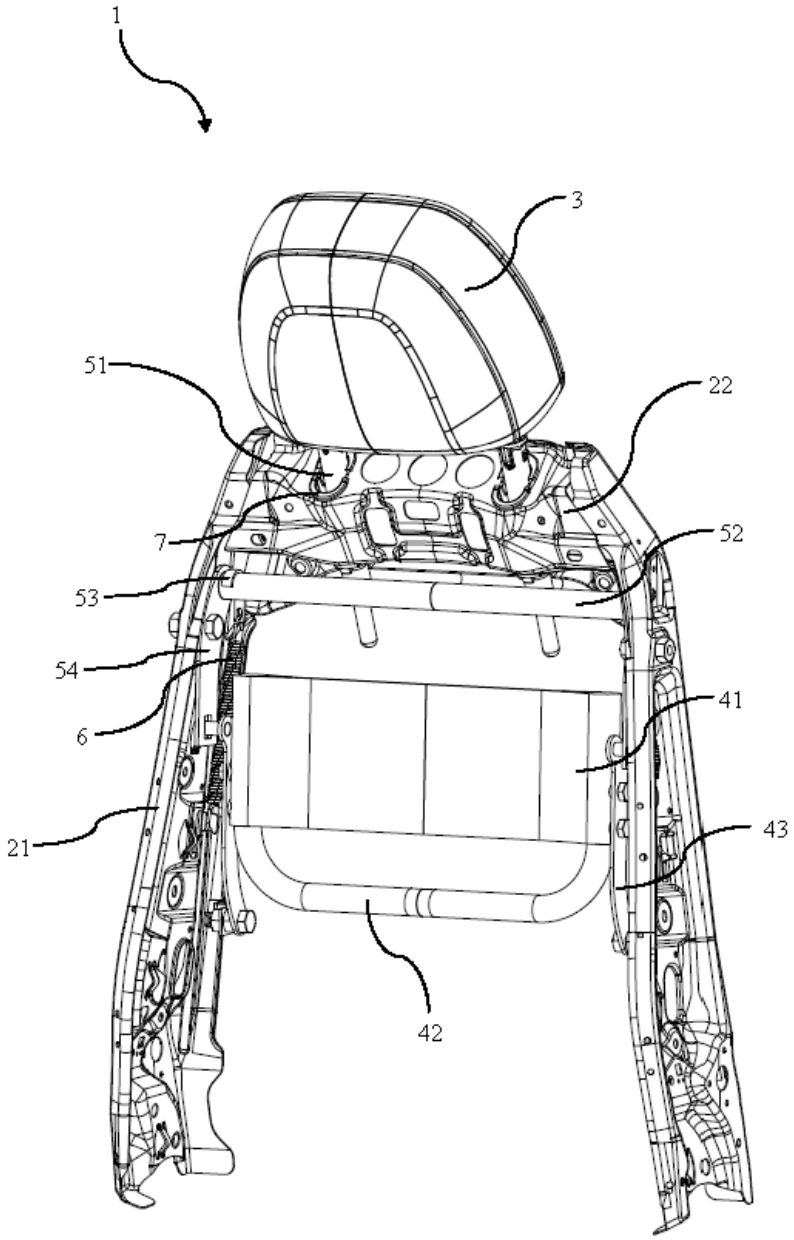

Figure 85 Perspective view of a vehicle seat with a quick forward mechanism

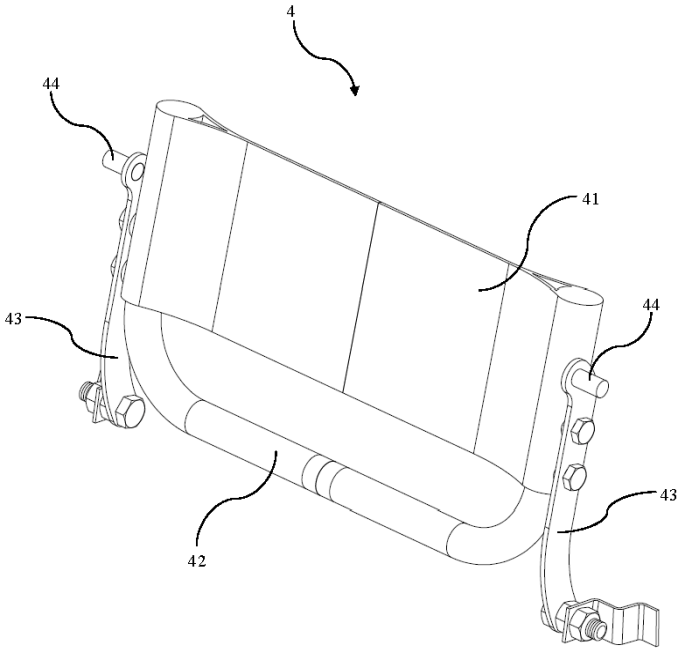

Figure 86 Detailed perspective view of the lower assembly

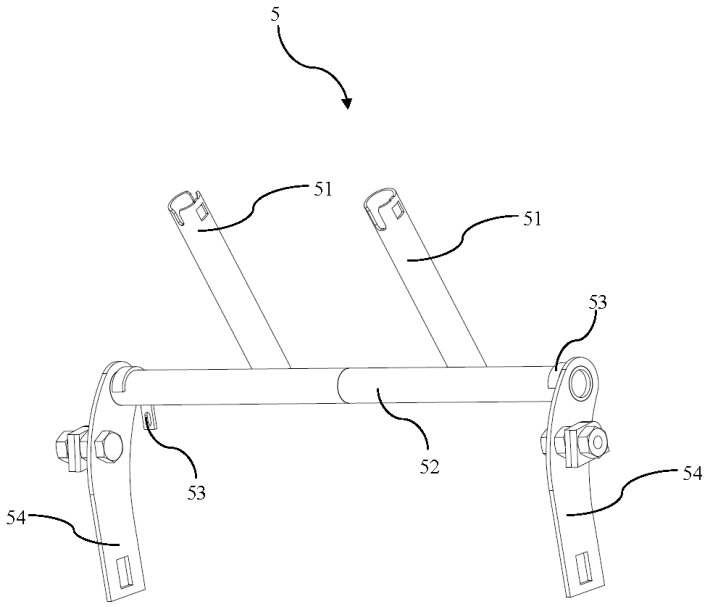

Figure 87 Detailed perspective view of the upper assembly

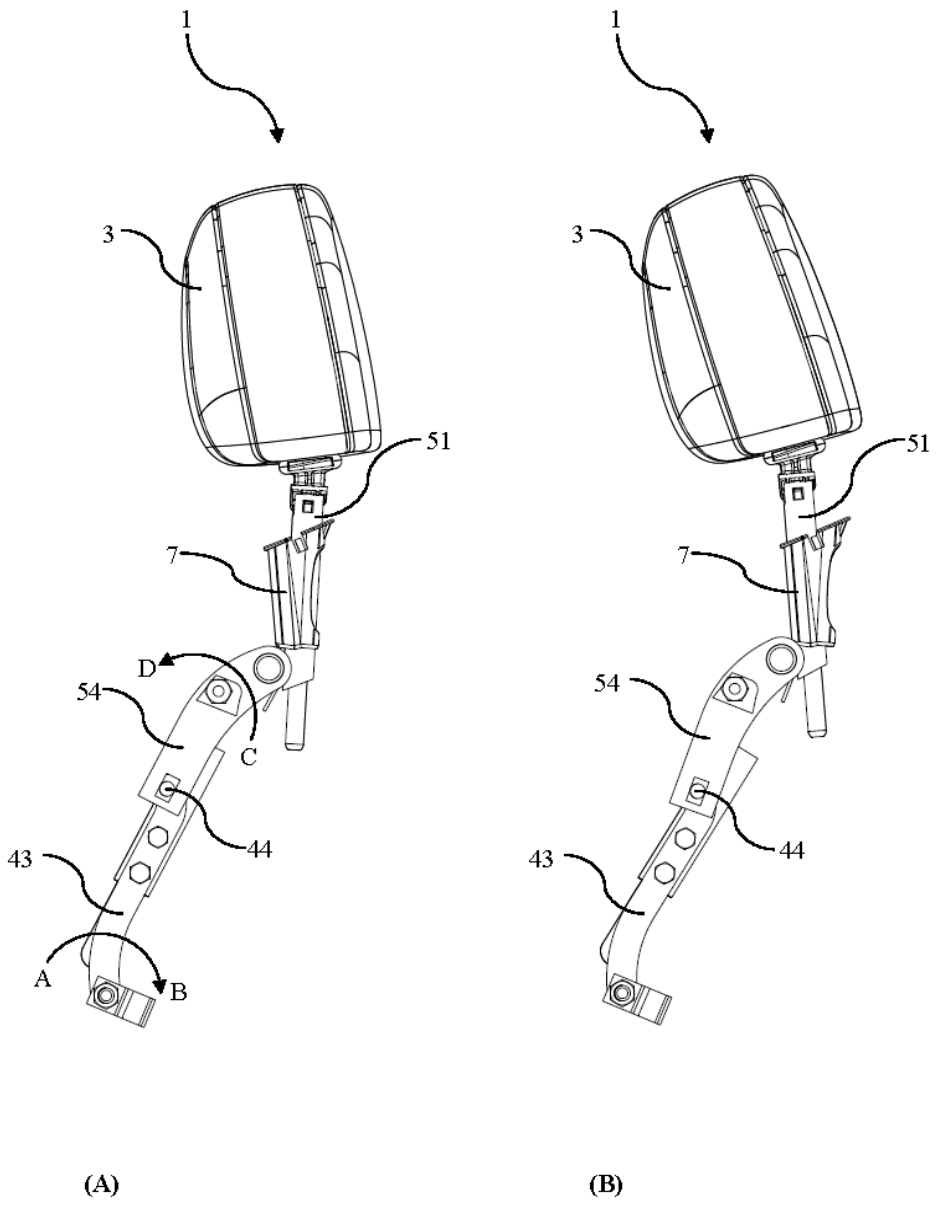

Figure 88 Left view of the seat before (A) and after (B) the crash, describing the working principle of the mechanism

5.3 Kinematic Synthesis and Analysis of the Quick Forward Anti-whiplash Seat Mechanism

A kinematic sketch of the quick forward anti-whiplash mechanism is shown in Figure 89. Here, link 2 and link 3 represent its lower and upper assemblies, respectively. The mechanism has one degree-of-freedom. θ_{12}, θ_{13} and s_{32} denote the joint variables of the mechanism, where $|B_0P_2| = s_{32}$. Let the link dimensions of the mechanism be labeled as $|A_0Q| = b_1$, $|QB_0| = c_1$ and $|A_0P_2| = a_2$.

The position level loop closure constraint equations can be written as

$$a_2 \cos\theta_{12} = b_1 + s_{32} \cos\theta_{13} \tag{5.1}$$

$$a_2 \sin\theta_{12} = c_1 + s_{32} \sin\theta_{13} \tag{5.2}$$

Leaving the terms including s_{32} alone on one side and dividing side by side yields

$$\tan\theta_{13} = \frac{a_2 \sin\theta_{12} - c_1}{a_2 \cos\theta_{12} - b_1} \tag{5.3}$$

Hence, θ_{13} can be obtained as

$$\theta_{13} = \operatorname{atan}_2\left(a_2 \sin\theta_{12} - c_1, a_2 \cos\theta_{12} - b_1\right) \tag{5.4}$$

Once θ_{13} is calculated through Eq. (5.4), s_{32} can be calculated either using Eqs. (5.1) or (5.2). For example, by using Eq. (5.1), one can write s_{32} as follows:

$$s_{32} = \frac{a_2 \cos\theta_{12} - b_1}{\cos\theta_{13}} \tag{5.5}$$

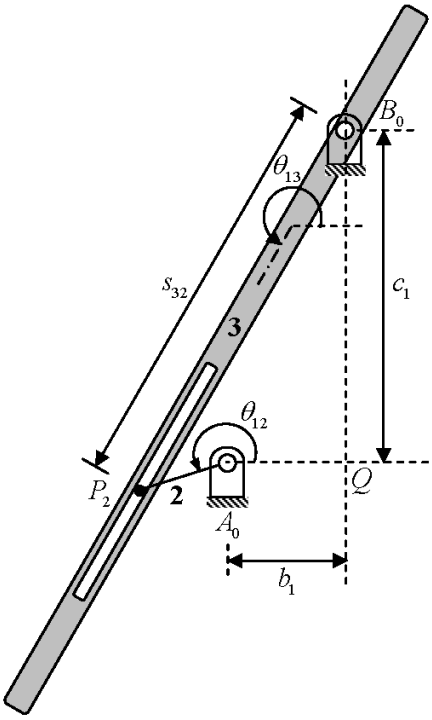

Figure 89 Kinematic sketch of the quick forward anti-whiplash mechanism

In this study, the kinematic parameters of the developed mechanism are selected considering the geometry of the backrest of the selected seat to which the mechanism is to be integrated. First of all, by examining the CAD data of the backrest with its cushion, it is determined that the backrest frame requires to make an angle of 27.6° in the clockwise direction with the vertical axis passing through its pivot point in order to yield a torso angle of 26.5°±2.5°, which is the target torso angle according to the Euro NCAP whiplash testing protocols. Since it is desired for the output link 3 to be parallel to the side members of the backrest frame with the aim of minimizing the interaction of the said link with the backrest cushion in normal seating posture, the initial value of θ_{13} is selected to be 242.4°, i.e., $\theta_{13}{}^{i} = 242.4°$. Then, considering the other attachments to the side members of the backrest frame like side airbags and ensuring that any disturbance to them is avoided, a suitable set of points is chosen on the side members for rotatably mounting the link 2 and link 3, respectively. After that, the required amount of the forward rotation of the output link 3 is determined to be 7.8° for about a 30-mm travel of the headrest in the forward direction, i.e., $\Delta\theta_{13} = \theta_{13}{}^{f} - \theta_{13}{}^{i} = 7.8°$, and hence, $\theta_{13}{}^{f} = 250.2°$. Finally, for a quick action, the ratio

$\Delta\theta_{13}/\Delta\theta_{12}$ is desired to be about -2, i.e., $\Delta\theta_{12} \approx -4°$ where $\Delta\theta_{12} = \theta_{12}{}^{f} - \theta_{12}{}^{i}$. Here, $\theta_{12}{}^{i}$ and $\theta_{12}{}^{f}$ denote the initial and final values of θ_{12} in the working range of the mechanism, respectively. It is worthwhile to mention at this point that the minus signs above indicate the clockwise rotation of the link 2 in opposition to the counterclockwise rotation of the link 3.

With all these design criteria stated above and the workspace constraints imposed by the geometry of the seat in mind, an iterative trial and error strategy is followed to select the link dimensions of the mechanism. As a result, they are determined to be as follows: $b_1 = 75$ mm, $c_1 = 205$ mm and $a_2 = 145$ mm.

According to these specifications, the full-cycle position analysis results are presented in Figure 90 and Figure 91. In the planned working range of the mechanism where $\theta_{13}{}^{i} = 242.4°$ and $\theta_{13}{}^{f} = 250.2°$, it is found out that $\theta_{12}{}^{i} = 73.7°$, $\theta_{12}{}^{f} = 69.8°$, $s_{32}{}^{i} = 74.25$ mm, $s_{32}{}^{f} = 73.29$ mm and $\Delta s_{32} = s_{32}{}^{f} - s_{32}{}^{i} = -0.96$ mm (see Figure 92 and Figure 93). Here, $s_{32}{}^{i}$ and $s_{32}{}^{f}$ denote the initial and final values of s_{32} in the working range of the mechanism, respectively.

An examination of Figure 90 shows that, with $\theta_{12}{}^{i} = 73.7°$ and $\theta_{12}{}^{f} = 69.8°$, the mechanism is operated in the quick forward phase as it is planned. With these concluding comments, the kinematic synthesis and analysis of the mechanism is completed.

5.4 Assessment of the Quick Forward Anti-whiplash Seat Mechanism

Assessment of the developed quick forward anti-whiplash seat mechanism is based on the sled tests performed at the METU-BILTIR Center Vehicle Safety Unit which are presented in Chapter 6. Three different types of vehicle seats are tested for this purpose. Among these, one type is the prototype seat with the developed quick forward anti-whiplash seat mechanism. Another type is a standard seat that has no specific whiplash injury prevention action, and the last type is a different anti-whiplash seat with a different re-active head restraint system. These three types of seats are selected such that they differ only by their head restraint types.

Test results are assessed using two different assessments systems, namely the European New Car Assessment Program (Euro NCAP) and the Research Council for Automobile Repairs-International Insurance Whiplash Prevention Group (RCAR-IIWPG) systems. After the fundamentals of the Euro NCAP and RCAR-IIWPG

whiplash assessment systems are introduced in Chapter 7, the evaluation results of the tested seats according to both of these rating systems are given in Chapter 8.

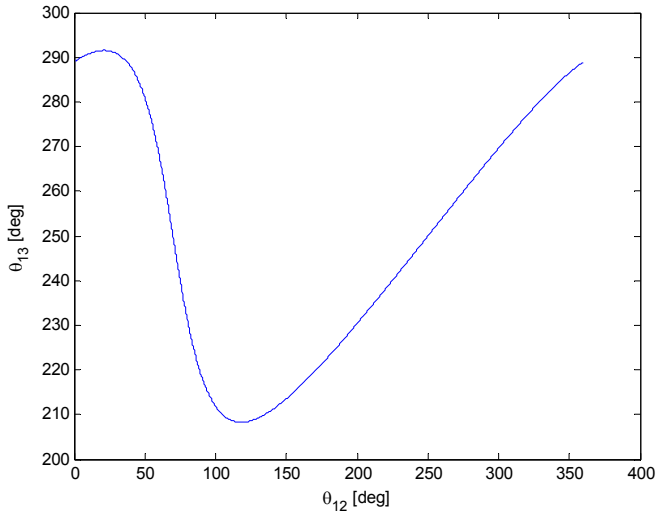

Figure 90 θ_{13} vs. θ_{12} during the full cycle of the mechanism

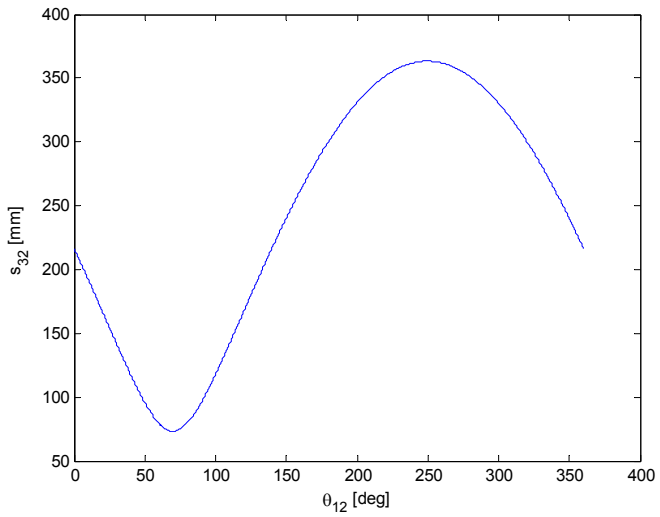

Figure 91 s_{32} vs. θ_{12} during the full cycle of the mechanism

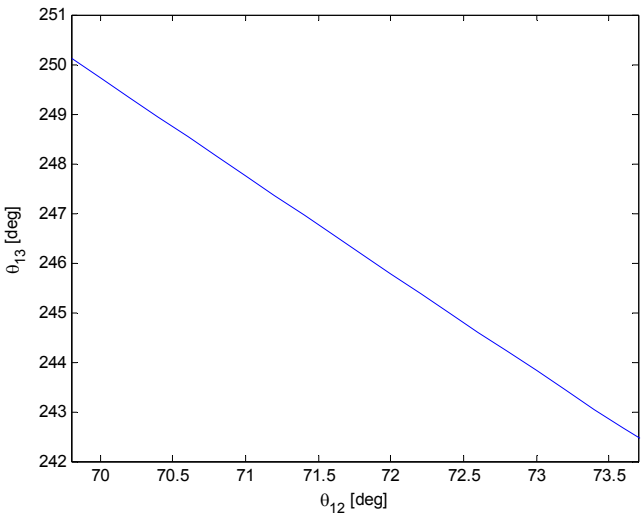

Figure 92 θ_{13} vs. θ_{12} in the working range of the mechanism

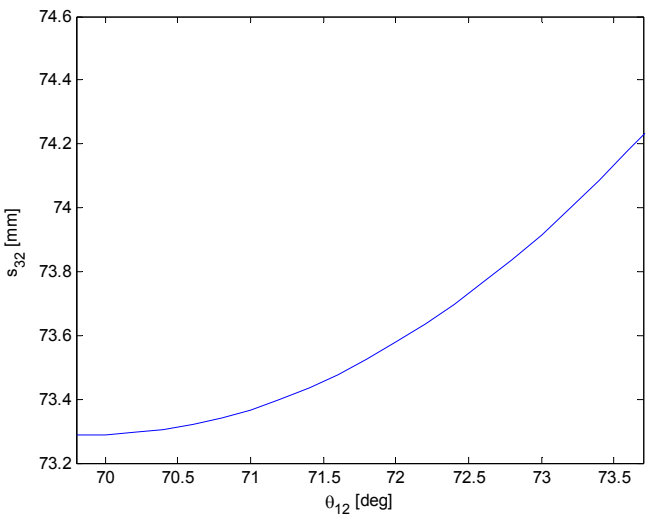

Figure 93 s_{32} vs. θ_{12} in the working range of the mechanism

CHAPTER 6

SLED TESTS OF THE SEAT WITH THE PROPOSED QUICK FORWARD ANTI-WHIPLASH SEAT MECHANISM

In order to measure the success of the proposed quick forward anti-whiplash mechanism, three identical prototype seats have been built and evaluated by sled tests that are performed with the low, medium and high severity Euro NCAP sled pulses (see Figure 52) at the Vehicle Safety Unit of the METU-BILTIR Center using the BioRID II test dummy. For comparing and revealing the improvements achieved by the seat with the proposed mechanism, the standard seats and the anti-whiplash seats which are currently used in a particular OEM have also been evaluated. With this aim, in addition to the three proposed seats, three identical standard seats that do not have any anti-whiplash action, and three identical anti-whiplash seats with a different headrest moving mechanism have been tested with the same Euro NCAP sled pulses. Hence, totally nine individual whiplash tests have been carried out.

In order to be able to focus only on the changes in the injury avoidance performance of the seat due to the developed headrest moving mechanism, the quick forward anti-whiplash mechanism is integrated to the tested type of the standard seat with minimum possible modifications that are inevitable for such integration. This approach is also valid for the tested seats with a different re-active head restraint system. For this reason, all the tested seat types have the same construction, cushion, cover, adjustment controls and seat belt anchorages, i.e. they are nearly identical except the head restraint types integrated to each of them. In the sled tests, unused seats have been tested. The Dynamic Assessment of Car Seats for Neck Injury Protection Testing Protocol by the Euro NCAP (2011) has been strictly followed during the entire test preparations and testing. This is the last updated version of the dates that these tests have been conducted. The following sections provide main features of the sled system used in the tests and a detailed explanation of the performed sled tests.

6.1 Sled Test System

Instron Structural Testing (IST) Hydropuls sled test system available in METU-BILTIR Center Vehicle Safety Unit has been used for the tests. Its technical specifications are as follows:

- 2500 kg payload
- 1800 x 4100 mm sled dimensions
- 90 g max. acceleration
- 90 km/hr max. velocity
- 32 m long precise rails
- 2500 kN Nominal Force
- 1700mm Working Stroke
- 140.000 l/min 4-Stage Servovalve
- Hydraulic Power Supply: 250 l/min flow rate
- Hydraulic Power Supply: 280 bar (4000 psi)Pressure

Five high-speed, high-g cameras are available in the Center. The lighting system with 150000 lux capacity and the data acquisition system exist. The sled test system available in the Center is also capable of performing the low, medium and high severity Euro NCAP whiplash tests. In addition to several adult and child test dummies, the BioRID II test dummy which is required for whiplash test is also available in the Center. All the information given in this section is taken from the website of the Center (METU-BILTIR Center, 2013). A general view of the test facility can be seen in Figure 94.

Figure 94 A general view of the test facility (METU-BILTIR Center, 2013)

6.2 Basic Steps in Euro NCAP Whiplash Assessment Tests

The Euro NCAP whiplash assessment is based on static and dynamic assessments for the particular seat. The static assessment is realized by using HPM and HRMD. The dynamic assessments are based on the results of the sled tests (i.e., dynamic tests) which are conducted on the sled test facility used for simulation of the rear-end crash. A general flow chart that summarizes the basic steps in tests according to the Euro NCAP whiplash testing protocol (2011) is given in Figure 95. All these steps are detailed in the following sections.

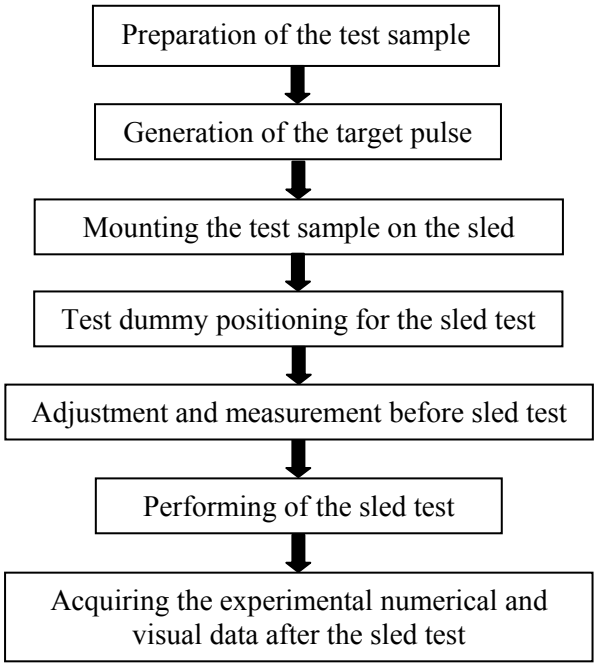

Figure 95 General flow chart of the Euro NCAP whiplash tests

6.3 Test Sample Preparation

Referring to Figure 96, a typical test sample for the Euro NCAP whiplash test is composed of:

- a sled plate (1) which is attached to the sled of the test system,
- a seat mounting fixture (2) which is secured on the sled plate (1),
- a heel surface plate (3) which is fixed to the sled plate (1),
- a toe board (4) which is attached to the sled plate (1),
- a seat (5) which is mounted to the seat mounting fixture (2),
- seat belt anchorage frames (6) which are attached on the sled plate (1),
- the lap/shoulder seat belt (7) which is anchored to the seat belt anchorage frames (6),
- the BioRID II test dummy (8) sitting on the seat (5),

The existing sled plate in the Center has been used. The seat mounting fixture which will be fixed to the sled plate by bolts should be designed such that the orientation of the seat to be tested relative to the floor plate of the vehicle is reproduced on the sled. Similarly, the heel surface plate should be employed such that the height of the heel rest point inside the vehicle relative to the non-moving seat rails is reproduced on the sled. The toe board should make an angle of 45° with the sled plate.

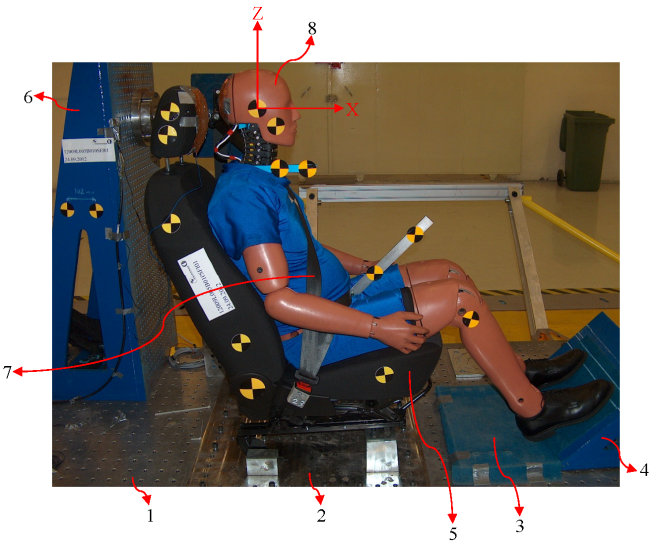

Figure 96 Euro NCAP whiplash test sample

In the test preparation, orthogonal Cartesian coordinate system is used for all the Coordinate Measuring Machine (CMM) measurements. Positive X-axis is horizontally forward in the direction of the looking of the dummy, positive Y-axis is to the left hand side of the dummy, and positive Z-axis is vertically upward (Figure 96). The origin is located at the center of the upper circle of the rear seat mounting bolt hole that is drilled into the fixed left hand seat rail (Figure 97).

The coordinate systems used for the dummy sensors are in accordance with the Society of Automotive Engineers (SAE) J211 specifications.

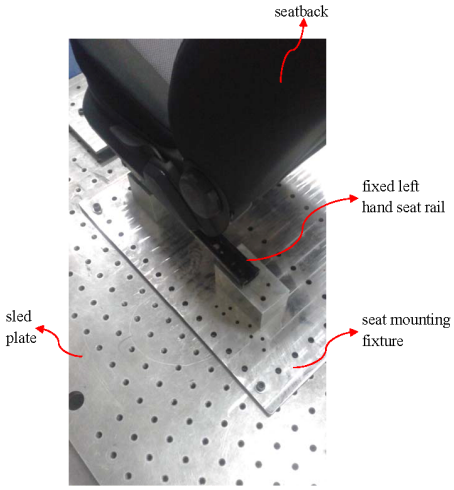

Figure 97 Origin of the coordinate system used

6.3.1 Seat Mounting and Adjustment

For mounting the seats to be tested to the sled plate, a suitable fixture, which is designed to reproduce on the sled their vehicle-specific design orientation relative to the horizontal plane, is used. Together with this fixture, a suitable heel surface plate is also used in order to match the height of the heel rest point relative to the non-moving seat rails while the seat is on the sled to its corresponding vehicle-specific design value. In addition to these, a toe board is attached to the sled plate such that it makes an angle of 45° with the sled plate, and both the heel surface plate and the toe board

are covered with a carpet with short piles. A seat that is attached to the sled as described above is seen in Figure 98.

The seats to be tested have only two adjustment controls. These are the seat track and height adjustments. The track adjuster is adjusting incrementally, whereas the height adjuster is adjusting continuously, and both are operated manually.

After the seat is attached to the sled, first the seat track and then the seat height are brought to their rearmost and lowermost limit positions, respectively. Then, first the seat track and then the seat height are set to their corresponding midrange values with the aid of the CMM.

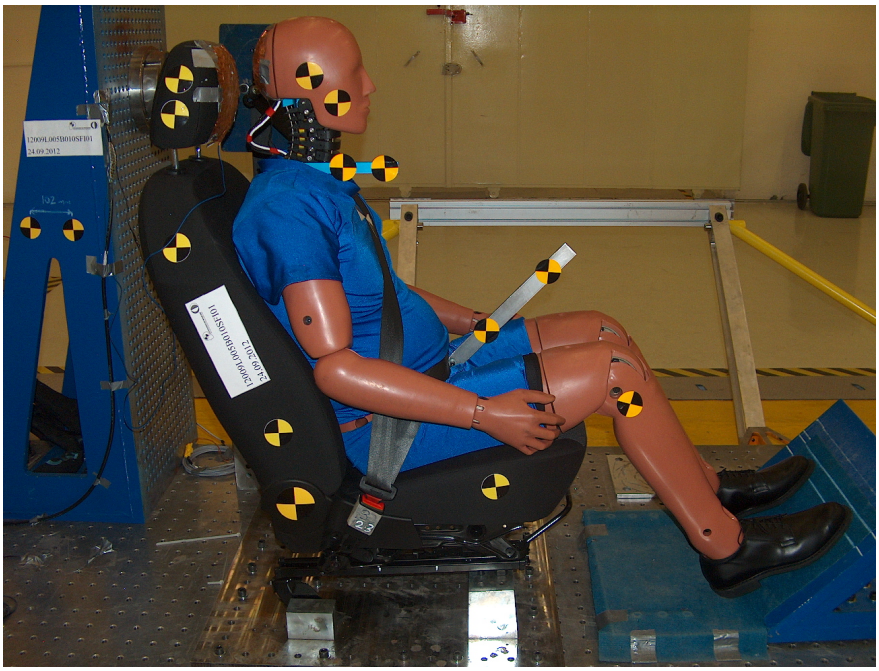

Figure 98 A general view of the seat and the dummy prior to test

6.3.2 Seat Belt Anchorage Arrangement

The three point lap/shoulder seat belt comprising a self-locking inertia reel is used in each test. The seat belt anchorage mounting according to the test protocol is

given in Figure 99. There is a tolerance of 50 mm for each of these anchorage points. Referring to Figure 99, the seats to be tested are already equipped with the anchorage point A. Highly rigid attachment frames (Figure 100) provided by the Center are used for the rest of the anchorages. The seat belt height adjuster is also attached to this fixture set-up. In addition to the three anchorage points for securing the seat belt, a fourth anchorage point is also created to attach the retractor. It is written in the test protocol that this fourth anchorage should be located on the same vertical plane on which K lays and 770 mm below it (in accordance with Figure 99). The seat belt is replaced with a new one for each test. A time to fire (TTF) of 10 ms is used to trigger the seat belt pretensioner.

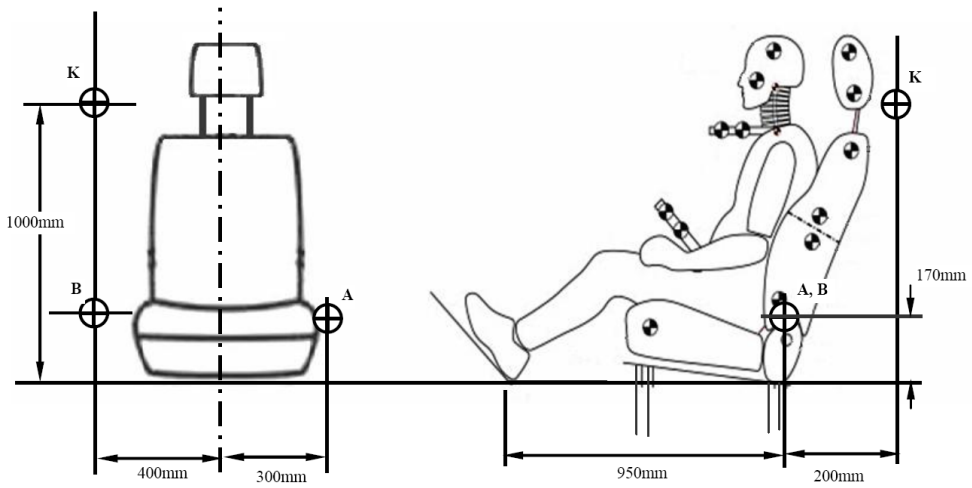

Figure 99 Generic seat belt anchorage mounting (Euro NCAP whiplash testing protocol, 2011)

6.3.3 HPM and HRMD Measurements

H-Point manikin (HPM) and Head Restraint Measuring Device (HRMD) measurements are required for the test positioning of the seatback, obtaining the reference measurements for dummy positioning, and static assessment of the head

restraint geometry. The rest of this section describes step by step the procedure followed for these purposes.

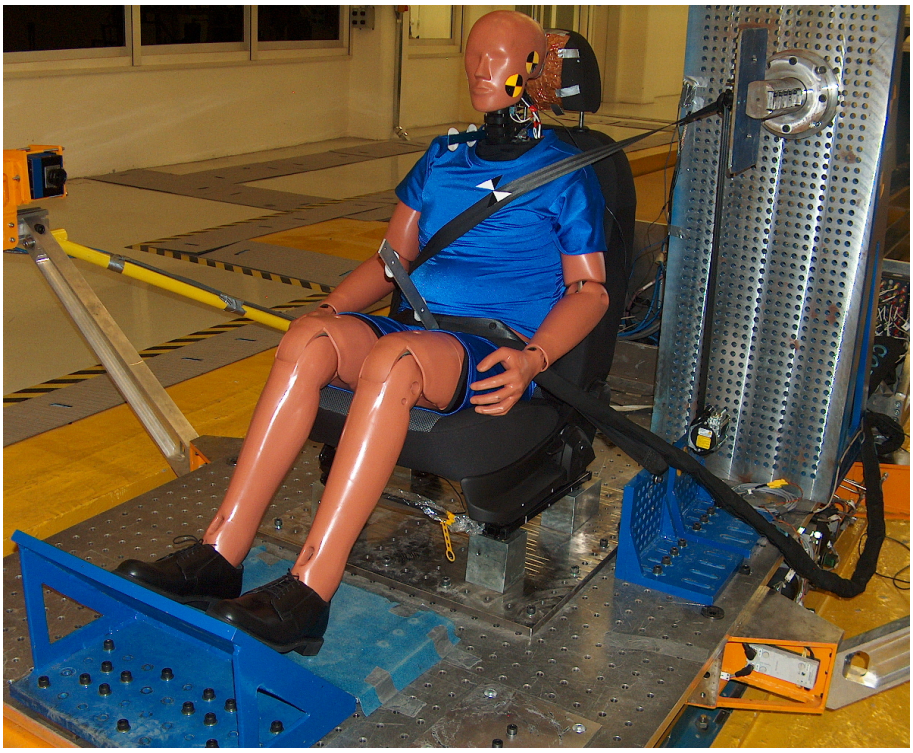

Figure 100 Seat belt anchorage fixture set-up

Prior to the installation process, the test position of the seatback is estimated roughly, and the seatback is adjusted accordingly. Then, the seat is covered with cotton fabric, and then the HPM is put onto the seat. Before the attachment of the legs, the lengths of the lower and upper legs are set to be equal to those of the 50th and 10th percentile dummies, respectively, and the feet are adjusted to make an angle of 90° with the tibias. After that, the legs are attached to the T-bar of the HPM such that the knees are spaced apart from each other by a distance of 250 mm. This state of the manikin will be a return point if the installation is required to be repeated due to the failure of the achievement of the target H-point tolerances. With the legs attached and the back pan brought forward, the HPM is made sure to center the seat and, following this, the back pan is leaned into the seatback. At this configuration, the feet are brought to the most forward position possible as the toe board is being too far away to

meet them. Subsequently, the lower leg and thigh weights are attached to the HPM, and the HPM is leveled using the integrated bubble level on it. The configuration of the manikin after this step will be another return point if the installation is required to be repeated due to the failure of the achievement of the target torso angle. Then, the whole assembly is pushed twice against the seatback with a 100-N horizontal force applied to the hip angle quadrant structure using an electronic force gauge, while the back pan is tilted forward by 45°. Before the force is stopped to be applied in the second repeat, the back pan is returned back into the seatback. While releasing the force being applied, the T-bar is supported with a light force in order to avoid any longitudinal slip of the HPM. The said support of the T-bar is continued from this stage until its end is explicitly mentioned. After a check of that the HPM is leveled and centered on the seat, the right and left buttock weights are mounted first, and next the six chest weights are attached by alternating left to right. From these six chest weights, the two larger ones are assembled last such that their flat portions are facing downward. When the assembly process is completed with these two said larger chest weights, the back pan is tilted to a vertical position, and the HPM is rocked three times from one side to the other in a 10° range, 5° in each side. During this step, it is paid attention that the feet are free to move, and any changes in the positions of the feet are left as they are. Then, the back pan is again returned into the seatback and the HPM is leveled. The continued support of the T-bar up to this step is ended at this point. After the back pan molding is exerted a rearward horizontal force of 10 N from the level of the center of the torso weights, each foot is put up in order, one by one, so that it is ensured that no additional forward movement is possible for them. Then, the toe board is brought near to the feet, and the final position of the feet is given without disturbing the HPM configuration such that the heel and sole of each foot are in contact with the heel surface plate and the toe board, respectively, and the toe of each of them is in the region between the 230 mm and 270 mm lines from the intersection of the toe board with the heel surface plate. The HPM is leveled again after the final positioning of the feet if needed. From this step on, the HPM is ready for the installation of the HRMD.

With its backset and height probes mounted and the leveling knob loosened, the HRMD is fitted to the HPM by taking care of that the manikin position is not disturbed during this installation. Then, the head is leveled with the aid of the bubble level available on the HRMD and secured at that level position by tightening the leveling knob. A general view of the HPM sitting on the seat and the HRMD fitted to it is given in Figure 101.

After the HRMD is installed, the torso angle is measured by placing an electronic protractor on the calibrated block of the weight hanger frame (Figure 102). When the measured angle is not within 25±1°, the HRMD and the chest and buttock weights are removed, the seatback is readjusted, and the steps from the corresponding return point described above up to here are repeated. Once the target torso angle is attained, the X and Z coordinates of the H-points on both sides of the HPM are

measured using CMM (Figure 103). If there is a difference of 2.5 mm or larger in the X or Z coordinate values of the right and left H-points, then all the steps from the corresponding return point described above are repeated.

Figure 101 Use of HPM and HRMD

A single installation and measurement cycle takes about 15 minutes, and if three adjacent installations are performed on the same seat, then the seat is left unloaded for 15 minutes to recover itself before the subsequent fourth attempt.

The head restraints of the seats that are to be tested are only height adjustable. As the test position, first, the head restraint is brought to the mid vertical position with the aid of the CMM. But since there is no locking notch at this geometric midpoint, the head restraint is raised up to 10 mm, and the locking notch encountered during this lift is used as the test position according to the definition of the test protocol.

With the head restraint set to its test position as well, it is then time to measure the position of the head restraint. The HRMD backset and height should be measured for the head restraint geometric assessment. The HRMD backset is defined as the reading from the backset probe in its first contact with the head restraint (Figure 104). By definition, it is read to the nearest millimeter. HRMD height, on the other hand, is defined as the height from the top of the head restraint to the height probe. This height is measured using a ruler (Figure 105). These two values are recorded for the head restraint geometry assessment.

Besides, according to the test protocol, the backset is measured once more for the reference geometry for BioRID set up in a different way than the HRMD backset reading given above. For this purpose, the X coordinates of an identifiable point on the head restraint and the rearmost point on the HRMD skull, which is the backset probe screw in the retracted position of the probe, are measured using a CMM. The BioRID reference backset is then defined as the absolute value of the difference between the X coordinates of these two points + 15 mm. The most forward point on the head restraint at its test position is selected as the identifiable point on the head restraint, and the said measurements are performed using the CMM.

As a last head restraint geometry measurement, the HRMD backset and height are measured once more at the lowest position of the head restraint for the worst case geometry (formerly known as ease of adjustment) assessment. After that, the head restraint is returned back to the previously obtained test position.

For each and every seat to be tested, the HPM and HRMD installations and measurements are repeated from the beginning two more times. For the repeat installations, the seatback angle is not changed in order to obtain a torso angle of 25±1°. But if such a change is needed in order to maintain a torso angle of 25±1°, then the installations should have been continued until three consecutive installations during which no seatback readjustment is required are performed. It is also ensured that the absolute values of the differences in the values of the X coordinate of the H-point, the Z coordinate of the H-point and the BioRID reference backset are within 5 mm among the three measurements performed for each individual seat. When any of the said differences exceeds this limit, the outlying measurements should have been repeated again until consistent records are obtained.

Figure 102 Torso angle measurement

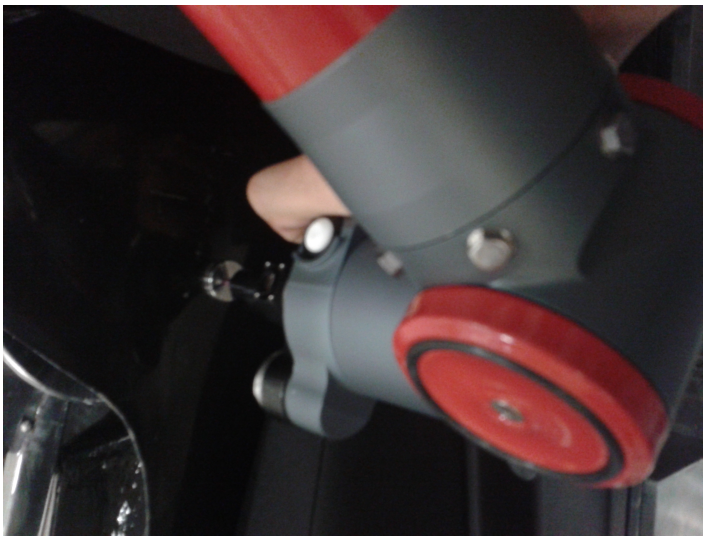

Figure 103 H-point measurement with CMM

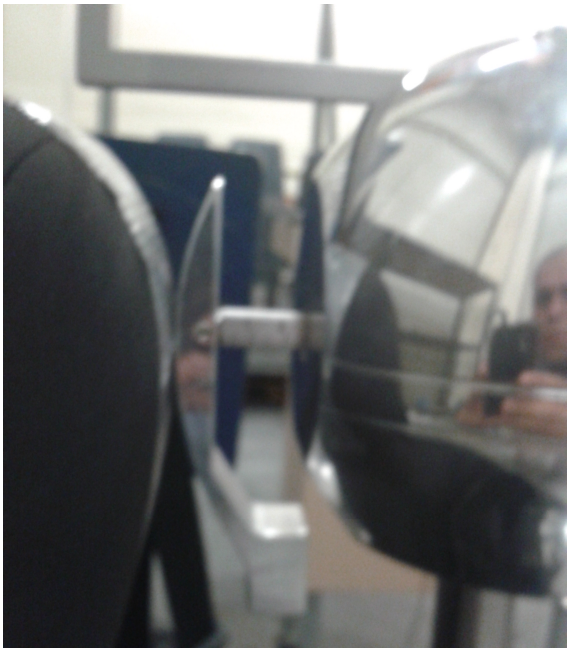

Figure 104 HRMD backset

Figure 105 HRMD height

In addition, the same head restraint test position is used for all the three seats of the same type. Furthermore, since the adjustment and locking characteristics of the three types of the seats to be tested are identical, the test head restraint test positions of all the nine test seats are the same.

The BioRID set up target values of the X coordinate of the H-point, the Z coordinate of the H-point and the BioRID reference backset are then determined for each individual seat by using the average values of the corresponding measurements recorded in the set of three measurements conducted for that seat. These are summarized in Table 6 where * denotes the average value of the corresponding HPM/HRMD measurements.

Table 6 Target and tolerance values of the BioRID installation parameters (Euro NCAP whiplash testing protocol, 2011)

Installation Parameter	Target Value	Tolerance
H-point (X-axis)	* + 20 mm	±10 mm
H-point (Z-axis)	*	±10 mm
Pelvis angle (Y-axis)	26.5°	±2.5°
Head angle (X-axis)	0°	±1°
Head angle (Y-axis)	0°	±1°
Backset	*	±5 mm

6.4 Generation of the Target Sled Pulses

Three different sled pulses, namely the low, medium and high severity sled pulses, are used by the Euro NCAP in the dynamic assessment of vehicle seats. In this study, the associated target sled pulses to be used for these three different test severities are generated by the Center's staff according to the definitions given in the test protocol. With this purpose, the weight of the test sample is measured, and dummy weights of which the total weight is nearly equal to the total weight of the test sample are attached to the sled (Figure 106). After that, the parameters of the electronic control unit of the sled's accelerator are adjusted iteratively in a trial-and-error approach until each target is successfully achieved for these dummy weights. The obtained target pulse for each test severity is presented in Figure 107.

After the target sled pulses are successfully obtained, the dummy weights are disassembled and the test sample is placed and securely fixed on the sled.

Figure 106 The dummy weights used during the iteration of the parameters of the electronic control unit of the sled's accelerator for each pulse severity

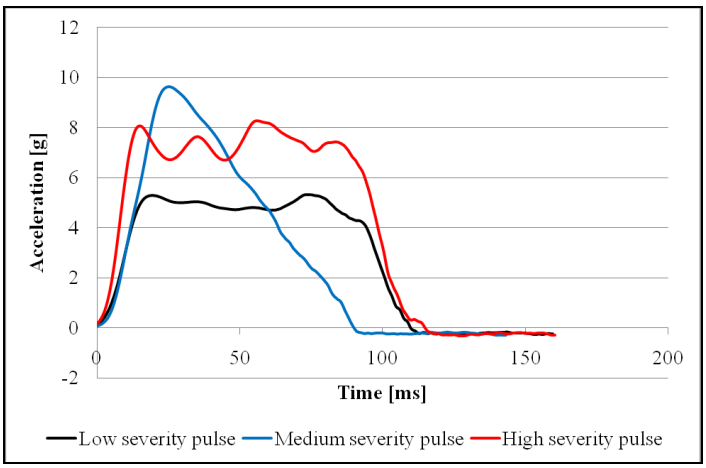

Figure 107 The target sled pulse obtained for each test severity

6.5 Dummy Positioning, Adjustments, Measurements and Performing of the Sled Test

The tests are conducted using the BioRID II dummy available in the Center. It is dressed in standard form with two shorts, two t-shirts, and Oxford-style, hard soled, work shoes that are supplied together with it. Before the installation of the dummy, the seat to be tested is kept unloaded for a sufficient time for recovery following the HPM/HRMD measurements. Then, the dummy is placed on the seat with the aid of the lab crane lifting from its lifting eye, and centered and laterally leveled. Next, the seat belt is secured across the dummy, leaving a sufficient slack for positioning. This state of the dummy will be a return point if the installation is required to be repeated when the target BioRID backset tolerances are not satisfied. The installation is continued by setting the pelvis angle and H-point point according to Table 6 with the use of the associated electronic tilt sensor within the dummy and the CMM, respectively. Following this, the legs are adjusted such that the centerlines of the knees and ankles are 200±10 mm apart from each other, and the knees are leveled by placing a bubble level on them. Similarly, the feet of the dummy are positioned such that the heels of its shoes are in contact with the heel surface plate, and the tips of them are in the region between the 230 mm and 270 mm lines from the intersection of the toe board with the heel surface plate. Subsequently, the arms are adjusted such that the upper arms are as close as possible to the torso and contacting the seatback from rear, and the elbows are rotated such that each small finger is touching the top surface of the seat cushion while the palms are facing towards the thighs. By leveling the head according to Table 6 in both the XZ and YZ planes via the associated tilt sensors integrated within the dummy, the positioning of the dummy becomes nearly finished. At this given configuration of the dummy, the BioRID backset is measured using the CMM. This parameter is defined as the horizontal distance between the rearmost point on the head and the same identifiable point on the head restraint used to measure the BioRID reference backset. The rearmost point on the head is obtained by measuring 95 mm from the top of the skull of the dummy along its midsagittal plane using a tape. When the BioRID backset is within ±5 mm of the BioRID reference backset as given in Table 6, the slack in the seat belt is removed and the test positioning of the dummy is completed. In the cases where the BioRID backset is not in the allowable range, it is dictated in the test protocol to rotate the head in the XZ plane without exceeding its associated allowable tolerance band in order to meet the requirement. If the backset requirement is still not satisfied with this adjustment, the steps from the corresponding return point described above up to here should be repeated. During the test preparations of this study, such a return is never needed. A general view of the BioRID and the seat prior to test is already given in Figure 98.

As explained previously, three different types of vehicle seats are tested using the BioRID II dummy in this study. These are the prototype seat with the developed quick forward anti-whiplash seat mechanism, a standard seat that does not have any specific whiplash injury prevention action, and a different anti-whiplash seat having a different re-active head restraint system. For the assessment of each type, three identical and unused driver seats are tested with the low, medium and high severity Euro NCAP sled pulses. Each seat is numbered as given in Table 7 considering its type and the pulse severity used in its test. The tested seats are referred according to this numbering system in the rest of the thesis.

The BioRID transducer channels used for the dynamic assessment of the tested seats are presented in Table 8 together with their purposes of use. Here, T1 Left and T1 Right denote the accelerometers located on the left-hand side and the right-hand side, respectively, of its first thoracic vertebra. The dummy is freshly calibrated at its calibration center in Germany just prior to the tests, and the tests performed in this study are its first tests after its calibration. Besides, another transducer channel, Sled X-Acceleration, which is provided within the electronic sled control system, is also employed for recording the sled pulse.

All the transducer data are acquired at a frequency of 20 kHz, and their portions from trigger to 300 ms are considered for evaluation. In addition, the quiescent period of each channel is also recorded for a sufficient duration before the triggering for the purpose of cancelling the quiescent signal biases.

The starting and ending times of the contact of the head of the dummy with the head restraint (T-HRC and T-$HRC_{(end)}$, respectively) are recorded using a foil contact switch method. For this purpose, the front surface of the head restraint and the rear surface of the head are covered with a thin, lightweight, conductive foil (Figure 108).

The sled acceleration signals attained in each and every test are given together with the associated target sled pulses through Figure 109 to Figure 111. The test sled acceleration signals shown here for each seat are suitably offset adjusted and then filtered at channel frequency class (CFC) 60, as dictated by the test protocol.

In addition, the velocity change (dV) and mean acceleration (A_{mean}) are tabulated in Table 9 for the attained sled acceleration signals of each tested seats. Here, dV is determined as the difference between the maximum and minimum sled velocities attained during the period between the time that the sled acceleration becomes 1.0g for the first time (it is taken as 4.6 ms, 5.8 ms and 3.7 ms for the for the low, medium and high pulses, respectively) and the time that the sled acceleration again falls below 0 for the first time. In this study, the sled velocities are obtained by integrating the offset adjusted and CFC60 filtered sled accelerations using the trapezoidal rule.

Table 7 The numbering system used for the tested seats

Seat No	Seat Type	Pulse Severity
1.1	The standard seat (Type #1)	Low severity
2.1	The prototype anti-whiplash seat (Type #2)	Low severity
3.1	The different anti-whiplash seat (Type #3)	Low severity
1.2	The standard seat (Type #1)	Medium severity
2.2	The prototype anti-whiplash seat (Type #2)	Medium severity
3.2	The different anti-whiplash seat (Type #3)	Medium severity
1.3	The standard seat (Type #1)	High severity
2.3	The prototype anti-whiplash seat (Type #2)	High severity
3.3	The different anti-whiplash seat (Type #3)	High severity

Table 8 Dummy transducer channels used (Euro NCAP whiplash testing protocol, 2011)

Transducer Channel	Function
Head X-Acceleration (a_x^{Head})	NIC
T1 Left X-Acceleration ($T1_{left}$)	T1 and NIC
T1 Right X-Acceleration ($T1_{right}$)	T1 and NIC
Upper Neck Shear Force (F_x^{upper})	F_x and N_{km}
Upper Neck Tension Force (F_z^{upper})	F_z
Upper Neck Y-Moment (M_y^{upper})	N_{km}

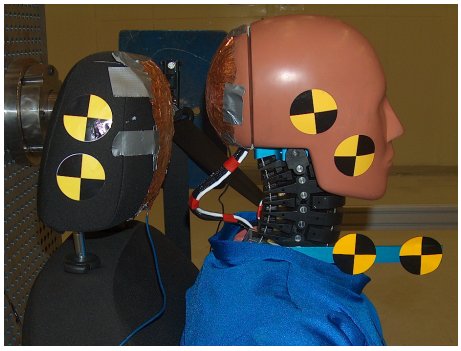

Figure 108 Measurement foil application for determining the head restraint contact starting and ending times

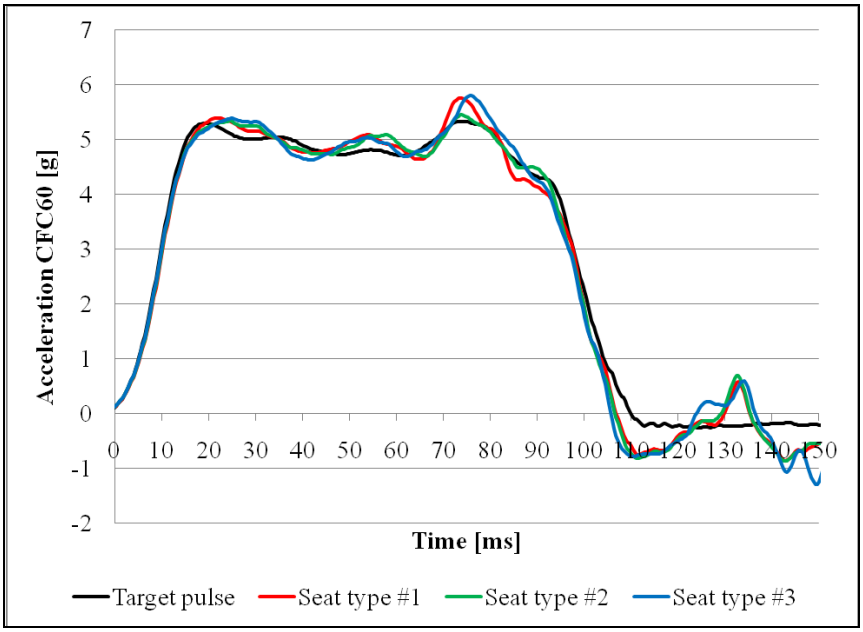

Figure 109 Sled acceleration signals attained during the low severity tests of each seat type together with the associated target pulse

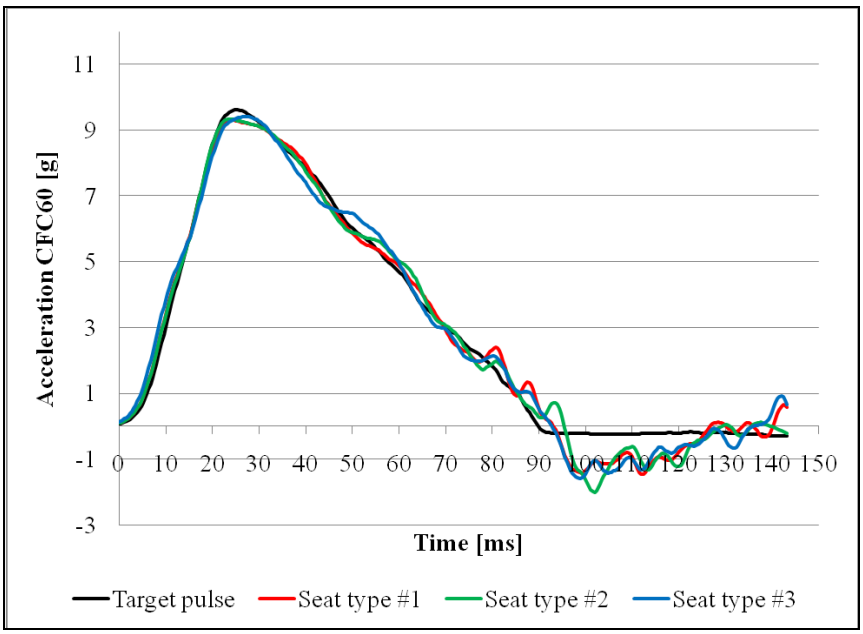

Figure 110 Sled acceleration signals attained during the medium severity tests of each seat type together with the associated target pulse

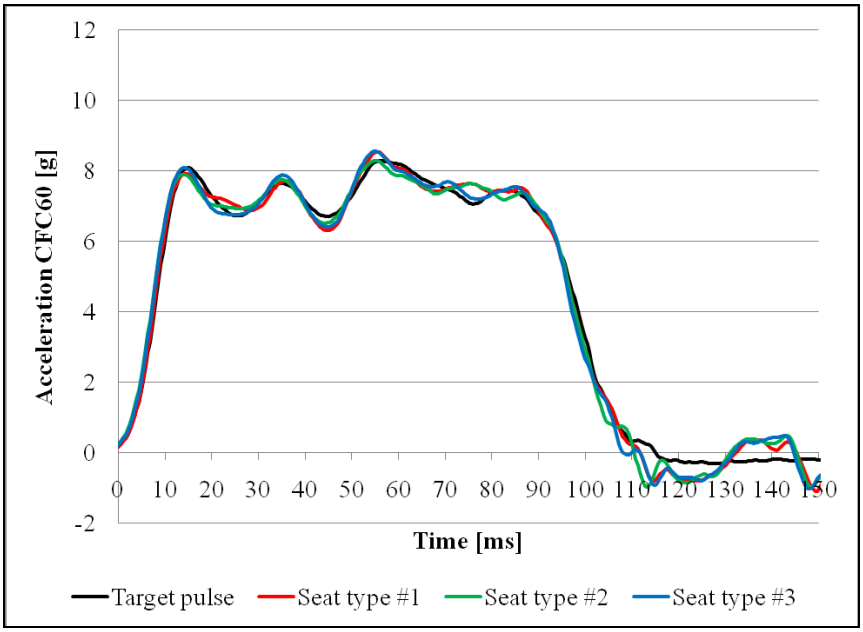

Figure 111 Sled acceleration signals attained during the high severity tests of each seat type together with the associated target pulse

Table 9 Sled pulse specifications

Seat No	dV [km/h]	A_{mean} [m/s^2]
1.1	15.63	42.32
2.1	15.63	42.28
3.1	15.67	42.78
1.2	15.73	49.51
2.2	15.72	48.41
3.2	15.68	49.62
1.3	24.08	61.41
2.3	24.01	61.99
3.3	23.94	63.53

The states of the dummy and seat just prior to and just after each and every test are recorded with photographs taken from several different views. Some examples of them are presented through Figure 112 to Figure 117 for seat #2.3.

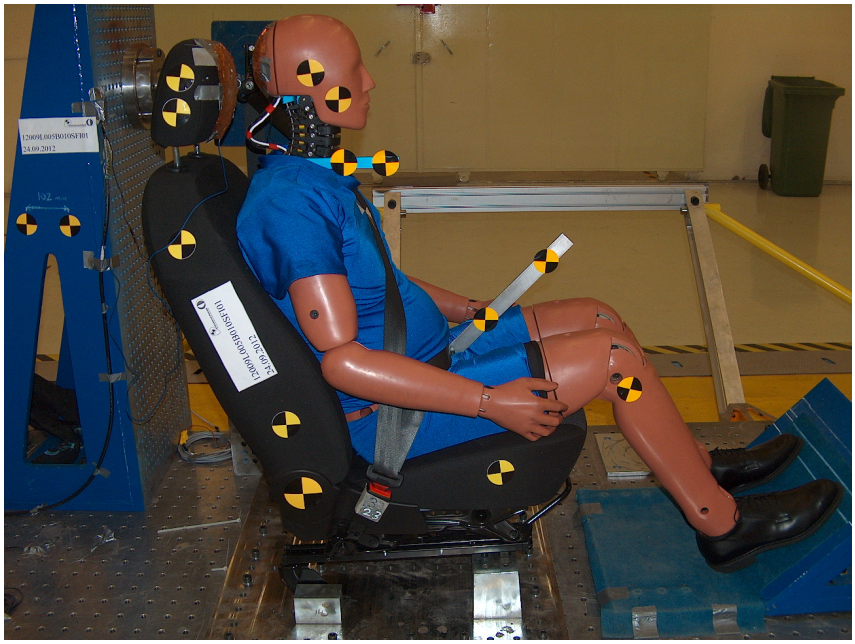

Figure 112 Left side view of the dummy and seat prior to the test of the seat #2.3

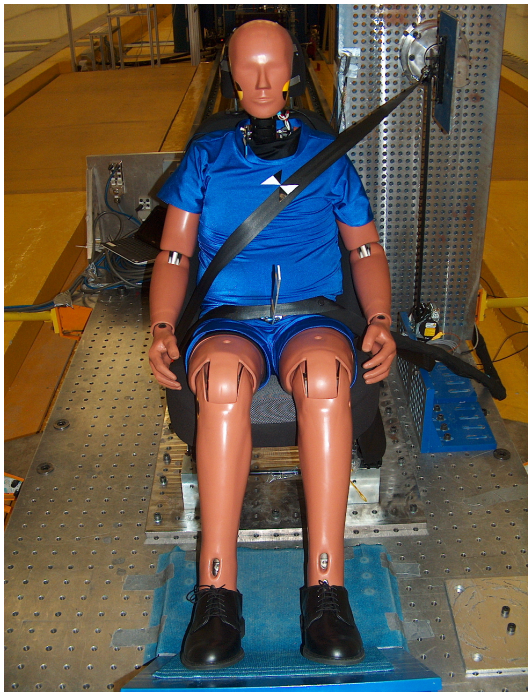

Figure 113 Front view of the dummy and seat prior to the test of the seat #2.3

Figure 114 Right side view of the dummy and seat prior to the test of the seat #2.3

Figure 115 Left side view of the dummy and seat after the test of the seat #2.3

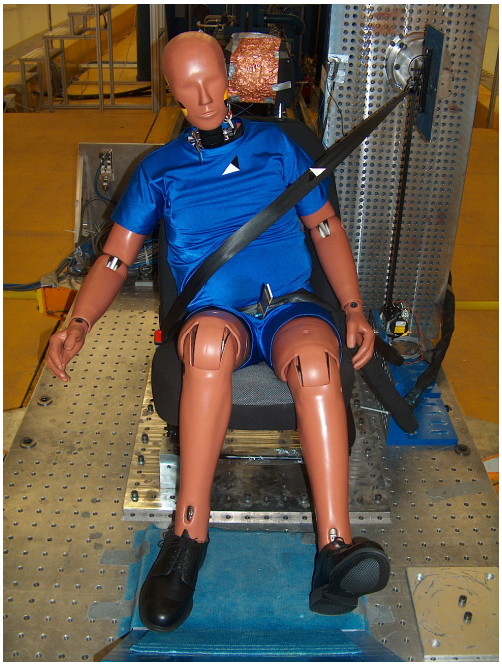

Figure 116 Front view of the dummy and seat after the test of the seat #2.3

All the tests performed are also recorded using two high speed on-board cameras at 1000 fps for 300 ms from trigger. One of them is adjusted to record the entire sled and seat whereas the other one is adjusted to record the zoom in the region of the dummy's head and neck. Film targets (i.e., trackers) are used on the sled, seat and dummy as can be seen in Figure 112. The video target distances shown in Figure 118 are measured by a tape measure for the purpose of providing them as a correction input to the motion analysis software used. The response of the dummy in the low severity pulse test of the seat type #2 is presented in Figure 119 as an example.

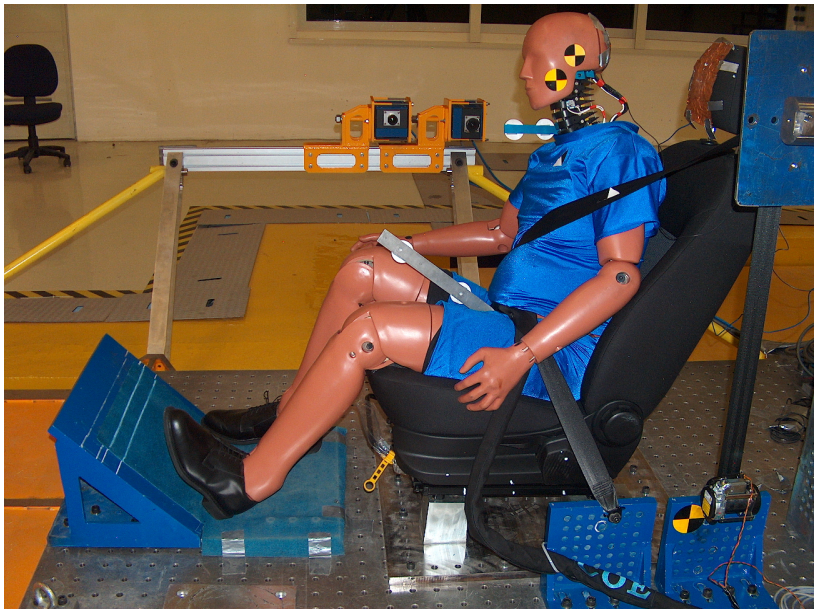

Figure 117 Right side view of the dummy and seat after the test of the seat #2.3

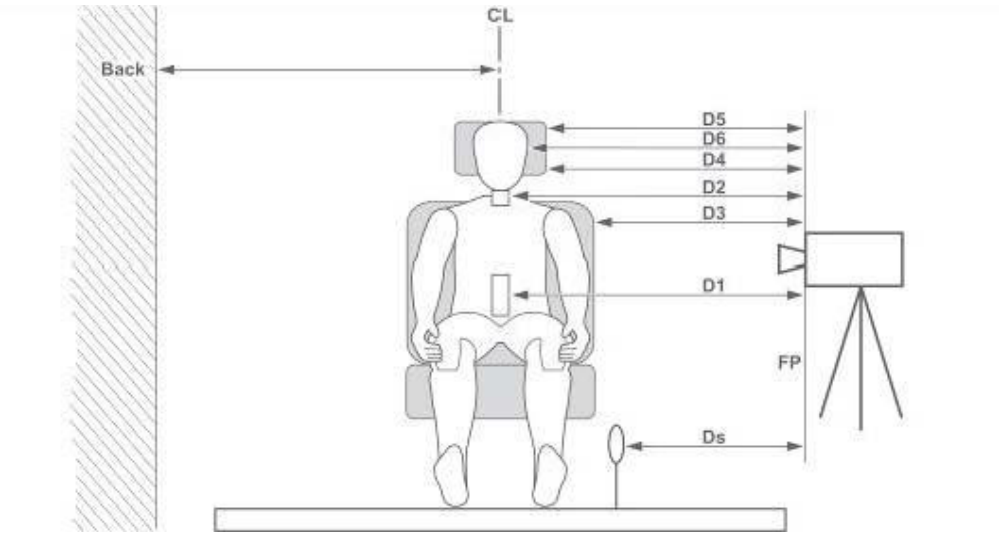

Figure 118 Required video tracking measurements (Euro NCAP whiplash testing protocol, 2011)

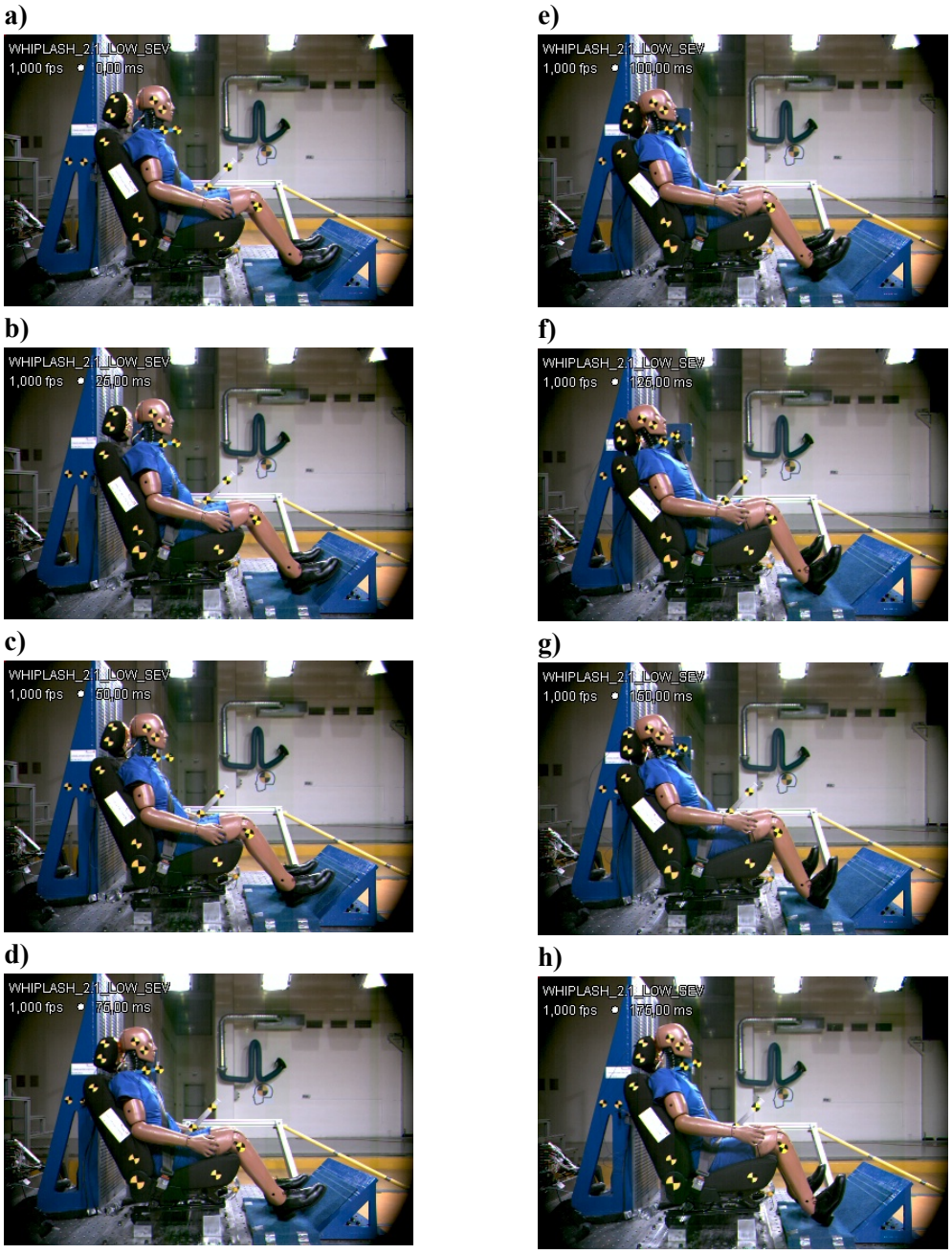

Figure 119 The response of the dummy in the low severity pulse test of the seat type #2 at (a) t =0 ms, (b) t= 25 ms, (c) t =50 ms, (d) t = 75 ms, (e) t = 100 ms, (f) t = 125 ms, (g) t= 150 ms, (h) t = 175 ms, (i) t = 200 ms, (j) t = 225 ms, (k) t = 250 ms, (l) t = 275 ms, (m) t = 300 ms

i)

j)

k)

l)

m)

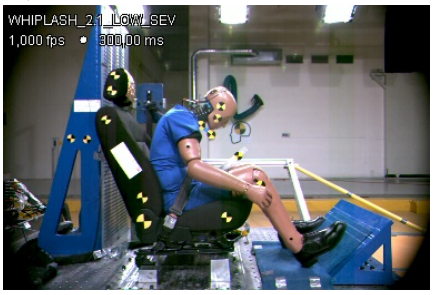

Figure 119 (continued)

CHAPTER 7

WHIPLASH ASSESSMENT SYSTEMS

Two different whiplash assessment systems are used in this study to rate the seats which have been tested at the METU-BILTIR Center Vehicle Safety Unit as described in Chapter 6. These are the European New Car Assessment Program (Euro NCAP) and the Research Council for Automobile Repairs-International Insurance Whiplash Prevention Group (RCAR-IIWPG) systems. Their details are given in the following sections.

7.1 Euro NCAP Assessment

The Assessment Protocol – Adult Occupant Protection by Euro NCAP (2011) is followed in this study together with the Euro NCAP whiplash testing protocol (2011) for determining the Euro NCAP ratings of the tested seats. These are the current versions of the corresponding protocols at the test dates.

Overall Euro NCAP whiplash protection evaluation is based on both the static and dynamic assessment of the seats. The injury criteria, their limit values, and the scoring system used in these protocols are summarized below.

7.1.1 Static Assessment

Static evaluation of a seat is based on the assessment of the head restraint geometry considering the average HRMD backset and height values obtained from the nine measurements that are performed on the three identical seats at the test position. The lower and higher performance limits (LPL and HPL, respectively) for these

parameters are given in Table 10. Each of these parameters is rated on a scale from -1 to 1, and the minimum of the two is then assigned as the geometry assessment score of the seat.

Similarly, the geometry of the head restraint is evaluated once more considering the average HRMD backset and height values obtained from the nine worst case measurements that are performed on the three identical seats with their head restraints in their lowermost and rearmost positions. An additional 1 point is then given for seats that score positive in this worst case assessment only in cases when they also perform well dynamically, with a raw score greater than 4.50 points after capping and all modifiers are applied.

Table 10 Geometry assessment parameters and their lower and higher performance limits (Euro NCAP whiplash assessment protocol, 2011)

Parameter	LPL	HPL
Height	80 mm below from the height probe of the HRMD	0 mm below from the height probe of the HRMD
Backset	100 mm	40 mm

7.1.2 Dynamic Assessment

Since the exact mechanism of whiplash injury has not been fully revealed yet, seven different injury criteria, namely, Neck Injury Criterion (NIC), N_{km}, head rebound velocity in the X-direction ($V_{rebound}$), upper neck shear force (F_x), upper neck tension force (F_z), T1 X-acceleration (T1) and starting time of the contact of the head of the dummy with the head restraint (T-HRC), are used by Euro NCAP to scale the injury risk. These are selected as a combination of the associated criteria used by the corresponding RCAR-IIWPG and Swedish Road Administration (SRA) protocols, but none of them has been yet proven biomechanically (Van Ratingen, et al., 2009). The calculation details of these injury criteria can be found in the next section.

Each dynamic test is evaluated over three points. Two and a half points come from each of NIC, N_{km}, $V_{rebound}$, F_x and F_z. A remaining half point is given by taking into account the best scored one among either T1 or T-HRC. If a test value lies between its relevant HPL and LPL, the score is determined using linear interpolation.

If any of NIC, N_{km}, $V_{rebound}$, F_x and F_z takes values higher than their corresponding capping limits (CL), no score is awarded for that dynamic test. Besides, if both T1 and T-HRC go beyond their corresponding LPLs and at the same time either one also exceeds its relevant CL, again no score is awarded for that dynamic test. The numerical values of HPL, LPL and CL for each injury criteria and for each pulse are summarized in Table 11.

7.1.3 Dynamic Assessment Criteria

Before starting to calculate these criteria, sled's trigger time is set as zero time (T-zero), and each required dummy transducer data channel is offset to zero by subtracting the average value of the data recorded during its quiescent period (i.e., the period before T-zero) from its each and every data point after T-zero to 300 ms. Following this, all the data channels are filtered using the appropriate channel frequency class (CFC) filter according to Table 12.

7.1.3.1 T-HRC

T-HRC is recorded as the first time (calculated from T-zero) that the head of the dummy remains in contact with the head restraint for longer than 40 ms. It is rounded to the nearest integer value in [ms]. Besides, ending time of the contact of the head of the dummy with the head restraint ($T\text{-}HRC_{(end)}$) is recorded as the first time (calculated from T-zero) at which the head loses its contact with the head restraint for longer than 40 ms. Both are determined using the aforementioned foil contact switch method.

7.1.3.2 T1

A new average T1 X-Acceleration data channel, T1(t), is created from the $T1_{left}$ and $T1_{right}$ data channels as follows:

$$T1(t) = \frac{T1_{left}(t) + T1_{right}(t)}{2} \tag{7.1}$$

Here and in the rest of the manuscript, t denotes the time from T-zero to 300 ms. The maximum value of this data vector is then recorded considering its portion only between T-zero and T-HRC$_{(end)}$.

Table 11 Higher and lower performance and capping limits for each dynamic assessment criteria (Euro NCAP whiplash assessment protocol, 2011)

Criterion	Unit	Low Severity			Medium Severity			High Severity		
		HPL	LPL	CL	HPL	LPL	CL	HPL	LPL	CL
NIC	m^2/s^2	9.00	15.00	18.30	11.00	24.00	27.00	13.00	23.00	25.50
N_{km}	-	0.12	0.35	0.50	0.15	0.55	0.69	0.22	0.47	0.78
$V_{rebound}$	m/s	3.0	4.4	4.7	3.2	4.8	5.2	4.1	5.5	6.0
F_x	N	30	110	187	30	190	290	30	210	364
F_z	N	270	610	734	360	750	900	470	770	1024
T1	g	9.40	12.00	14.10	9.30	13.10	15.55	12.50	15.90	17.80
T-HRC	ms	61	83	95	57	82	92	53	80	92

Table 12 CFC filter classes used for the dummy transducer channels during the calculation of the injury criteria (Euro NCAP whiplash testing protocol, 2011)

Dummy Transducer Channel	Injury Criterion	CFC Filter Class
a_x^{Head}	NIC	CFC 60
$T1_{left}$	T1 and NIC	CFC 60
$T1_{right}$	T1 and NIC	CFC 60
F_x^{upper}	F_x	CFC 1000
F_z^{upper}	F_z	CFC 1000
F_x^{upper}	N_{km}	CFC 600
M_y^{upper}	N_{km}	CFC 600

7.1.3.3 NIC

The NIC is defined according to the following formula:

$$NIC(t) = a_{rel}(t) \cdot 0.2 + v_{rel}^2(t) \tag{7.2}$$

where

$$a_{rel}(t) = T1(t) - a_x^{Head}(t) \tag{7.3}$$

$$v_{rel}(t) = \int a_{rel}(t)\,dt \tag{7.4}$$

Before substituting into this formula, $T1(t)$ and $a_x^{Head}(t)$ should be converted to be in [m/s^2]. The positive peak value of the portion of the $NIC(t)$ vector between T-zero and T-HRC$_{(end)}$ is then recorded.

7.1.3.4 F_x and F_z

The positive peak values of the portions of the $F_x^{upper}(t)$ and $F_z^{upper}(t)$ vectors between T-zero and T-HRC$_{(end)}$ are recorded.

7.1.3.5 N_{km}

The N_{km} criterion takes into account the combined effect of neck moment and shear forces. It is formulated as follows:

$$N_{km}(t) = \frac{F_x^{upper}(t)}{F_{int}} + \frac{M_{OCy}(t)}{M_{int}} \tag{7.5}$$

where

$$M_{OCy}(t) = M_y^{upper}(t) - D \cdot F_x^{upper}(t) \tag{7.6}$$

Here, $F_x^{upper}(t)$ and $M_y^{upper}(t)$ are in [N] and [N.m], respectively, whereas D is the distance between the axes of the force sensor and the occipital condyle, and is equal to 0.01778 m. F_{int} and M_{int} are the critical intercept values that are required for normalization while calculating $N_{km}(t)$ (Table 13).

Before attempting to use Eq. (7.5), positive and negative valued parts of $F_x^{upper}(t)$ and $M_{OCy}(t)$ should be separated from each other by defining the following variables regarding the four different possible load cases:

$$F_{xa}(t) = \begin{cases} F_x^{upper}(t), & F_x^{upper}(t) > 0 \\ 0, & F_x^{upper}(t) < 0 \end{cases} \tag{7.7}$$

$$F_{xp}(t) = \begin{cases} F_x^{upper}(t), & F_x^{upper}(t) < 0 \\ 0, & F_x^{upper}(t) > 0 \end{cases} \tag{7.8}$$

$$M_{yf}(t) = \begin{cases} M_{OCy}(t), & M_{OCy}(t) > 0 \\ 0, & M_{OCy}(t) < 0 \end{cases} \tag{7.9}$$

$$M_{ye}(t) = \begin{cases} M_{OCy}(t), & M_{OCy}(t) < 0 \\ 0, & M_{OCy}(t) > 0 \end{cases} \tag{7.10}$$

Table 13 Critical intercept values for calculation of N_{km} (Euro NCAP whiplash testing protocol, 2011)

Load Case	**Value**
Extension	47.5 N.m
Flexion	88.1 N.m
Negative and positive shear	845 N

The four components of N_{km}, namely N_{ep}, N_{ea}, N_{fp} and N_{fa}, are then defined based on these four different possible loading combinations as given below:

1. "Neck Extension Posterior" (N_{ep})

$$N_{ep}(t) = \frac{F_{xp}(t)}{F_{int}} + \frac{M_{ye}(t)}{M_{int}} \tag{7.11}$$

where $F_{int} = -845$ N and $M_{int} = -47.5$ N.m.

2. "Neck Extension Anterior" (N_{ea})

$$N_{ea}(t) = \frac{F_{xa}(t)}{F_{int}} + \frac{M_{ye}(t)}{M_{int}} \tag{7.12}$$

where $F_{int} = 845$ N and $M_{int} = -47.5$ N.m.

3. "Neck Flexion Posterior" (N_{fp})

$$N_{fp}(t) = \frac{F_{xp}(t)}{F_{int}} + \frac{M_{yf}(t)}{M_{int}} \tag{7.13}$$

where $F_{int} = -845$ N and $M_{int} = 88.1$ N.m.

4. "Neck Flexion Anterior" (N_{fa})

$$N_{fa}(t) = \frac{F_{xa}(t)}{F_{int}} + \frac{M_{yf}(t)}{M_{int}} \tag{7.14}$$

where $F_{int} = 845$ N and $M_{int} = 88.1$ N.m.

The maximum value among the four maximum values attained by each of these four components of N_{km} between T-zero and T-$HRC_{(end)}$ is then recorded.

7.1.3.6 $V_{rebound}$

$V_{rebound}$ is determined using a suitable target tracking film analysis software package. For this purpose, two new traces are generated: absolute X-velocities of the head's center of gravity (CoG) target (referring to Figure 120, DT6) and the sled ($V_{Head\ CoG}(t)$ and $V_{sled}(t)$, respectively). Both traces are then offset adjusted and then filtered at CFC 30. After this, $V_{rebound}(t)$ is calculated as

$$V_{rebound}(t) = V_{Head\ CoG}(t) - V_{sled}(t) \tag{7.15}$$

and its maximum value before the breaking of the sled starts is recorded. This extremum should occur in the close neighborhood of T-HRC$_{(end)}$. TEMA Automotive® motion analysis software is available in the Center and is used in this study in order to perform this analysis.

7.1.4 Modifiers

A three-point reduction is applied to the seats that have 32.0° or greater seatback rotations in the high severity pulse tests. For this purpose, high speed video records of the associated tests are analyzed using a suitable target tracking and motion analysis software package. Associated calculation details can be found in the following subsection. Besides, a two-point reduction is also applied in dummy artifact loading situations.

7.1.4.1 Seatback Deflection

Referring to Figure 120, seatback deflection is defined as the maximum change in the angle between the lines ST2-ST3 and B1-B2 attained during the period between T-zero and T-HRC$_{(end)}$. Similar to the calculation of $V_{rebound}$, a suitable target tracking and motion analysis software package is used also for the calculation of this criterion.

Seatback deflection is not used directly as a dynamic assessment criterion. Instead, it is considered as a modifier only for high severity dynamic tests. However, in this study, the seatback deflections obtained in the conducted low and medium severity dynamic tests are also recorded. These related analyses are also performed using TEMA Automotive® motion analysis software.

It should be mentioned that, again referring to Figure 120, ST2' and ST3' are not used in this study because both of them are required for only bipartite hinged seatbacks whereas the tested seats do not have such an adjustment feature.

7.1.5 Overall Scoring

Total dynamic score is modified by the modifiers and combined with the static assessment results in order to obtain the raw whiplash score of the seat. The maximum possible raw whiplash score is 11 points, and its components are summarized in Table 14. This score is then finally scaled to four points by multiplying with 4/11. A scaled score of 0 to 1.499 points is colored "Red", 1.500 to 2.999 is colored "Orange", and 3.000 to 4.000 is colored "Green".

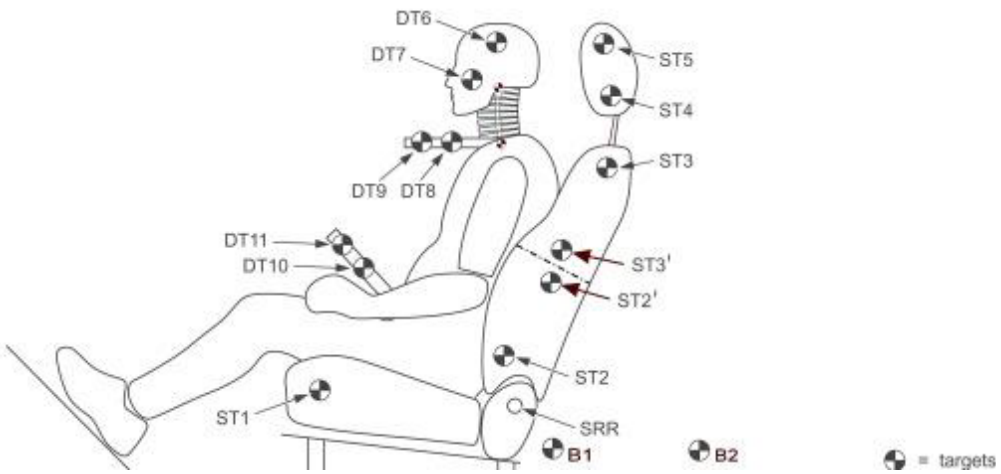

Figure 120 Required film target application to the sled, seat and dummy (Euro NCAP whiplash testing protocol, 2011)

Table 14 Raw scoring (Euro NCAP whiplash assessment protocol, 2011)

	Points
Static assessment	
Head restraint geometry assessment	-1 to 1
Worst case geometry assessment	1
Dynamic assessment	
Low severity pulse	3
Medium severity pulse	3
High severity pulse	3
Modifiers	
Seatback deflection	-3
Dummy artifact loading	-2
Maximum raw whiplash score	11

7.2 RCAR-IIWPG Assessment

Insurance Institute for Highway Safety (IIHS, USA) and other IIWPG members, which are The Motor Insurance Repair Research Centre (or Thatcham as widely known, UK), Allianz Centre for Technology (Germany), German Insurance Association (GDV, Germany), The Insurance Corporation of British Columbia (ICBC, Canada), Insurance Australia Group (IAG) Folksam (Sweden), AXA Winterthur (Switzerland), Mapfre Centre for Road Traffic Safety and Research (CESVIMAP, Spain), Centro Zaragoza (Spain), rate vehicle seats using the RCAR-IIWPG whiplash testing and assessment system (Edwards, Smith, Zuby, & Lund, 2005).

The RCAR-IIWPG Seat/Head Restraint Evaluation Protocol (2008) and the RCAR Procedure for Evaluating Motor Vehicle Head Restraints (2008) are considered together in this study in order to obtain the RCAR-IIWPG ratings of the tested seats. These are the current versions of the corresponding protocols at the test dates.

The RCAR-IIWPG whiplash assessment basically involves a static geometry assessment of the head restraint based on the HRMD backset and height measurements, and following this, a single dynamic test of the seat using a 16 km/h dV triangular sled pulse. In this manner, the RCAR-IIWPG evaluation system differs from the one of Euro NCAP in which three dynamic tests are used as described previously. However, the medium severity Euro NCAP sled pulse is directly taken from the RCAR-IIWPG dynamic testing protocol (Van Ratingen, et al., 2009), and

similarly, Japan New Car Assessment Program (JNCAP) has also decided to use a triangular sled pulse which is similar to the one of the RCAR-IIWPG (Ikari, Kaito, Nakajima, Yamazaki, & Ono, 2009).

The static geometry evaluation of the head restraint is a rather complicated system, and the rating position of the head restraint changes according to whether the head restraint is fixed or adjustable, and if adjustable, then whether these adjustment controls are lockable or not. In addition to this, it is also different than the Euro NCAP head restraint geometry assessment because of the following reasons: (i) The seat should be measured such that it is mounted on the vehicle of concern. (ii) The seat should be adjusted to be at its lowermost and rearmost position for the related measurements (iii) no repeat measurements are required to ensure consistency.

The head restraints of the seats tested in this study have only height adjustment, and it is lockable. The RCAR protocol says for such head restraints to measure the HRMD backset and height twice, one at the lowest and one at the highest locking position of the head restraint. The rating is then made by using the average backset and height values of these two measurements. The RCAR-IIWPG head restraint rating scale is given in Figure 121.

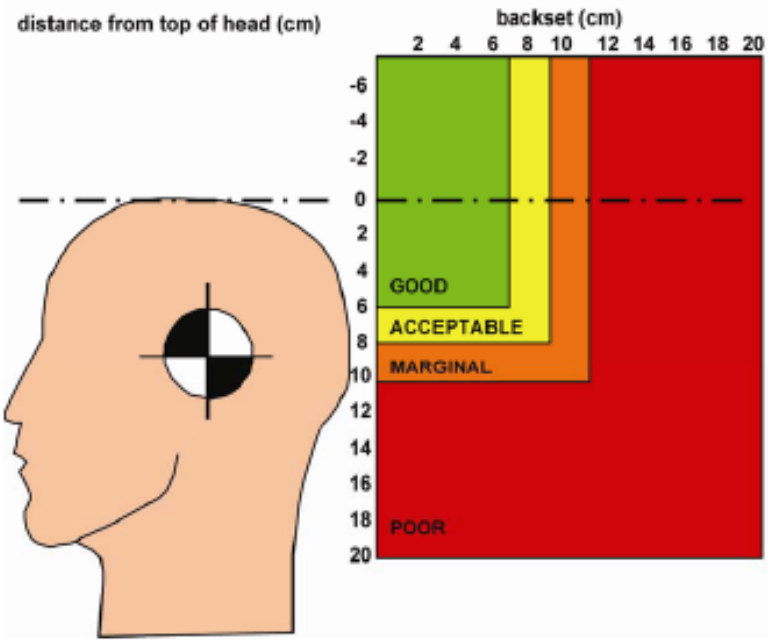

Figure 121 RCAR-IIWPG head restraint rating scale (RCAR static evaluation protocol, 2008)

The dynamic test is performed only if the head restraint geometry is evaluated to be at least acceptable. Then, the dynamic rating of the seat is determined according to Table 15. The associated neck force classification boundaries are given in Figure 122. The static assessment ratings are then combined with the dynamic assessment ratings according to Table 16 to obtain the overall RCAR-IIWPG ratings. Similar to the Euro NCAP, the portions of the transducer data channels from trigger to 300 ms are considered for evaluation, any DC bias in the data is removed by subtracting the average value of that data vector recorded during its quiescent period (i.e., the period before T-zero) from its each and every data point after T-zero to 300 ms, each data channel is filtered according to Table 17, and then the maximum values of the related data vectors are recorded considering their portions only between T-zero and T-$HRC_{(end)}$.

Actually, the entire RCAR-IIWPG dynamic testing protocol has been directly adopted during the preparation of the Euro NCAP protocol. The only differences of the Euro NCAP protocol from the RCAR-IIWPG protocol are summarized below:

- In addition to the RCAR-IIWPG sled pulse that has been adopted as the medium severity pulse, it has also adopted the low and high severity trapezoidal pulses from the SRA whiplash assessment protocol (Van Ratingen, et al., 2009).
- In addition to the RCAR-IIWPG dynamic assessment criteria that have been adopted, it has also adopted three additional dynamic assessment criteria that are being used by SRA, namely the NIC, N_{km}, and $V_{rebound}$ (Van Ratingen, et al., 2009).
- It has introduced a sliding scale scoring system.
- It has also included two modifiers to modify the overall dynamic score.

Hence, due to the similarities between these two evaluation systems, the Euro NCAP medium pulse test data of a seat can be used to determine its RCAR-IIWPG dynamic rating. For example, Australasian New Car Assessment Program (ANCAP) does so (ANCAP, 2012)

As mentioned previously, none of the Euro NCAP dynamic assessment criteria, which are adopted from the RCAR-IIWPG and SRA protocols, has been yet fully verified biomechanically. Muser, Hell, & Schmitt (2003) studied the significance of the three criteria that are used in the Euro NCAP system in addition to the ones used in the RCAR-IIWPG system, i.e., NIC, N_{km} and $V_{rebound}$, by comparing the sled test results with the real-world accident data and found out that NIC is in a good correlation with the real-world accidents. However, they also noted that inaccuracies in the sled tests may make NIC far from being a measure of the real-world risk. In addition, it was found in that study that only the N_{ea} component of the N_{km} correlates well with the real-world injury risk. Besides, this is the strongest correlation among the correlations calculated for the three criteria handled in their paper. Lastly, they reported nothing important regarding $V_{rebound}$. However, Euro NCAP tries to make use

of the every proposed criterion in the literature while evaluating seats for whiplash risk as a result of its "best practice" approach. Therefore, Euro NCAP ratings may only be an indicator of the relative injury risk, but not the absolute injury risk. So, it can be said that excluding these three aforementioned criteria from the assessment, i.e. the use of the RCAR-IIWPG whiplash rating system, would not be a big loss, especially for a non-commercial evaluation of a seat (Himmetoglu, Acar, Bouazza-Marouf, & Taylor, 2011).

Moreover, the RCAR-IIWPG whiplash ratings, especially the "good" and the "poor" ones, are in a perfect match with the real-world injury claims (Van Ratingen, et al., 2009; Aylor, & Zuby, 2011). In fact, what Euro NCAP mainly wants to improve with its introduced whiplash evaluation system is the correlation of the mid whiplash ratings of the vehicle seats with the real-world whiplash injury risk. With this aim, it has combined the "acceptable" and "marginal" ratings of the RCAR-IIWPG whiplash assessment system into one "marginal" rating and has increased the demanding of each rating band (Van Ratingen, et al., 2009).

Table 15 RCAR-IIWPG dynamic rating scale (RCAR-IIWPG dynamic evaluation protocol, 2008)

Seat Design Criteria	Neck Force Classification	Dynamic Rating
T1 X-acceleration ≤9.5 g OR Time to head restraint contact ≤70 ms	Low	Good
	Moderate	Acceptable
	High	Marginal
T1 X-acceleration >9.5 g AND Time to head restraint contact >70 ms	Low	Acceptable
	Moderate	Marginal
	High	Poor

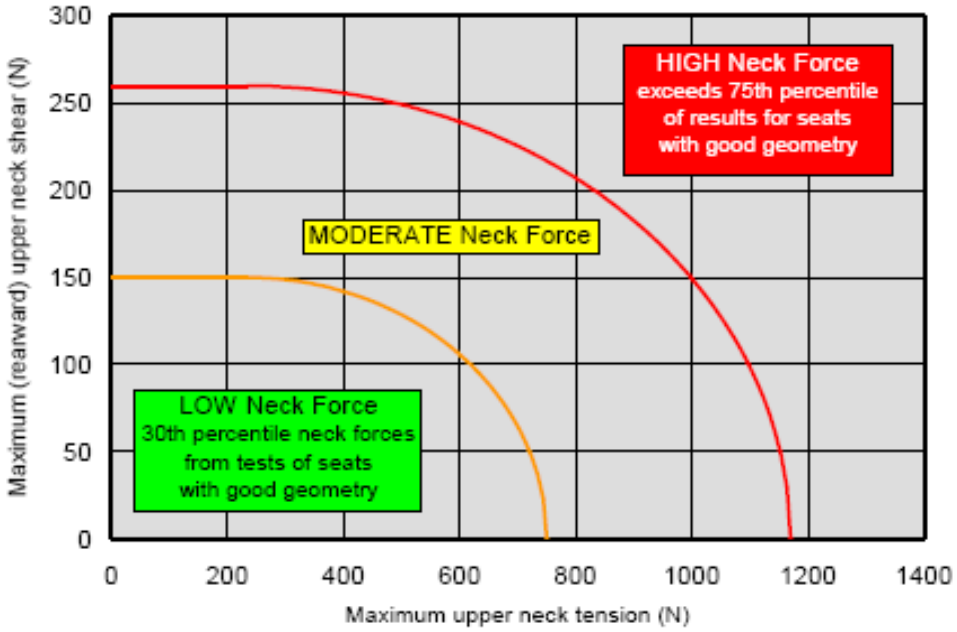

Figure 122 RCAR-IIWPG neck force classification scale (RCAR-IIWPG dynamic evaluation protocol, 2008)

Table 16 RCAR-IIWPG overall rating scale (RCAR-IIWPG dynamic evaluation protocol, 2008)

Geometric Rating	Dynamic Rating	Overall Rating
Good	Good	Good
	Acceptable	Acceptable
	Marginal	Marginal
	Poor	Poor
Good Height		Good
Acceptable	Good	Acceptable
	Acceptable	Acceptable
	Marginal	Marginal
	Poor	Poor
Marginal	No dynamic test	Poor
Poor	No dynamic test	Poor

Table 17 CFC filter classes used for the RCAR-IIWPG dynamic rating (RCAR-IIWPG dynamic evaluation protocol, 2008)

Dummy Transducer Channel	CFC Filter Class
$T1_{left}$	CFC 60
$T1_{right}$	CFC 60
F_x^{upper}	CFC 1000
F_z^{upper}	CFC 1000

CHAPTER 8

EURO NCAP AND RCAR-IIWPG EVALUATION RESULTS OF THE TESTED SEATS

This chapter aims to present the Euro NCAP and RCAR-IIWPG assessment results of the tested seats in tabular form in order to show the performance of the developed anti-whiplash seat mechanism.

8.1 Euro NCAP Assessment Results

The HRMD backset and height measurements performed for the head restraint geometry assessment are summarized for each seat type through Table 18 to Table 20. Table 21 gives the head restraint geometry assessment score of each seat.

Similarly, the HRMD backset and height measurements performed for the worst case assessment are summarized for each seat type through Table 22 to Table 24. Table 25 gives the worst case assessment score of each seat.

Dynamic test results of each seat type are given through Table 26 to Table 28. It should be mentioned that the results presented here should be understood in the sense of the relative performance of the developed mechanism when compared to the cases where no mechanism is used at all and where a different but same purpose mechanism is used. If the developed mechanism was incorporated into a different seat having different raking characteristics, and/or cushions with different viscoelastic properties and/or having differing outer contours and/or headrest tubes with different elasticity, the dynamic test results might be better or worse, but would be absolutely different. However, optimization of the absolute performance of a particular seat is not a purpose of this thesis.

Table 18 HRMD backset and height measurements summary for the head restraint geometry assessment of seat type #1

Seat No	1.1			1.2			1.3			Average	Score
Repeat Measurement No	1	2	3	1	2	3	1	2	3		
HRMD Backset (mm)	25	25	26	27	27	26	24	23	24	25	1.000
Difference between measurement nos. 1 and 2 (mm)	0			0			1				
Difference between measurement nos. 1 and 3 (mm)	-1			1			0				
Difference between measurement nos. 2 and 3 (mm)	-1			1			-1				

Seat No	1.1			1.2			1.3			Average	Score
Repeat Measurement No	1	2	3	1	2	3	1	2	3		
Vertical distance below from the top of the HRMD (mm)	29	29	30	35	37	34	34	33	33	33	0.175
Difference between measurement nos. 1 and 2 (mm)	0			-2			1				
Difference between measurement nos. 1 and 3 (mm)	-1			1			1				
Difference between measurement nos. 2 and 3 (mm)	-1			3			0				

Table 19 HRMD backset and height measurements summary for the head restraint geometry assessment of seat type #2

Seat No	2.1			2.2			2.3			Average	Score
Repeat Measurement No	1	2	3	1	2	3	1	2	3		
HRMD Backset (mm)	28	29	29	29	28	26	28	27	28	28	1.000
Difference between measurement nos. 1 and 2 (mm)	-1			1			1				
Difference between measurement nos. 1 and 3 (mm)	-1			3			0				
Difference between measurement nos. 2 and 3 (mm)	0			2			-1				

Seat No	2.1			2.2			2.3			Average	Score
Repeat Measurement No	1	2	3	1	2	3	1	2	3		
Vertical distance below from the top of the HRMD (mm)	28	29	29	30	33	31	27	28	27	29	0.275
Difference between measurement nos. 1 and 2 (mm)	-1			-3			-1				
Difference between measurement nos. 1 and 3 (mm)	-1			-1			0				
Difference between measurement nos. 2 and 3 (mm)	0			2			1				

Table 20 HRMD backset and height measurements summary for the head restraint geometry assessment of seat type #3

Seat No	3.1			3.2			3.3			Average	Score
Repeat Measurement No	1	2	3	1	2	3	1	2	3		
HRMD Backset (mm)	33	33	33	30	29	28	29	28	29	30	1.000
Difference between measurement nos. 1 and 2 (mm)	0			1			1				
Difference between measurement nos. 1 and 3 (mm)	0			2			0				
Difference between measurement nos. 2 and 3 (mm)	0			1			-1				

Seat No	3.1			3.2			3.3			Average	Score
Repeat Measurement No	1	2	3	1	2	3	1	2	3		
Vertical distance below from the top of the HRMD (mm)	30	31	30	39	38	37	29	28	29	32	0.200
Difference between measurement nos. 1 and 2 (mm)	-1			1			1				
Difference between measurement nos. 1 and 3 (mm)	0			2			0				
Difference between measurement nos. 2 and 3 (mm)	1			1			-1				

Table 21 Head restraint geometry assessment scores of each seat type

Seat No	Geometric Assessment
1	0.175
2	0.275
3	0.200

As apparent from its name, the main aim of the developed mechanism is to minimize the time required for the head restraint to meet and support the head of the occupant, and this is achieved with the maximum available T-HRC scores attained in all the three dynamic tests. Besides, the minimum T-HRC values are obtained by the developed design in all the three dynamic tests when compared to the corresponding values obtained by the other two seat types.

It should be noted that the height adjusting mechanism of the seat collapsed during the high severity pulse test of seat type #3 (i.e. seat no 3.3). However, this test could not be repeated since there is no additional seat. For this reason, the corresponding dynamic test result of the said seat should be approached with caution and skepticism.

Table 22 HRMD backset and height measurements summary for the worst case assessment of seat type #1

Seat No	1.1			1.2			1.3			Average	Score
Repeat Measurement No	1	2	3	1	2	3	1	2	3		
HRMD Backset (mm)	29	29	30	32	33	31	29	28	29	30	1.000
Difference between measurement nos. 1 and 2 (mm)	0			-1			1				
Difference between measurement nos. 1 and 3 (mm)	-1			1			0				
Difference between measurement nos. 2 and 3 (mm)	-1			2			-1				

Seat No	1.1			1.2			1.3			Average	Score
Repeat Measurement No	1	2	3	1	2	3	1	2	3		
Vertical distance below from the top of the HRMD (mm)	67	67	68	73	74	73	72	71	72	71	-0.775
Difference between measurement nos. 1 and 2 (mm)	0			-1			1				
Difference between measurement nos. 1 and 3 (mm)	-1			0			0				
Difference between measurement nos. 2 and 3 (mm)	-1			1			-1				

Table 23 HRMD backset and height measurements summary for the worst case assessment of seat type #2

Seat No	2.1			2.2			2.3			Average	Score
Repeat Measurement No	1	2	3	1	2	3	1	2	3		
HRMD Backset (mm)	36	37	37	33	33	32	34	32	34	34	1.000
Difference between measurement nos. 1 and 2 (mm)	-1			0			2				
Difference between measurement nos. 1 and 3 (mm)	-1			1			0				
Difference between measurement nos. 2 and 3 (mm)	0			1			-2				

Seat No	2.1			2.2			2.3			Average	Score
Repeat Measurement No	1	2	3	1	2	3	1	2	3		
Vertical distance below from the top of the HRMD (mm)	67	68	68	69	68	68	65	65	65	67	-0.675
Difference between measurement nos. 1 and 2 (mm)	-1			1			0				
Difference between measurement nos. 1 and 3 (mm)	-1			1			0				
Difference between measurement nos. 2 and 3 (mm)	0			0			0				

Table 24 HRMD backset and height measurements summary for the worst case assessment of seat type #3

Seat No	3.1			3.2			3.3			Average	Score
Repeat Measurement No	1	2	3	1	2	3	1	2	3		
HRMD Backset (mm)	38	39	38	33	33	32	33	32	33	35	1.000
Difference between measurement nos. 1 and 2 (mm)	-1			0			1				
Difference between measurement nos. 1 and 3 (mm)	0			1			0				
Difference between measurement nos. 2 and 3 (mm)	1			1			-1				

Seat No	3.1			3.2			3.3			Average	Score
Repeat Measurement No	1	2	3	1	2	3	1	2	3		
Vertical distance below from the top of the HRMD (mm)	68	69	68	79	78	76	69	67	69	71	-0.775
Difference between measurement nos. 1 and 2 (mm)	-1			1			2				
Difference between measurement nos. 1 and 3 (mm)	0			3			0				
Difference between measurement nos. 2 and 3 (mm)	1			2			-2				

Table 25 Worst case assessment scores of each seat type

Seat No	Worst Case Geometry
1	0.000
2	0.000
3	0.000

The overall Euro NCAP rating of each tested seat type is summarized in Table 29. With these results, it is shown that both anti-whiplash mechanisms, by decreasing the backset immediately after the crash, have made an improvement in the sense of decreasing the injury risk when compared to the standard seat. However, the proposed prototype mechanism is found to be not as effective in injury prevention as the other tested anti-whiplash mechanism. Another important conclusion might be that the backset reduction strategy as being the dominant approach in the related literature to avoid whiplash injuries might need a revision for being successful in the assessment of the Euro NCAP because the said technique does not prevent both anti-whiplash seats from being in the same injury risk level with the standard seat.

Table 26 Dynamic test results of seat type #1

Seat No: 1.1					
Criterion	**Value**	**HPL**	**LPL**	**CL**	**Score**
NIC (m^2/s^2)	12.31	9.00	15.00	18.30	0.224
Nkm	0.31	0.12	0.35	0.50	0.087
Rebound Velocity (m/s)	3.7	3.0	4.4	4.7	0.250
Fx (N)	44	30	110	187	0.413
Fz (N)	108	270	610	734	0.500
T1 acceleration (g)	15.47	9.40	12.00	14.10	0.000
T-HRC (ms)	80	61	83	95	0.068
Total Score					1.542

	Value	**Limit Value**
Seatback Deflection (deg)	9.0	-

Seat No: 1.2					
Criterion	**Value**	**HPL**	**LPL**	**CL**	**Score**
NIC (m^2/s^2)	19.40	11.00	24.00	27.00	0.177
Nkm	0.57	0.15	0.55	0.69	0.000
Rebound Velocity (m/s)	4.0	3.2	4.8	5.2	0.250
Fx (N)	50	30	190	290	0.438
Fz (N)	158	360	750	900	0.500
T1 acceleration (g)	13.39	9.30	13.10	15.55	0.000
T-HRC (ms)	77	57	82	92	0.100
Total Score					1.465

	Value	**Limit Value**
Seatback Deflection (deg)	9.4	-

Seat No: 1.3					
Criterion	**Value**	**HPL**	**LPL**	**CL**	**Score**
NIC (m^2/s^2)	18.15	13.00	23.00	25.50	0.243
Nkm	0.48	0.22	0.47	0.78	0.000
Rebound Velocity (m/s)	4.5	4.1	5.5	6.0	0.357
Fx (N)	105	30	210	364	0.292
Fz (N)	120	470	770	1024	0.500
T1 acceleration (g)	18.12	12.50	15.90	17.80	0.000
T-HRC (ms)	67	53	80	92	0.241
Total Score					1.633

	Value	**Limit Value**
Seatback Deflection (deg)	14.9	32.0

Table 27 Dynamic test results of seat type #2

Seat No: 2.1					
Criterion	**Value**	**HPL**	**LPL**	**CL**	**Score**
NIC (m^2/s^2)	13.61	9.00	15.00	18.30	0.116
Nkm	0.32	0.12	0.35	0.50	0.065
Rebound Velocity (m/s)	3.8	3.0	4.4	4.7	0.214
Fx (N)	66	30	110	187	0.275
Fz (N)	139	270	610	734	0.500
T1 acceleration (g)	13.98	9.40	12.00	14.10	0.000
T-HRC (ms)	57	61	83	95	0.500
Total Score					1.670

	Value	**Limit Value**
Seatback Deflection (deg)	9.4	-

Seat No: 2.2					
Criterion	**Value**	**HPL**	**LPL**	**CL**	**Score**
NIC (m^2/s^2)	20.25	11.00	24.00	27.00	0.144
Nkm	0.41	0.15	0.55	0.69	0.175
Rebound Velocity (m/s)	4.2	3.2	4.8	5.2	0.188
Fx (N)	84	30	190	290	0.331
Fz (N)	222	360	750	900	0.500
T1 acceleration (g)	15.09	9.30	13.10	15.55	0.000
T-HRC (ms)	52	57	82	92	0.500
Total Score					1.838

	Value	**Limit Value**
Seatback Deflection (deg)	10.4	-

Seat No: 2.3					
Criterion	**Value**	**HPL**	**LPL**	**CL**	**Score**
NIC (m^2/s^2)	20.49	13.00	23.00	25.50	0.126
Nkm	0.53	0.22	0.47	0.78	0.000
Rebound Velocity (m/s)	4.3	4.1	5.5	6.0	0.429
Fx (N)	195	30	210	364	0.042
Fz (N)	165	470	770	1024	0.500
T1 acceleration (g)	15.89	12.50	15.90	17.80	0.001
T-HRC (ms)	50	53	80	92	0.500
Total Score					1.597

	Value	**Limit Value**
Seatback Deflection (deg)	14.7	32.0

Table 28 Dynamic test results of seat type #3

Seat No: 3.1					
Criterion	**Value**	**HPL**	**LPL**	**CL**	**Score**
NIC (m^2/s^2)	10.98	9.00	15.00	18.30	0.335
Nkm	0.28	0.12	0.35	0.50	0.152
Rebound Velocity (m/s)	3.7	3.0	4.4	4.7	0.250
Fx (N)	46	30	110	187	0.400
Fz (N)	119	270	610	734	0.500
T1 acceleration (g)	14.06	9.40	12.00	14.10	0.000
T-HRC (ms)	64	61	83	95	0.432
Total Score					2.069

	Value	**Limit Value**
Seatback Deflection (deg)	9.6	-

Seat No: 3.2					
Criterion	**Value**	**HPL**	**LPL**	**CL**	**Score**
NIC (m^2/s^2)	15.94	11.00	24.00	27.00	0.310
Nkm	0.39	0.15	0.55	0.69	0.200
Rebound Velocity (m/s)	4.1	3.2	4.8	5.2	0.219
Fx (N)	66	30	190	290	0.388
Fz (N)	169	360	750	900	0.500
T1 acceleration (g)	13.32	9.30	13.10	15.55	0.000
T-HRC (ms)	54	57	82	92	0.500
Total Score					2.117

	Value	**Limit Value**
Seatback Deflection (deg)	10.3	-

Seat No: 3.3					
Criterion	**Value**	**HPL**	**LPL**	**CL**	**Score**
NIC (m^2/s^2)	17.01	13.00	23.00	25.50	0.300
Nkm	0.67	0.22	0.47	0.78	0.000
Rebound Velocity (m/s)	3.9	4.1	5.5	6.0	0.500
Fx (N)	99	30	210	364	0.308
Fz (N)	133	470	770	1024	0.500
T1 acceleration (g)	18.53	12.50	15.90	17.80	0.000
T-HRC (ms)	50	53	80	92	0.500
Total Score					2.108

	Value	**Limit Value**
Seatback Deflection (deg)	15.3	32.0

Table 29 Overall Euro NCAP rating of each tested seat type

	Seat No		
	1	2	3
Geometry	0.2	0.3	0.2
Worst Case Geometry	0.0	0.0	0.0
Low Severity (unscaled)	1.5	1.7	2.1
Medium Severity (unscaled)	1.5	1.8	2.1
High Severity (unscaled)	1.6	1.6	2.1
Seatback Deflection (deg)	14.9	14.7	15.3
Dynamic	4.6	5.1	6.3
Raw Whiplash Score	4.8	5.4	6.5
Final Scaled Score	1.8	2.0	2.4
Color	Orange	Orange	Orange

The BioRID backset distances measured prior to each test are summarized in Table 30. They are recorded to be close to each other, but not the same at all, and this should be kept in mind while comparing the results of the same severity dynamic tests of different seat types.

Table 30 BioRID backset distances recorded prior to each test

Seat No	Backset (mm)
1.1	40
1.2	43
1.3	40
2.1	41
2.2	44
2.3	44
3.1	46
3.2	42
3.3	47

While comparing the results, another thing that should be considered is that the seatback deflections of the three different seat types are again close but not the same for each sled pulse severity. Actually, they differ in a range of 0.6-1° (see Table 31). Although the differences might be thought to be minor at first, they will result in substantial differences in the effective dynamic backset distances since the deflections are measured around the pivot point of the seatback. A careful examination of Table 31 reveals that the seatback deflections are recorded to be the minimum for the standard seat in the low and medium severity tests. This fact may be responsible for not increasing the performance of the both types of anti-whiplash seats in these tests with respect to the standard seat as much as expected.

Table 31 Seatback deflections in each test

Seat No	Seatback Deflection (deg)
1.1	9.0
1.2	9.4
1.3	14.9
2.1	9.4
2.2	10.4
2.3	14.7
3.1	9.6
3.2	10.3
3.3	15.3

8.2 RCAR-IIWPG Assessment Results

The HRMD backset and height measurements conducted for the Euro NCAP head restraint geometry assessment of the seats to be tested are converted into the RCAR-IIWPG static rating results for each seat type as shown in Table 32. These ratings are based on the average values of the nine Euro NCAP head restraint geometry measurements performed for each seat type (see Table 18 through Table 20). Over and above this, each of these 27 measurements would also be rated as "good" according to the scale given in Figure 121.

However, these backset and height measurements are not conducted on a seat mounted to the vehicle of concern as required by the RCAR-IIWPG system. Even so, the seat mounting fixture and the heel surface plate used to mount the seats to be tested to the sled plate reproduce accurately the orientation of the seat inside the vehicle on the sled.

Besides, these measurements are taken at the Euro NCAP test position of the head restraint, which is within 10 mm rise from the geometric midpoint of the allowable travel range of the head restraint. However, according to the RCAR-IIWPG system, they should have been conducted twice, one at the lowest and one at the highest locking position of the head restraint. The rating then should have been made by using the average backset and height values of these two measurements. Since the travel of the head restraint between the up and down positions is linear, this would correspond to measure the head restraint at its geometric mid. However, even if the corresponding measurements were performed in accordance with the RCAR-IIWPG system, they would still yield "good" static ratings according to the scale of Figure 121, because the "worst" recorded backset and height values among these 27 measurements are still 37 mm and 21 mm far away from the associated "good"-"acceptable" boundaries, respectively. Moreover, the "worst" recorded backset value among the 27 worst case geometry measurements is still 31 mm far away from the associated "good"-"acceptable" boundary.

Lastly, the seat track and height adjustments are set to their midranges before these head restraint geometry measurements, as required by the Euro NCAP protocol. On the other hand, the reason why the RCAR protocol dictates to adjust the seat to be at its lowermost and rearmost position prior to these measurements is explained as to allow sufficient space for the feet of the HPM to be raised freely. In this study, such a constraint problem is not encountered on the sled, and in addition, the relative orientation of the HPM and HRMD with respect to the seat and head restraint would not be affected significantly when the seat adjustment controls were set according to the RCAR-IIWPG system. Furthermore, as mentioned above, all the 27 head restraint geometry measurements are too far away from the "good"-"acceptable" boundary. For these reasons, the ratings would be the same again (i.e., "good") even if they were repeated at the lowest and rearmost position of the seat.

The neck forces are classified as low for each seat type tested in Table 33 according to the classification scheme given in Figure 122. Then, each seat is rated dynamically in Table 34 according to the dynamic rating formulation given in Table 15. Table 35 combines the geometric and dynamic ratings obtained for each tested seat type to yield the overall RCAR-IIWPG rating of each of them.

Both anti-whiplash mechanisms are rated with the highest possible score, i.e., "good", whereas the standard seat is rated one grade below, i.e., "acceptable". It should be made clear that T-HRC values seen in Table 34 for seat type #1 and seat type #3 are slightly different than the ones seen in Table 26 and Table 28,

respectively. This is because the T-HRC values presented in Table 34 are calculated using the time indexing method described in the RCAR-IIWPG dynamic evaluation protocol (2008).

Table 32 Head restraint static rating of each seat type

Seat No	Backset (mm)	Height (mm)	Geometric Rating
1	25	33	Good
2	28	29	Good
3	30	32	Good

According to this time indexing method, first the time is shifted such that the time at which the peak value of the bias removed and CFC 60 filtered sled acceleration occurs is 27 ms. The T-HRC is determined in accordance with this shift in time. Let it be denoted by T-HRC^s. Then, the sled velocity is obtained by integrating the sled acceleration in the interval between the last time of passing through the zero-acceleration at the beginning of the pulse and the first time of passing through the zero-acceleration at the end of the pulse. Following this, the time at which the sled velocity reaches to 4 m/s is found and rounded to the next highest integer. Let this value be denoted by t_v. This t_v is then subtracted from 70 ms and this differences is added to the T-HRC^s to determine the RCAR-IIWPG T-HRC.

Table 33 Neck force classification of each seat type

Seat No	F_x (N)	F_z (N)	Neck Force Classification
1	50	158	Low
2	84	222	Low
3	66	169	Low

Table 34 Dynamic rating of each seat type

Seat No	T1 (g)	T-HRC (ms)	Neck Force Classification	Dynamic Rating
1	13.4	78	Low	Acceptable
2	15.1	52	Low	Good
3	13.3	55	Low	Good

Table 35 Overall RCAR-IIWPG rating of each seat type

Seat No	Geometric Rating	Dynamic Rating	Overall Rating
1	Good	Acceptable	Acceptable
2	Good	Good	Good
3	Good	Good	Good

CHAPTER 9

CONCLUSIONS

This chapter gives a brief summary of the findings and contributions of this thesis work and presents general conclusions and recommendations for future works.

9.1 General Conclusions

Neck injury, or whiplash syndrome, is one of the most common types of injuries encountered in low-speed rear end crashes. Although not life-threatening, because of its long-lasting pain and the labor force loss due to the resulted discomfort, this health and socio-economic problem recently attracted more and more interest from both academia and industry. Although the exact injury mechanism is still not known, headrest position and raking characteristics of the seatback in vehicle seats are encountered to be the two major risk factors for whiplash injury, as discussed in Chapter 1.

The main aim of this thesis is to develop and evaluate a novel anti-whiplash seat mechanism. The existing anti-whiplash system patents have been studied, and a classification of them has been made based on their working principles. According to this classification, the following eight groups have been identified: (i) systems where the head restraint is moved forward by a mechanical trigger mechanism, (ii) systems where the head restraint is moved forward by an electrical control system, (iii) systems where the backrest moves, (iv) systems where the entire seat moves, (v) special-shaped backrest and head restraint designs made of special materials, (vi) air-bagged head restraints, (vii) other headrest forms, (viii) helmet and collar designs. However, it is found that the dominant approach followed by most of these systems is to reduce the gap between the head and the headrest during a rear-end collision in order to meet and properly support the head of the occupant. Allowing the movement of the entire seat with respect to the vehicle and absorbing some of the crash energy that is

transmitted to the occupant through a controlled plastic deformation of a deformation element is another encountered technique for this purpose.

At the preliminary stages of this study, two functional design alternatives have been considered. One of them is the widely used backset reducing system and the other one is a novel concept of horizontal anti-whiplash seat suspension. For the preliminary evaluation of these alternatives, a simplified seat model has been developed, and using this finite element model and the commercially available finite element model of the BioRID II dummy, these two design concepts have been evaluated through simulations in the LS-DYNA® environment. The developed simplified seat model is easily adaptable to evaluate different seats with different designs and characteristics.

As a result of the simulations wherein the effect of backset has been investigated, as one may expect from the related literature, the NIC_{max} value has been observed to decrease with decreasing backset.

As a second alternative, a vehicle seat that slides backwards along a pair of rails against a horizontal suspension arrangement, during a rear collision has been proposed. For the purpose of avoiding any undesired backward sliding of the seat during normal use, an initial bias is given to the spring of this suspension arrangement, and the damper within the suspension absorbs some of the crash energy. Hence, as being an important advantage of the suggested anti-whiplash suspension, no member is plastically deformed during the backward travel of the seat, and the system resets itself automatically after the accident without any additional effort or cost. A parametric analysis of this system has revealed a strong linear inverse correlation between NIC_{max} and the maximum seat sliding distance while the stiffness and damping coefficients of the suspension arrangement are varied. It has been also found that, for a given crash pulse and a predetermined initial seat spring bias force, the same NIC_{max} value is obtained with different suspension stiffness and damping coefficients that result in the same maximum sliding distance of the seat. These conclusions constitute the general design guidelines of such an anti-whiplash seat suspension.

Although the use of the suggested seat suspension promises good performance for injury prevention, the backward movement of the seat may bring out adverse effects on the passengers sitting on the rear seat. For this reason, it has been decided to continue with the first alternative in this study.

Two different and novel vehicle seat mechanisms have been developed for reducing the backset immediately after the crash. One of these systems is a lock/release system. In this system, with the rotation of a back plate lying underneath the back rest cushion, the inner wire of a Bowden cable is pulled to release a trigger lock which maintains the nominal position of the headrest. After this lock is released, the headrest is rotated forward by a pair of biased headrest springs. With a sufficient amount of bias given to the headrest springs, the headrest maintains its frontmost

position when it is subjected to forces due to its contact with the head. In an alternative embodiment of this design, a secondary lock is proposed to be used with the same aim. Any of these two alternative embodiments does not comprise a component that is plastically deformed. However, occupant effort will be required in order to reset both of them after the accident, and if the occupant cannot re-set-up the system properly, this will deteriorate the driving comfort. For this reason, it has been believed to be very beneficial to eliminate the lock unit from the system in order to have a system that autonomously re-sets-up itself for reuse.

This has been achieved by adapting a quick forward mechanism to be used for vehicle seats. In this system, as a back plate rotates backwards during a rear impact, the headrest rotates forward. The mechanism is operated in the working range wherein the headrest rotates faster than the back plate so that the ratio of the angle rotated by the headrest to the angle rotated by the back plate can be achieved as high as required. After the accident, the mechanism is reversely operated by a pair of biased back plate springs, and it becomes ready to work again automatically without requiring any interference of the occupant.

For the assessment of the developed quick forward anti-whiplash mechanism, three different types of vehicle seats, namely the prototype seat with the developed mechanism, a standard seat that has no specific whiplash injury prevention action and a different anti-whiplash seat with a different re-active head restraint system, have been tested at the METU-BILTIR Center Vehicle Safety Unit. These three types differ only by their head restraint types. For each type, three identical new driver seats have been tested using the low, medium and high severity Euro NCAP sled pulses, respectively. The test data have been evaluated by using both the Euro NCAP and the RCAR-IIWPG rating systems.

In accordance with its name, the minimum starting times of the contact of the head of the dummy with the head restraint (T-HRC) have been attained by the developed quick forward anti-whiplash mechanism in all of the three dynamic tests when compared to the corresponding values obtained by the other two seat types. Besides, the developed mechanism has made the maximum available score reserved for T-HRC performance in the Euro NCAP rating system in all of the three dynamic tests. Moreover, it has been shown that both anti-whiplash mechanisms, by decreasing the backset immediately after the crash, have made an improvement in the sense of decreasing the injury risk when compared to the standard seat. This finding is valid for both the Euro NCAP and the RCAR-IIWPG ratings of the same seats.

According to the Euro NCAP assessment system, although some improvement has been achieved by both anti-whiplash systems when compared to the standard seat, all the three tested types have been rated with the same mid-level of injury risk, i.e., they have been all colored in "orange". However, the proposed prototype seat mechanism has not been found as successful as the other tested anti-whiplash seat mechanism according to this rating. This might be due to the fact the rotations of the

input links, i.e., the back plates of the two headrest moving mechanisms are in the opposite sense of each other. Another important conclusion might be that the backset reduction strategy, although widely followed, might not suffice alone for being successful in the Euro NCAP assessment because this technique has not prevented both anti-whiplash seats from being in the same injury risk level with the standard seat.

It should be noted that the recorded seatback deflections of the three different seat types have differed in a range of 0.6-1°. Although these differences might seem to be minor, they might have significantly affected the dynamic backset distances. The seatback deflections have been recorded to be the minimum for the standard seat in the low and medium severity tests, and this fact might be responsible for not increasing the performance of the both types of anti-whiplash seats with respect to the standard seat as much as expected.

According to the RCAR-IIWPG assessment system, both anti-whiplash mechanisms have been rated with the highest possible score, i.e., "good", whereas the standard seat has been rated one grade below, i.e., "acceptable". The reason behind the relatively lower performance of the standard seat is due to its relatively higher T-HRC value. Based on the RCAR-IIWPG ratings of the tested seats, one can say that reducing the backset will help a lot for minimizing the injury risk.

It is worth to recall that the RCAR-IIWPG evaluation puts more emphasis on the real-world validation of its results, whereas the evaluation system of SRA, and hence that of the Euro NCAP by adopting its criteria, welcome also unproven and unvalidated hypotheses. Hence, more biomechanical investigation of the injury predictors is required for a robust evaluation of vehicle seats for whiplash protection.

Main contributions of this thesis research can be summarized as follows:

- ✓ Development of a simplified vehicle seat model
  - ➢ An easily adaptable model for the preliminary evaluation of different vehicle seat design concepts
- ✓ Parametric analysis and design guidelines for a novel anti-whiplash seat suspension concept
  - ➢ No deformation element used
  - ➢ No additional cost or user effort required for making the system ready to use again after the accident
- ✓ A novel anti-whiplash vehicle seat mechanism having a lock
  - ➢ Two alternative embodiments
  - ➢ No deformation element used in any of these two embodiments
  - ➢ No additional cost required for making any of these two embodiments ready to use again after the accident
- ✓ A novel quick forward anti-whiplash vehicle seat mechanism
  - ➢ No deformation element used

- No additional cost or user effort required for making the system ready to use again after the accident

- ✓ Evaluation and validation of the performance of the proposed quick forward anti-whiplash mechanism through a series of sled tests
  - Totally nine sled tests have been performed for three different types of seats
- ✓ Comparison of the evaluation of the same test data according to two different whiplash rating systems
  - Differences have been shown between the overall Euro NCAP and RCAR-IIWPG ratings of the same seats

9.2 Recommendations for Future Works

In this thesis, firstly, effect of the backset distance on the whiplash syndrome has been analyzed using the developed simplified seat model and the finite element model of the BioRID II crash test dummy. Any specific headrest moving mechanism is not included in this simplified seat model, and position of the headrest has been adjusted by simply moving the headrest back and forth prior to the simulation. Then, an evaluation of the proposed quick forward anti-whiplash mechanism has been performed through a series of sled tests.

As a continuation of this thesis work, an evaluation of the proposed mechanism can also be performed through simulations in the computer environment using the finite element models of the actual tested seats including the corresponding headrest moving mechanism and the BioRID II crash test dummy model. Trajectories followed by the trackers on the sled, seat and the dummy, the recorded dummy transducer data and the resulting injury criteria values in the sled tests of this study can be used for the validation of these simulations. Such simulations would be helpful for decreasing the cost of the evaluation of any further improvements that might be needed later in the prototype anti-whiplash seat.

Recorded high speed videos of the conducted sled tests have been used in this study only for the calculation of the two injury criteria, namely the rebound velocity ($V_{rebound}$) and the seatback deflection, as required by the assessment protocols used. However, these videos can be further analyzed using suitable motion analysis software like the TEMA Automotive®, which is available at the METU-BILTIR Center.

Kinematic parameters of the developed mechanism have been selected in this research such that minor modifications are required for its integration to the tested standard seat in order to be able to concentrate only on the effect of the headrest

moving mechanism on the injury prevention. However, in a future work, the synthesis of the proposed mechanism can be optimized to maximize the whiplash avoidance, which might require more dramatic changes to the seat construction.

As another extension of this thesis, a prototype of the proposed anti-whiplash system having lock(s) can be built and tested in order to study the possible advantages and disadvantages of a system with locking action over continuous systems. Such a lock/release system will operate independently from the magnitude of the force applied by the occupant on the back rest or its change in time once it exceeds a threshold value that is predetermined for activation of the system.

Still another future work suggestion would be that a slidable seat-seat suspension prototype can be built and tested for identifying its advantages and disadvantages when compared to the backset reducing systems.

One another recommendation might be to develop and evaluate a novel anti-whiplash system by combining the two strategies considered in this study, i.e. a vehicle seat that can slide against a horizontal seat suspension while the backset is reduced at the same time. Such a system would be much more successful than each of the systems where only one of these strategies is used. With such a system, the distance that the seat travels backwards can be reduced substantially for the passengers sitting in the rear seats while the accompanying increase in the injury risk due to the decrease in the maximum sliding distance can be compensated with a reduction in backset by moving the headrest forward. Such a system will especially provide a better prevention for the occupants sitting with a large initial backset distance. The forward travel of the headrest might not suffice alone in such cases for a proper support of the head and neck, and the backward sliding of the seat against a horizontal suspension arrangement as proposed in this study will aid to the overall prevention of the system.

A last remark is that all the analyses and evaluations have been carried out in this study using the BioRID II crash test dummy. This crash dummy is a representative of a 50th percentile, i.e., mid-size, adult male. In a future research, the proposed systems in this thesis work can be evaluated for different size male and female occupants.

REFERENCES

Akaike, F., & Nishimura, S. (2005). *US Patent No. 2005280304.*

Albrecht, D. (2003). *US Patent No. 2003001413.*

Aldman, B. (1995). *WO Patent No. 9511818.*

Andersson, S. (2001). *US Patent No. 6179379.*

Australasian New Car Assessment Program (ANCAP). (January 2012). ANCAP notes on the assessment protocol, (Version 5.1).

Aylor, D. A., & Zuby, D. S. (2011). Comparison of BioRID injury criteria between dynamic sled tests and vehicle crash tests. *Proceedings of the 22nd Enhanced Safety of Vehicles Conference*, Washington DC, USA.

Bossecker, M., & Karlbauer, U. (2002). *US Patent No. 2002014760.*

Boström, O., Fredriksson, R., Haland, Y., Jakobsson, L., Krafft, M., Lovsund, P., ... & Svensson, M. Y. (2000). Comparison of car seats in low speed rear-end impacts using the BioRID dummy and the new neck injury criterion (NIC). *Accident Analysis and Prevention*, *32* (2), 321-328.

Breed, D. S. (1996). *GB Patent No. 2301906.*

Breed, D. S. (2000). *US Patent No. 6088640.*

Breed, D. S. (2006). *US Patent No. 2006186713.*

Breed, D. S. (2008). *US Patent No. 2008042477.*

Bring, G., Björnstig, U., & Westman, G. (1996). Gender patterns in minor head and neck injuries: an analysis of casualty register data. *Accident Analysis and Prevention*, *28* (3), 359-369.

Bring, G., & Westman, G. (1991). Chronic posttraumatic syndrome after whiplash injury: a pilot study of 22 patients. *Scandinavian Journal of Primary Health Care*, *9* (2), 135-141.

Caiati, M. I., & Lehle, W. L. (1972). *US Patent No. 3643972.*

Chapline, J. F., Ferguson, S. A., Lillis, R. P., Lund, A. K., & Williams, A. F. (2000). Neck pain and head restraint position relative to the driver's head in rear-end collisions. *Accident Analysis and Prevention*, *32* (2), 287-297.

Chen, H.-B., Yang, K. H., & Wang, Z.-G. (2009). Biomechanics of whiplash injury. *Chinese Journal of Traumatology (English Edition)*, *12* (5), 305-314.

Cholewicki, J., Panjabi, M. M., Nibu, K., Babat, L. B., Grauer, J. N., & Dvorak, J. (1998). Head kinematics during in vitro whiplash simulation. *Accident Analysis and Prevention, 30* (4), 469-479.

Croft, A. C. (1996). Low speed rear impact collisions: In search of an injury threshold. *Journal of Musculoskeletal Pain, 4* (4), 39-46.

Croft, A. C., Herring, P., Freeman, M. D., & Haneline, M. T. (2002). The neck injury criterion: future considerations. *Accident Analysis and Prevention*, *34* (2), 247-255.

Dellanno, R. P. (1996). *US Patent No. 5580124.*

Dellanno, R. P. (2004). *US Patent No. 2004070239.*

Dellanno, R. P., & Gualtier, Q. E. (1992). *WO Patent No. 9204847.*

Dellanno, R. P., & Gualtier, Q. E. (1993). *US Patent No. 5181763.*

Dellanno, R. P., & Gualtier, Q. E. (1994). *US Patent No. 5290091.*

Deter, T., Malczyk, A., & Kuehn, M. (2007). Validation of a seat-dummy simulation model for rear-impact. *German Insurance Association-Accident Research*, *Paper Number 07-0151*.

Edwards, M., Smith, S., Zuby, D. S., & Lund, A. K. (2005). Improved seat and head restraint evaluations. Insurance Institute for Highway Safety, United States, Paper No. 05-0374.

Eichberger, A., Steffan, H., Geigl, B., Svensson, M., Boström, O., Leinzinger, P. E., & Darok, M. (1998). Evaluation of the applicability of the neck injury criterion (NIC) in rear end impacts on the basis of human subject tests. *Proceedings of the 1998 International IRCOBI Conference on the Biomechanics of Impac*t, Goteborg, Sweden.

Eichorst, H. H. (1964). *US Patent No. 3151911.*

Eriksson, L. (2005). Influence of head restraint position on long-term AIS 1 neck injury risk. *International Journal of Crashworthiness*, *10* (6), 545-555.

European New Car Assessment Program (Euro NCAP). (May 2008). The dynamic assessment of car seats for neck injury protection testing protocol, (Version 2.8).

European New Car Assessment Program (Euro NCAP). (June 2008). Assessment protocol and biomechanical limits, (Version 4.2).

European New Car Assessment Program (Euro NCAP). (June 2011). The dynamic assessment of car seats for neck injury protection testing protocol, (Version 3.1).

European New Car Assessment Program (Euro NCAP). (November 2011). Assessment protocol – Adult occupant protection, (Version 5.4).

Farmer, C. M., Wells, J. K., & Lund, A. K. (2003). Effects of head restraint and seat redesign on neck injury risk in rear-end crashes. *Traffic Injury Prevention*, *4* (2), 83-90.

Farmer, C. M., Wells, J. K., & Werner, J. V. (1999). Relationship of head restraint positioning to driver neck injury in rear-end crashes. *Accident Analysis and Prevention*, *31* (6), 719-728.

Farquhar, M., McQueen, K., Humer, M., & Smallwood D. (2004) *US Patent No. 2004061362*.

Golinski, W. Z., & Gentle, C. R. (2001). Biomechanical simulation of whiplash-some implications for seat design. *International Journal of Crashworthiness*, *6* (4), 573-584.

Golinski, W. Z., & Gentle, R. (2005). The influence of seat back rake on ligament loadings in rear-end impact. *Proceedings of the Institution of Mechanical Engineers, Part D: Journal of Automobile Engineering*, *219* (2), 197-205.

Göçmen, U. (2009). Experimental whiplash analysis with Hybrid III 50 percentile test dummy. M.S. Thesis, Middle East Technical University Graduate School of Natural and Applied Sciences Department of Mechanical Engineering.

Grandoni, L. (1990). *CA Patent No. 1273375.*

Grenda, R., Jacobs, F., Verunac, M., & Lariviere, G. (2001). *GB Patent No. 2354936.*

Gujarati, D. N. (2003). Basic Econometrics (4th ed.). The McGraw-Hill Companies.

Güzel, A. G., Karaduman, M., Koçum, M. A., Kuzucuoğlu, M., Sipahi, M., Topuz, R. D., & Naderi, S. (2000). Whiplash yaralanmaları. *The Journal of Turkish Spinal Surgery*, *11* (1), 13-16.

Haglund, L., Simonsson, L., & Holgers, A. (2004). *GB Patent No. 2403137.*

Haland, L. Y., & Boström, O. (1997). *GB Patent No. 2311212.*

Hartling, L., Pickett, W., & Brison, R. J. (2002). Derivation of a clinical decision rule for whiplash associated disorders among individuals involved in rear-end collisions. *Accident Analysis and Prevention, 34* (4), 531-539.

Hesen, J. A. (1965). *US Patent No. 3222084.*

Himmetoglu, S., Acar, M., Bouazza-Marouf, K., & Taylor, A. J. (2008). Energy-absorbing car seat designs for reducing whiplash. Traffic injury prevention, 9(6), 583-591.

Himmetoglu, S., Acar, M., Bouazza-Marouf, K., & Taylor, A. J. (2011). Car seat design to improve rear-impact protection. *Proceedings of the Institution of Mechanical Engineers, Part D: Journal of Automobile Engineering*, *225* (4), 441-459.

Ikari, T., Kaito, K., Nakajima, T., Yamazaki, K., & Ono, K. (2009). Japan New Car Assessment Program for minor neck injury protection in rear-end collisions. *Proceedings of the 21st International Technical Conference on the Enhanced Safety of Vehicles*, Stuttgart, Germany.

Ivancic, P. C., Sha, D., & Panjabi, M. M. (2009). Whiplash injury prevention with active head restraint. *Clinical Biomechanics*, *24* (9), 699-707.

Jacobs, F., Verunac, M., & Zellmer, H. (2001). *GB Patent No. 2359482.*

Jakobsson, L., Lundell, B., Norin, H., & Isaksson-Hellman, I. (2000). WHIPS - Volvo's whiplash protection study. *Accident Analysis and Prevention, 32* (2), 307-319.

Krafft, M., Kullgren, A., Tingvall, C., Boström, O., & Fredriksson, R. (2000). How crash severity in rear impacts influences short- and long-term consequences to the neck. *Accident Analysis and Prevention, 32* (2), 187-195.

Krafft, M., Kullgren, A., Ydenius, A., & Tingvall, C. (2002). Influence of crash pulse characteristics on whiplash associated disorders in rear impacts-Crash recording in real life crashes. *Traffic Injury Prevention*, *3* (2), 141-149.

Kumar, S., Narayan, Y., & Amell, T. (2000). Role of awareness in head-neck acceleration in low velocity rear-end impacts. *Accident Analysis and Prevention, 32* (2), 233-241.

Lenz, T. (1997). *WO Patent No. 9743142.*

Lenz, T. (1998). *US Patent No. 5833312.*

Lerjestad, J., Blaus, M., Ewald, M., & Halvardsson, C. (1998). *WO Patent No. 9818356.*

Lindblad, K.-G. (2004). *GB Patent No. 2395114.*

Linder, A. (2000). A new mathematical neck model for a low-velocity rear-end impact dummy: Evaluation of components influencing head kinematics. *Accident Analysis and Prevention, 32* (2), 261-269.

Lindström, M. (2000). *WO Patent No. 0050258.*

Luo, M., & Zhou, Q. (2010). A vehicle seat design concept for reducing whiplash injury risk in low-speed rear impact. *International Journal of Crashworthiness*, *15* (3), 293-311.

Maher, J. (2000). Report investigating the importance of head restraint positioning in reducing neck injury in rear impact. *Accident Analysis and Prevention, 32* (2), 299-305.

Masuda, K., & Ito, T. (2002). *US Patent No. 2002195846.*

McCreesh, K., Arthurs, S., Horgan, S., Keane, L., & Meagher, L. (2012). Vehicle head restraint positioning knowledge and behaviours in a sample of Irish drivers. *International Journal of Injury Control and Safety Promotion*, *19* (4), 340-346.

METU-BILTIR Center. (2013, May 04). Retrieved from http://www.biltir.metu.edu.tr/tasitguven_ing.html

Meyer, T. (2000). *US Patent No. 6149232.*

Meyer, T., Haller, E., Eidenhammer, P., & Hermann, S. (2000). *US Patent No. 6017086.*

Minton, R., Murray, P., Stephenson, W., & Galasko, C. S. B. (2000). Whiplash injury - Are current head restraints doing their job? *Accident Analysis and Prevention, 32* (2), 177-185.

Muser, M., Hell, W., & Schmitt, K. U. (2003). How injury criteria correlate with the injury risk-A study analyzing different parameters with respect to whiplash injury. *Proceedings of the 18th International Technical Conference on the Enhanced Safety of Vehicles*, Nagoya, Japan, Paper No. 68-W.

Muser, M., & Schmitt, K.-U. (2005). *EP Patent No. 1551664.*

Muser, M., & Schmitt, K.-U. (2005). *US Patent No. 2005253408.*

Niitsuma, K., Negishi, H., Tanabe, J., Uno, K., Terauchi, T., Matsumoto, T., & Sano, K. (2007). *EP Patent No. 1842717.*

Nilsson, K. (2001). *US Patent No. 2001011830.*

Nilsson, K. (2002). *US Patent No. 6435591.*

Okano, N., Ishikawa, T., Kage, M., & Ishikura, K. (2001). *EP Patent No. 1084901.*

Olivegren, H., Jerkvall, N., Hagström, Y., & Carlsson, J. (1999). The long-term prognosis of whiplash-associated disorders (WAD). *European Spine Journal, 8* (5), 366-370.

Ommaya, A. K., & Hirsch, A. E. (1974). *GB Patent No. 1348239.*

Omori, M. (2008). *US Patent No. 2008129092.*

Palm, J. E. (2008). *US Patent No. 2008073886.*

Pan, J. Y. M. (2004). *US Patent No. 2004075252.*

Panjabi, M. M., Cholewicki, J., Nibu, K., Grauer, J. N., Babat, L. B., & Dvorak, J. (1998). Mechanism of whiplash injury. *Clinical Biomechanics*, *13* (4), 239-249.

Rasenberg, J. T. M. (2001). *WO Patent No. 0156830.*

Research Council for Automobile Repairs (RCAR). (March 2008). Procedure for evaluating motor vehicle head restraints, (Version 3).

Research Council for Automobile Repairs- International Insurance Whiplash Prevention Group (RCAR-IIWPG). (March 2008). Seat/head restraint evaluation protocol, (Version 3).

Riches, D. (1996). *GB Patent No. 2296855.*

Saczalski, T. K., & Saczalski, K. J. (2002). *US Patent No. 2002056980.*

Saczalski, T. K., & Saczalski, K. J. (2002). *US Patent No. 2002180197.*

Schmitt, K. U., Muser, M., Heggendorn, M., Niederer, P., & Walz, F. (2003). Development of a damping seat slide to reduce whiplash injury. *Proceedings of the Institution of Mechanical Engineers, Part D: Journal of Automobile Engineering*, *217* (11), 949-955.

Schmitt, K. U., Muser, M. H., Walz, F. H., & Niederer, P. F. (2002). Nkm-A proposal for a neck protection criterion for low-speed rear-end impacts. *Traffic Injury Prevention*, *3* (2), 117-126.

Sekizuka, M. (1998). Seat designs for whiplash injury lessening. *Proceedings of the 16th International Conference on the Enhanced Safety of Vehicles*, (pp. 1570-1578). Windsor, Ontario, Canada.

Sendur, P., Thibodeau, R., Burge, J., & Tencer, A. (2005). Parametric analysis of vehicle design influence on the four phases of whiplash motion. *Traffic Injury Prevention, 6* (3), 258-266.

Shin, M. K., Park, K. J., & Park, G. J. (2003). Occupant analysis and seat design to reduce neck injury from rear end impact. *International Journal of Crashworthiness*, *8* (6), 573-581.

Siegmund, G. P., Heinrichs, B. E., & Wheeler, J. B. (1999). The influence of head restraint and occupant factors on peak head/neck kinematics in low-speed rear-end collisions. *Accident Analysis and Prevention*, *31* (4), 393-407.

Siemiantkowski, P. (2007). *US Patent No. 2007158933.*

Stahlschmidt, S., Keding, B., Franz, U., & Hirth, A. (2006a). BioRID II dummy model development-Influence of parameters in validation and consumer tests. *9th International LS-DYNA Users Conference*, Detroit, USA.

Stahlschmidt, S., Keding, B., Witowski, K., Müllerschön, H., & Franz, U. (2006b). BioRID II dummy model development-Stochastic investigations. *DYNAmore LS-DYNA Conference*, Ulm, Germany.

Stemper, B. D., Yoganandan, N., & Pintar, F. A. (2006). Effect of head restraint backset on head–neck kinematics in whiplash. *Accident Analysis and Prevention, 38* (2), 317–323.

Svensson, M. Y., Boström, O., Davidsson, J., Hansson, H. A., Haland, Y., Lövsund, P., ... & Säljö, A. (2000). Neck injuries in car collisions-A review covering a possible injury mechanism and the development of a new rear-impact dummy. *Accident Analysis and Prevention*, *32* (2), 167-175.

Svensson, M. Y., Lövsund, P., Haland, Y., & Larsson, S. (1996). The influence of seat-back and head-restraint properties on the head-neck motion during rear-impact. *Accident Analysis and Prevention*, *28* (2), 221-227.

Szabo, T. J., Voss, D. P., & Welcher, J. B. (2003). Influence of Seat Foam and Geometrical Properties on BioRID P3 Kinematic Response to Rear Impacts. *Traffic Injury Prevention, 4* (4), 315-323.

Tabiei, A., & Nilakantan, G. (2007). Reduction of acceleration induced injuries from mine blasts under infantry vehicles. *6th European LS-DYNA Users Conference*, Gothenburg, Sweden.

Taylor, C. (2007). *US Patent No. 2007241594.*

Van Ratingen, M., Ellway, J., Avery, M., Gloyns, P., Sandner, V., & Versmissen, T. (2009). The Euro NCAP whiplash test. *Proceedings of the 21st International Technical Conference on Enhanced Safety of Vehicles*, Stuttgart, Germany (pp. 15-18).

Viano, D. C. (2003a). Influence of seat properties on occupant dynamics in severe rear crashes. *Traffic Injury Prevention*, *4* (4), 324-336.

Viano, D. C. (2003b). Seat influences on female neck responses in rear crashes: a reason why women have higher whiplash rates. *Traffic Injury Prevention*, *4* (3), 228-239.

Viano, D. C. (2003c). Seat properties affecting neck responses in rear crashes: a reason why whiplash has increased. *Traffic Injury Prevention*, *4* (3), 214-227.

Viano, D. C. (2008). Seat design principles to reduce neck injuries in rear impacts. *Traffic Injury Prevention*, *9* (6), 552-560.

Viano, D. C., & Gargan, M. F. (1996). Headrest position during normal driving: implication to neck injury risk in rear crashes. *Accident Analysis and Prevention*, *28*(6), 665-674.

Watanabe, Y., Ichikawa, H., Kayama, O., Ono, K., Kaneoka, K., & Inami, S. (2000). Influence of seat characteristics on occupant motion in low-speed rear impacts. Accident Analysis and Prevention, 32 (2), 243-250.

Welcher, J. B., & Szabo, T. J. (2001). Relationships between seat properties and human subject kinematics in rear impact tests. *Accident Analysis and Prevention, 33* (3), 289-304.

Yoganandan, N., Pintar, F. A., & Gennarelli, T. A. (2002). Biomechanical mechanisms of whiplash injury. *Traffic Injury Prevention*, *3*(2), 98-104.

Young, A. L., Ragel, B. T., Su, E., Mann, C. N., & Frank, E. H. (2005). Assessing automobile head restraint positioning in Portland, Oregon. *Injury Prevention*, *11* (2), 97-101.

Yu, C. H. (2007). *US Patent No. 2007209667.*

Yuen, M., & Bilston, L. (2004). Development of an anti-whiplash seat. *Australian Transport Safety Bureau*.

CURRICULUM VITAE

PERSONAL INFORMATION

Surname, Name: Özdemir, Mustafa
Nationality: Turkish (TC)
Date and Place of Birth: 19 January 1983, Çorlu
E-mail: mozdemir@metu.edu.tr
Phone: +90 312 210 5266
Fax: +90 312 210 2536

EDUCATION

Degree	Institution	Date of Graduation	C.GPA
M.S.	METU Department of Mechanical Engineering, Ankara	14 January 2008	3.79 / 4.00
B.S.	METU Department of Mechanical Engineering, Ankara	25 June 2005	3.47 / 4.00
High School	Ankara Fen Lisesi	15 June 2001	5.00 / 5.00

WORK EXPERIENCE

Period	Place	Position
September 2012-Present	METU Department of Mechanical Engineering, Ankara	Instructor
September 2005-September 2012	METU Department of Mechanical Engineering, Ankara	Research Assistant
December 2009-June 2010	A collaboration project between METU and TOFAŞ (Project Title: Detailed Design and Tests of an Anti-Whiplash Seat Mechanism)	Researcher

WORK EXPERIENCE (CONTINUED)

Period	Place	Position
June 2008-September 2009	A collaboration project between METU and TOFAŞ (Project Title: Design of an Anti-Whiplash Seat Mechanism)	Researcher
2004-2005 Academic Year	METU Department of Mechanical Engineering, Ankara	Student Assistant
June-July 2004	Volkswagen Electrical Systems, Inc., Çerkezköy	Intern Engineering Student
August 2003	BSH Profilo Home Appliances, Inc., Çerkezköy	Intern Engineering Student

FOREIGN LANGUAGES

Fluent English, Beginner German

PUBLICATIONS

1. **Özdemir, M.**, İder, S. K., Gökler, M. İ., Dicle, H., Anık, E., & İnce, M. S. (2012) Finite element analysis of effect of backset distance on whiplash syndrome using BioRID II and simplified seat models. *6th Automotive Technologies Congress-OTEKON 2012*, Bursa, Turkey, pp. 79-80.
2. **Özdemir, M.**, İder, S. K., Gökler, M. İ., Dicle, H., Anık, E., & İnce, M. S. (2012). Classification of anti-whiplash systems: A patent survey. *6th Automotive Technologies Congress-OTEKON 2012*, Bursa, Turkey, pp. 77-78.
3. **Özdemir, M.**, İder, S. K., Gökler, M. İ., Dicle, H., Anık, E., & İnce, M. S. (2010) "BioRID II" ve basitleştirilmiş koltuk modelleri ile "whiplash" analizi. *5th Automotive Technologies Congress-OTEKON 2010*, Bursa, Turkey, pp.313-320.
4. **Özdemir, M.**, İder, S. K., Anık, E., Dicle, H., & Gökler, M. İ. *Hızlı dönüş mekanizmasına sahip bir araç koltuğu*, TR Patent applied for (under review).
5. **Özdemir, M.**, İder, S. K., Anık, E., Dicle, H., Gökler, M. İ., & İnce, M. S. *Boyun incinmelerini önleyici bir araç koltuk mekanizması*, TR Patent applied for (under review).
6. **Özdemir, M.**, İder, S. K., & Gökler, M. İ. Parametric analysis of a novel anti-whiplash system of a vehicle seat for rear-end collisions. *International Journal of Crashworthiness* (under review).

PUBLICATIONS (CONTINUED)

7. Kavas, A., **Özdemir, M.**, Erdemli, Ö., Gürses, S., Keskin, D., & Tezcaner, A. (2012). Combinational effects of BMP9, Raloxifene and Pluronic F-68 on OA-like chondrocytes. *3rd TERMIS World Congress 2012*, Vienna, Austria (Poster Presentation).
8. Kavas, A., **Özdemir, M.**, Gürses, S., Keskin, D., & Tezcaner, A. (2011). In vitro investigation and biomechanical modeling of the effects of PLF-68 on osteoarthritis in a three-dimensional model. *Biomechanics and Modeling in Mechanobiology*, *10*(5), pp. 641-650.
9. Kavas, A., **Özdemir, M.**, Gürses, S., Keskin, D., & Tezcaner, A. (2009). Investigation of effect of PLF-68 on osteoarthritic chondrocytes embedded in agarose and Kelvin model development for further analysis. *International Symposium on Biotechnology: Developments and Trends-BIOTECH METU 2009*, Ankara, Turkey (Poster Presentation).
10. **Özdemir, M.**, & Söylemez, E. (2009). Verilen bir dört-çubuk mekanizmasının sabit eğrilik yarıçaplı noktalar eğrisini çizen bilgisayar programı. *14. Ulusal Makina Teorisi Sempozyumu-UMTS 2009*, Güzelyurt, Turkish Republic of Northern Cyprus, pp.443-448.
11. **Özdemir, M.**, Inverse dynamics control of parallel manipulators around singular configurations. M.S. Thesis, January 2008, METU Department of Mechanical Engineering, Ankara.

HONORS & SCHOLARSHIPS

- The Scientific and Technological Research Council of Turkey (TÜBİTAK) National Scholarship Program for Ph.D. Students
- The Scientific and Technological Research Council of Turkey (TÜBİTAK) National Scholarship Program for M.S. Students
- Dean's high-honor list for 3 semesters at the Department of Mechanical Engineering, Middle East Technical University: 2003-2004 Spring, 2004-2005 Fall & Spring
- Dean's honor list for 5 semesters at the Department of Mechanical Engineering, Middle East Technical University: 2001-2002 Fall & Spring, 2002-2003 Fall & Spring, 2003-2004 Fall